

# **STRUCTURAL DAMAGE IDENTIFICATION USING HIGH DIMENSIONAL MODEL REPRESENTATION**

Thesis

Submitted in partial fulfilment of the requirements for the degree of  
**DOCTOR OF PHILOSOPHY**

*by*

**NAVEEN B.O.**



**DEPARTMENT OF CIVIL ENGINEERING  
NATIONAL INSTITUTE OF TECHNOLOGY KARNATAKA  
SURATHKAL, MANGALORE – 575 025**

**March, 2018**

## **D E C L A R A T I O N**

*by the Ph.D. Research Scholar*

I hereby declare that the Research Thesis entitled “**Structural Damage Identification Using High Dimensional Model Representation**” which is being submitted to the **National Institute of Technology Karnataka, Surathkal** in partial fulfilment of the requirements for the award of the Degree of **Doctor of Philosophy** in Department of **Civil Engineering**, is a bonafide report of the research work carried out by me. The material contained in this Research Thesis has not been submitted to any University or Institution for the award of any degree.

**(NAVEEN B.O.)**

Register No. 145060CV14F04

Department of Civil Engineering

Place: NITK, Surathkal

Date: 02-03-2018

## C E R T I F I C A T E

This is to certify that the Research Thesis entitled “**Structural Damage Identification Using High Dimensional Model Representation**” submitted by **Mr. NAVEEN B.O.** (Register Number: **145060CV14F04**) as the record of the research work carried out by him, is accepted as the Research Thesis submission in partial fulfilment of the requirements for the award of degree of **Doctor of Philosophy**.

Dr. A.S. Balu

Research Guide

(Signature with date and seal)

Prof. Varghese George

Chairman - DRPC

(Signature with date and seal)

Dedicated to

*My Family and Teachers*

## ACKNOWLEDGEMENT

I would like to express my sincere gratitude to my research supervisor Dr. A.S. Balu, Department of Civil Engineering, National Institute of Technology Karnataka, Surathkal for providing continuous support and encouragement. I wish to acknowledge the precious time spent with my supervisor for technical discussions, and writings undertaken, which gave me confidence in perusing the research work.

I would like to express my sincere thanks to Head of the Department Dr. Varghese George, former Heads Prof. D. V. Reddy and Prof. Katta Venkataramana and all faculty members of the Department of Civil Engineering for their constant encouragement and for providing necessary facilities during the period of my research work.

I am thankful to the members of RPAC, Prof. K. Swaminathan, Department of Civil Engineering and Dr. Satyanarayana Engu, Department of Mathematical and Computational Sciences for their continuous evaluation of my research work and for their suggestions, and constant encouragement.

I would like to express my sincere thanks to all the research scholars of civil engineering department especially Basavana Gowda S.N., Punith B. Kotagi, Darshan C Sekhar, Renuka Prasad M. S., Parameshwar, Kesava Rao B., Spoorthi S. K., Sharan Kumar, and Vinod N. Tamburi, for their constant encouragement throughout my research work. Also, I extend my special thanks to my senior colleagues Naveen Kumar D.T., Sangeetha D.M., and K. Rajendra Prabhu for their suggestions.

My special thanks to my family members especially my parents, father in-law, mother in-law, my wife Mrs. Deeksha S.U., daughter Vaishnavi, brother Mr. Gururaja, Mrs. Sridevi Gururaja, Mr. Dhyan, Mr. Atharv, Ms. Aadhya, Mr. Suresh Babu, Mrs. Pushpa Suresh Babu and my friends Abhilash T.S., Prashanth S. K., Sridhar B.S., Vinay and Shruthi Badami, who always supported and encouraged me.

**Naveen B.O.**

## **ABSTRACT**

Any engineering structure is subject to various internal and external factors which may cause wear or malfunction due to deterioration, an incorrect construction process, lack of quality control or environmental effects. To be able to observe these changes in the material and to react in a proper way before serious damage is caused, the implementation of a damage identification system is crucial. In the past, many methods have attempted to identify damage by solving an inverse problem, which inevitably needs an analytical model. However, often the construction of these analytical model requires considerable effort in building a mathematical framework with acceptable level of accuracy and reliability which makes these approaches less attractive. In order to circumvent this complexity, this work presents a computationally efficient approach in structural damage identification (SDI) using high dimensional model representation (HDMR).

In general, most of the structural systems are simulated with the help of finite element (FE) models to predict static as well as dynamic behaviour of the systems with different boundary conditions. Therefore the FE models have to be in tune with the experimental observation to facilitate any modifications in the systems so that the future responses can be accurately predicted, and subsequently utilized in design optimization. Thus, finite element model updating (FEMU) is effective in improving the correlation between predicted and observed ones by correcting the inaccurate modelling assumptions.

The proposed methodology involves an integrated finite element modeling, development of response surface model using HDMR, establishment of objective function, and minimization of the function using genetic algorithm. An attempt has been made to reduce the computational effort with increase in the accuracy of updated parameters.

The proposed methodology is applied in model updating of a simulated beam and an existing reinforce cement concrete (RCC) box culvert structure. The results have demonstrated that the HDMR based FEMU is a good candidate featuring computational efficiency. Further to validate the proposed methodology in SDI, three

case-studies (an experimental beam, a frame structure and a bridge structure) have been considered. The damage patterns, locations and severity obtained using the proposed methodology are compared with the experimental results available in literature, and are found to be in good agreement. Based on the study conducted, it can be concluded that the HDMR based FEMU in SDI is computationally efficient.

**Keywords:** Finite element analysis; High dimensional model representation; Model update; Response surface method; Structural damage identification.

# CONTENTS

	Page No.
<b>TABLE OF CONTENTS</b>	i
<b>LIST OF FIGURES</b>	iii
<b>LIST OF TABLES</b>	v
<b>LIST OF ABBREVIATIONS AND SYMBOLS</b>	vii
<b>1. INTRODUCTION</b>	1
1.1 Structural Health Monitoring	2
1.2 Model Update	4
1.3 Structural Damage Identification	5
1.4 Need for the Present Work	8
1.5 Thesis Organisation	9
<b>2. LITERATURE REVIEW</b>	11
2.1 Finite Element Model Updating	11
2.2 Structural Damage Identification	19
2.3 High Dimensional Model Representation	22
2.4 Summary of Literature Review	27
2.5 Objectives of Research Work	28
<b>3. MODEL UPDATING USING HDMR</b>	29
3.1 HDMR	29
3.2 HDMR Expansions	30
3.3 Model Updating using HDMR	34
3.4 Numerical Examples	35
3.4.1 Example 1: Simply Supported Beam	35
3.4.1.1 Response Surface Generation	36
3.4.1.2 Optimization using GA	38
3.4.2 Example 2: Reinforced Concrete Box Culvert	43
3.5 Summary	47



<b>4. STRUCTURAL DAMAGE IDENTIFICATION USING HDMR</b>	49
4.1 Simulation Study : Simply Supported Beam	49
4.2 Case Study 1: Experimental Beam	54
4.3 Case Study 2: Reinforced Concrete Frame	66
4.4 Case Study 3: Bridge Structure	73
4.5 Summary	78
<b>5. CONCLUSIONS</b>	81
5.1 Summary and Research Findings	81
5.2 Suggestions for Future Work	83
<b>APPENDIX</b>	85
<b>REFERENCES</b>	91
<b>PUBLICATIONS</b>	100

## LIST OF FIGURES

	Page No.
1.1 Principle and organization of a SHM system	2
1.2 Applications of SHM	3
2.1 Summary of articles	12
3.1 Sampling scheme: First-order HDMR	33
3.2 Sampling scheme: Second-order HDMR	34
3.3 Flow chart of HDMR based model updating and damage identification	34
3.4 Simply supported concrete beam	35
3.5 Parameter screening results	41
3.6 Finite element model of RC box culvert	44
4.1 A simulated simply supported beam	49
4.2 Difference in frequencies after model updating ( $n=3$ )	51
4.3 Identified damage locations and stiffness distribution ( $n=3$ )	52
4.4 Difference in frequencies after model updating ( $n=5$ )	52
4.5 Identified damage locations and stiffness distribution ( $n=5$ )	53
4.6 Beam cross section and with two point loading	54
4.7 Crack pattern at each load steps	55
4.8 Stiffness distribution: Reference state model (After updating: $n=3$ )	56
4.9 Stiffness distribution: Reference state model (After updating: $n=5$ )	58
4.10 Stiffness distribution: Ref.-damage state model (After updating: $n=5$ )	60
4.11 Stiffness distribution: Damage state model (After updating: $n=5$ )	62
4.12 Variation of Young's modulus at different updating states	64
4.13 3D Numerical model of experimental beam	65
4.14 Reinforcement bars (Linear line elements of type T3D2)	65
4.15 Comparison of cracks	66
4.16 RC frame: Geometric dimensions and accelerometer arrangement	66
4.17 Modal test of an RC frame	67

4.18	Parameter screening results (RC frame)	67
4.19	Comparison of absolute errors (%) of initial and reference state model ( $n=5$ )	70
4.20	Comparison of absolute errors (%) of reference and damage state model ( $n=5$ )	72
4.21	Variation of $E$ at different updating states	72
4.22	General view of I – 40 Bridge	73
4.23	Damage scenarios: First and Second stage damage	73
4.24	Damage scenarios: Third and Fourth stage damage	74
4.25	Simplified I-40 bridge model with accelerator layout	75
4.26	Two dimensional beam model of bridge	75
4.27	Identified damage location at substructure S5 ( $n=3$ )	76
4.28	Identified damage location at substructure S5 ( $n=5$ )	77
4.29	Stiffness distribution at S5 substructure ( $n=5$ )	77

## LIST OF TABLES

		Page No.
3.1	Identified values of parameter using GA	40
3.2	Responses for development of HDMR expression (Beam example)	42
3.3	Variation of values (Error percentage) for Beam	43
3.4	Computational effort (Beam Example)	43
3.5	Variation of values (Error percentage) for Box-culvert	46
4.1	Initial frequencies of FE model: Simulated beam	51
4.2	Updated frequencies of simulated beam ( $n=5$ )	53
4.3	Six step static load magnitude	55
4.4	Frequencies and their differences: Experimental beam ( $n = 5$ )	59
4.5	Frequencies and its difference of Ref.-damage state model: Experimental beam ( $n = 5$ )	60
4.6	Frequencies and its difference of damage state model: Experimental beam ( $n = 5$ )	61
4.7	Differences in frequencies of Modal flexibility residual and HDMR before updating: Experimental beam (Reference state)	63
4.8	Differences in frequencies of Modal flexibility residual and HDMR before updating: Experimental beam (Damage state)	63
4.9	Updated values of reference state model Experimental RC frame	68
4.10	Modal frequencies of reference state model: Experimental RC frame ( $n = 5$ )	69
4.11	Updated values of E1 substructure in damage state: Experimental RC frame ( $n = 5$ )	70
4.12	Values of $E$ at different updating states: Experimental RC frame ( $n = 5$ )	70
4.13	Modal frequencies of damage state model:	

	Experimental RC frame ( $n = 5$ )	71
4.14	Frequency errors before updating: Bridge example	76
4.15	Frequency errors after updating:	
	Bridge model in damage state ( $n = 5$ )	78

## LIST OF ABBREVIATIONS AND SYMBOLS

### Abbreviations

ABC	: Artificial Bee Colony
ANN	: Artificial Neural Network
ANNOVA	: Analysis of Variance
C3D8R	: Continuum 3D 8-Node Reduced Integration
CCD	: Central Composite Design
DOE	: Design of Experiment
FE	: Finite Element
FEA	: Finite Element Analysis
FEM	: Finite Element Method
FEMU	: Finite Element Model Updating
FFT	: Fast Fourier Transform
FHDMR	: Factorized High Dimensional Model Representation
FRF	: Frequency Response Function
FRP	: Fibre Reinforced Polymer
GA	: Genetic Algorithms
GHDMR	: General High Dimensional Model Representation
GRSMU	: Generalized Response Surface Model Updating
HDMR	: High Dimensional Model Representation
HHDMR	: Hybrid High Dimensional Model Representation
IESM	: Inverse Eigen Sensitivity Method
ILs	: Influence Lines
MLS	: Moving Least Square
NDE	: Non-Destructive Evaluation
NN	: Neural Network
PSO	: Particle Swarm Optimization
PZT	: Piezoelectric ceramic material
RCC	: Reinforced Cement Concrete
RFM	: Response Function Method

RS	: Response Surface
RS-HDMR	: Random Sampling High Dimensional Model Representation
RSM	: Response Surface Method
SA	: Simulated Annealing
SDI	: Structural Damage Identification
SHM	: Structural Health Monitoring
T3D2	: 2-noded linear 3-D Stress/Displacement Truss Element

### **Symbols**

$A$	: Area of cross section of girder
$\rho$	: Density of concrete
$Y$	: HDMR response equation
$x$	: Input parameters/variables
$\phi$	: Lagrange interpolation function
$\mu_i$	: Mean
$N$	: Number of parameters/variables
$F_{obj}$	: Objective function
$\mu$	: Poisson's ratio
$c$	: Reference point
$n$	: Sample points
$I$	: Second moment of area
$\sigma_i$	: Standard deviation
$E$	: Substructure
$E$	: Young's modulus

# **CHAPTER 1**

## **INTRODUCTION**

In order to improve the safety and serviceability of any civil engineering structures, the present condition of the structures should be known. A periodical inspection facilitates to understand the condition of the structures which involves structural modifications, repairs and/or reconstructions. In economical point of view, maintenance and repair cost will be less than the reconstruction of major structural components which are distressed/damaged or the entire structure. The most commonly adopted method to detect damages is carried out by visual inspection using non-destructive methods. The process of implementing a damage detection strategy for aerospace, civil and mechanical engineering structures is referred to as structural health monitoring (SHM). Monitoring and early damage detection in a structure depends on the ability of an SHM technique implemented into the engineering system, where it aims to give a diagnosis of the state of the constituent materials of different parts, and of the full assembly of these parts constituting the structure as a whole at every moment during the life of a structure. Damage is defined as the changes in the physical properties introduced into a system that adversely affect current or future performance of the system, which occurs due to natural or man-made cause. SHM is considered as an efficient approach of non-destructive evaluation (NDE), which involves the utilization of smart materials, sophisticated sensors, data transmission mechanisms, and usage of advanced processing techniques having more computational power for monitoring a structure of interest. The implementation of SHM results in reduction of inspection costs, possibility to better understand the behaviour of structures under dynamic loads, seismic protection, observation in real or near real-time of the structural response and evolution of damage, so that it is possible to produce post-disaster scenarios and support rescue operations. Thus, SHM



is a multidisciplinary field, where a number of different skills and institutions can work together in order to increase the performance and reliability of structural systems. Figure 1.1 presents the organisation of a typical a SHM system in detail (Balageas et. al. 2006).

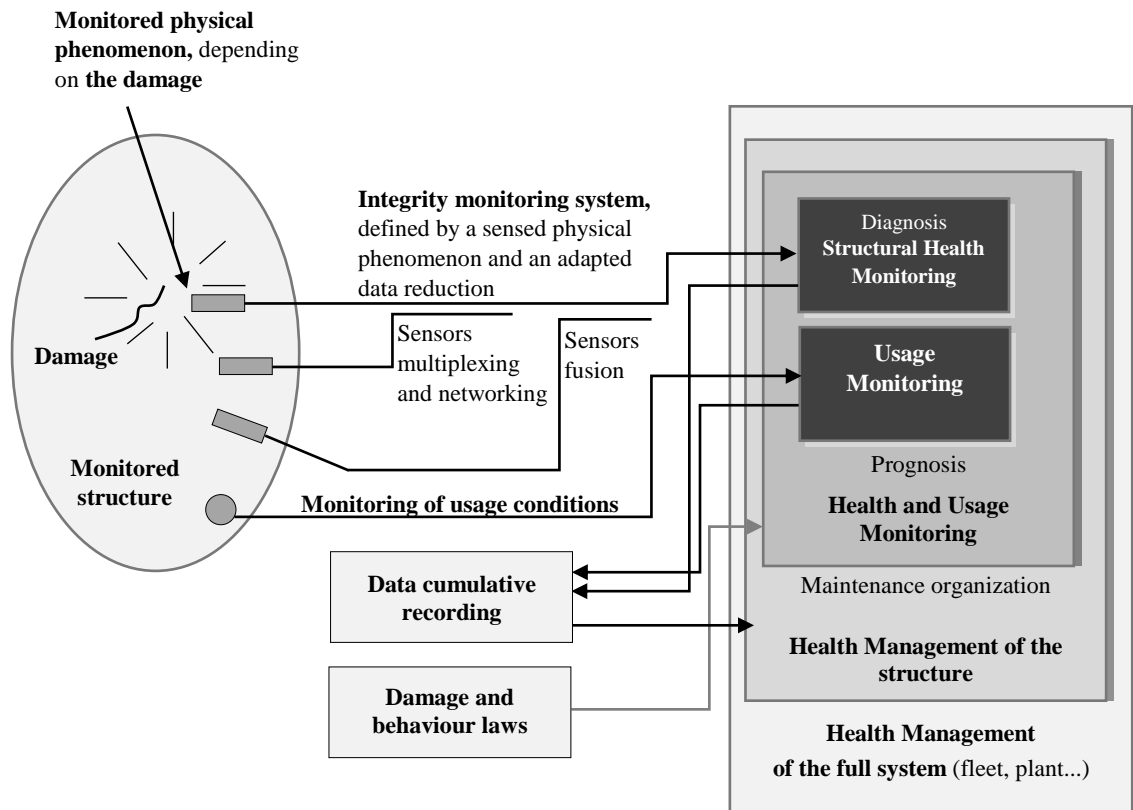


Fig. 1.1 Principle and organization of a SHM system

## 1.1 STRUCTURAL HEALTH MONITORING

The motivation of SHM in various applications of engineering field involves maximum utilization of structure over a period of time with better serviceability and improved maintenance without any major damage of structural components, or failure of the entire structural systems, thus improving safety and reliability. The various applications of SHM is shown in Fig.1.2, and a brief application of SHM is discussed below (<https://www.hbm.com/en/5530/structural-health-monitoring>).

- Civil engineering structures (ie, bridges, buildings, tunnels, etc.) are designed to resist enormous amount of applied loads and forces due to natural disasters. With the application of SHM the structure is monitored

by material testing and load assessment, measurement of displacements, deflections and rotations for extending the performance of the structure.

- Application of SHM in railway industry includes, fatigue analysis of structural members and railway components (ie, wheels and axels), remote monitoring of tracks, measurement of forces and mechanical stresses, and data determination for life cycle cost calculations.
- In wind energy sector, SHM is useful in condition monitoring of the critical components (ie, rotor blades, drivetrains, inverters) which are subjected to extreme mechanical stresses.
- In oil and gas industry, SHM has important role in pipe line monitoring using fibre optic strain sensors, and also in efficient measurement of drive power using torque transduces in gas compressor stations.

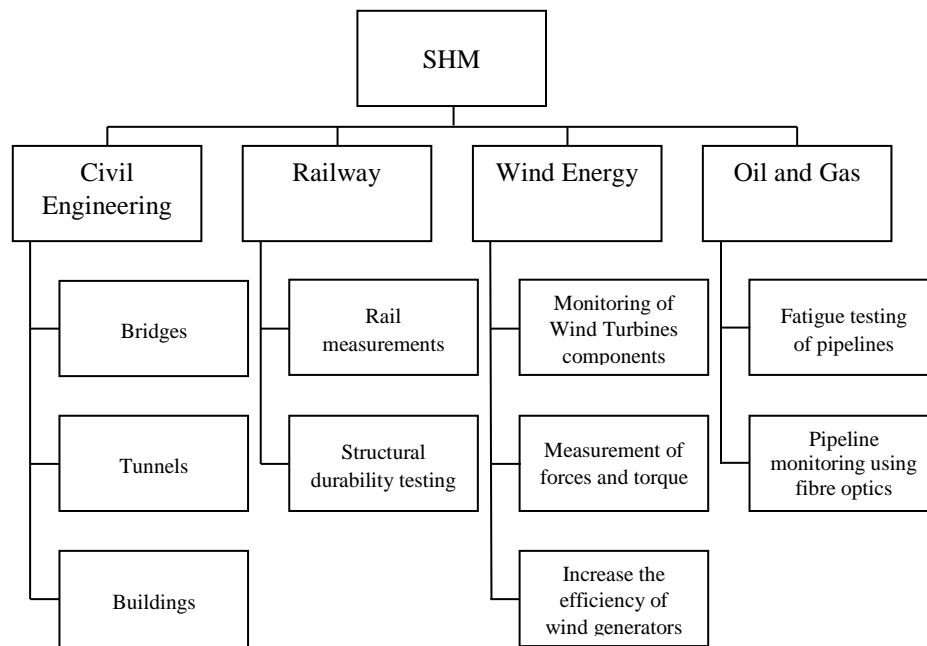


Fig. 1.2 Applications of SHM

The design of SHM system is influenced by different parts as follows (Hejll 2007).

- The structural phenomena to be studied (cracking, settlements, etc.)
- The time strategy (continuous, periodic or triggered monitoring)
- The condition of the phenomenon to be studied (global or local)
- The load effect (position/intensity/nature of loading)

- The evaluation method
- The model used to evaluate the cause-effect (i.e., knowledge of geometrical, material, load data, etc.)

The SHM and the damage identification are gaining larger importance in civil engineering. It is also defined as the use of in-situ, non-destructive sensing and analysis of structural characteristics in order to identify any damages. In addition, it defines the location, estimates the severity, and evaluates the consequences on the residual life of the structure. In the field of structural engineering and design, with respect to aging of steel and reinforced concrete (RC) structures, safety has become the most important criterion. Prolonging the life of the structure is the major role of SHM techniques by detecting the damages in the initial stages only.

The structural dynamic behaviour can be represented by many terms such as natural frequencies, Eigen values, damping ratio, and frequency response functions. From the dynamic analysis we can understand and evaluate the responses, and these can be modified as per the requirements of engineering design, if required. The dynamic analysis of structures can be done through either experimental route or by using theoretical approach. In most of the cases, performing experimental investigation requires more time and effort, and sometimes tedious due to extensive procedure. Hence, theoretical approaches such as classical methods and finite element method (FEM) are preferred. Classical methods are having limited applications, which include the application in simple structural elements like plates, shells, beam elements, laminates, composites, etc. For modelling and predicting the dynamic behaviour of structures with complex shapes, boundary and loading conditions, FEM is preferred (Sehgal and Kumar 2015).

## **1.2 MODEL UPDATE**

In most of the cases where simplifications and assumptions are made while defining the loads, modeling the joints and boundary conditions, optimizing the mesh pattern, and characterising the damping, there exists a conflict with the results obtained from FEM and the experimental observations. Inaccurate response prediction from finite element (FE) model leads to difficulties in understanding the dynamic behaviour of

the system. In order to overcome this drawback, model updating techniques have emerged to aid the FE model predictions with good accuracy, so that the vibrational behaviour of FE model matches with the actual dynamic response obtained experimentally. Modification of uncertain parameters to make certain analytical responses in tune with the experimental observations is the key role that can be considered as inverse method in finite element model updating (FEMU).

In the model updating procedure, the experimental results are considered as targets, and the inputs of FE model are updated to obtain accurate parameters. Dealing with FE model modifications, performing multiple runs needs more computational effort and time. Hence to reduce the complexity, FE model is replaced with an approximate mathematical expression which relates predetermined FE inputs and outputs. Model updating methods may be classified as sensitivity or direct methods (Sehgal and Kumar 2015). Sensitivity type methods rely on a parametric model of the structure and the minimization of some penalty function based on the error between the measured data and the predictions from the model. The alternative is the direct updating methods that change complete mass and/or stiffness matrices, although the updated models obtained are often difficult to interpret for health monitoring applications.

The concept of FEMU has been applied to build efficient formulations for the analysis of structural damages, for the investigation of material properties based on NDE characterization, and for the design based on dynamic responses. Applications of FEMU techniques can be found in various industries like, airport, automobile, power plants, bridges, multi-storey steel/RCC structures, mechanical tools and equipment etc.

### **1.3 STRUCTURAL DAMAGE IDENTIFICATION**

The SHM applications have an important role in the field of composites and aircraft industries. A significant amount of work has been conducted using SHM techniques to determine the various defects, damages and critical size of damage, which influences the strength and life of composite structures. Among the various NDE methods, the important ones are as follows: visual inspection; optical methods; Eddy

current; ultrasonic inspection; laser ultrasonic; acoustic emission; vibration analysis; radiography; thermography and Lamb waves (Balageas et al. 2006). Each method has its own advantages and limitations. For instance, offshore platforms can be analysed using visual examination. The acoustic emission technique plays an important role in the inspection of secondary structures in nuclear reactor core, and in case of ultrasonic method of SHM, it is necessary to know the damage location a priori, and it renders the structure unavailable throughout the length of the test. Many of the NDE methods can be applied only at the certain period of time. Application of impedance-based health monitoring techniques has gained importance, as the conventional NDE methods might be very tedious, expensive, or unreliable. Hence, automated NDE techniques are developed to enable real time health monitoring of civil engineering structures. While in operations, the techniques are embedded with built-in diagnostic system, which can be placed at desired and inaccessible locations. This built-in diagnostic system utilizes impedance-based damage detection technique, which uses a smart piezoelectric ceramic material (PZT). The PZT patches have been bonded to the surface of the structural member of interest or at critical locations, which will detect any changes in the structural/ mechanical impedance due to external loads (Park et al. 2000).

Vibration based techniques are rapidly expanding in the field of structural damage identification (SDI). In vibration based SHM techniques, the use of natural frequencies is considered as the most important diagnostic parameter in assessment of structural behaviour, since natural frequencies are sensitive to the modification in the structural integrity. Hence, by conducting systematic periodical measurement of changes in frequencies, the structure can be monitored. This method is more reliable, and less expensive, and hence it can be carried out frequently (Salawu 1997). The vibration based technique is based on the basic idea that, for any structure subjected to dynamic loads, the frequencies, mode shapes and modal damping are functions of the mass, damping and stiffness which constitute the physical properties of the structure. Hence, changes in these physical properties result in changes in modal properties (Doebbling et al. 1998).

In most of the cases, all the structural systems are subjected to various dynamic loads. Hence, study of those parameters, which affect the dynamic behaviour of structural systems, is an interesting area of research. In order to evaluate the accurate dynamic parameters of intact and damage state of structural component or structure as a whole, an efficient and cost effective tool is required to localize and quantify the damage scenarios. Further, based on the dynamic response parameters, the method is subdivided into modal analysis, time domain, frequency domain and impedance domain (Zou et al. 2000). Among the various NDE techniques, vibration based techniques have greater importance in identifying structural damages in the past decade, and also greater advancements in instrumentation have been achieved. Changes in the dynamic behaviour of any structural system due to localized damage is associated with the reduction in stiffness, increase in damping, decrease in natural frequencies, and variation of modes. Certain dynamic responses could not be measured in the field experiments due to various causes. Hence, using FEM, any complex structures can be modelled by considering all the degrees of freedom, so that the exact dynamic behaviour can be assessed and quantified (Dutta and Talukdar 2004). Damage detection using inverse methods is carried out by various researchers. A brief overview of the use of inverse methods in damage detection and location, using measured vibration data is available in Friswell (2007).

Development of statistical model plays an important role in enhancing the SHM process, and there is a lot of scope in this field since least attention is given to implementation of statistical models in current and previous applications of SHM. Generally, in all the engineering systems, a set of responses are dependent on certain selected parameters, and a change in these parameters results in change in behaviour of the systems. In majority of the cases, these parameters influence the type, location and severity of the damage. In order to assess the changes in the selected features to identify the damaged system, the statistical models can be effectively utilized. The algorithms used to develop statistical model need data from both the undamaged and the damaged structures. The statistical pattern recognition algorithms are generally classified as supervised and unsupervised learning. Group classification and regression analysis are supervised learning algorithms. Response surface (RS), metamodeling, linear discriminants, neural networks (NN) and genetic algorithms

(GA) fall under the supervised learning. Unsupervised learning methods include control chart analysis and novelty detection methods (Sohn et al. 2001). Metamodeling has been widely used for design optimisation, where surrogate models are built and applied in various engineering problems (Zhao et al.2011). Additionally, surrogate models are utilized in the analysis of stochastic structures, where the statistical properties of dynamic variables are obtained accurately. One of the methods adopted by Liu et al. (2015) deals with problems in load identification for stochastic structure by combining the Gegenbauer polynomial approximation and regularization method. The response surface method (RSM) is widely adopted in many fields owing to its numerical efficiency. Nonetheless, the RSM is time consuming for large-scale applications, and sometimes indicates large errors in the calculation of the sensitivity of the parameters. In order to overcome these problems, an improved method called high dimensional model representation (HDMR), which is basically a dimension-reduction technique widely used in kinetic chemistry and structural reliability areas, is widely used in many areas of specializations.

#### **1.4 NEED FOR THE PRESENT WORK**

In general, most of the structural systems are simulated with the help of FE models to predict static as well as dynamic behaviour of the systems with different boundary conditions. Therefore, the FE models have to be in tune with the experimental observation to facilitate any modifications in the systems so that the future responses can be accurately predicted, and subsequently utilized in design optimization. Thus, FEMU is effective in improving the correlation between predicted and observed ones by correcting the inaccurate modelling assumptions.

Many damage detection methods have attempted to identify damage by solving an inverse problem, which inevitably needs an analytical model. However, often the construction of these analytical model requires considerable effort in building a mathematical framework with acceptable level of accuracy and reliability which makes these approaches less attractive. In order to circumvent this complexity, a computationally efficient approach in SDI using HDMR is presented in this thesis.

## 1.5 THESIS ORGANISATION

The proposed methodology involves an integrated FE modeling, development of RS model using HDMR, establishment of objective function, and minimization of the function using GA in order to identify the damages by updating the FE model. An attempt has been made to reduce the computational effort, with increase in the accuracy of updated parameter. The thesis is organised as follows.

- i) The first chapter describes a brief introduction to SHM, applications and importance of SHM in SDI. Various damage identification methods have been mentioned including NDE and vibrations based methods. Importance of FEMU in SHM and damage identification has been discussed along with the need of the present study.
- ii) The second chapter presents a detailed review of relevant literature on FEMU, SDI and HDMR, followed by summary of literature and objectives of the proposed research work.
- iii) The third chapter demonstrates the application of HDMR concepts in model updating. Two numerical examples (simply supported beam and box culvert) have been presented to verify the efficient application of HDMR in FEMU.
- iv) The fourth chapter presents a detailed study on HDMR based damage identification. A simulated numerical example of simply supported beam with assumed damages is considered. To substantiate the merit of the method, three case studies are considered from the literature to validate the proposed methodology.
- v) The last chapter presents the conclusions based on the key findings from the present work, and also the scope for the future work.





## **CHAPTER 2**

### **LITERATURE REVIEW**

A detailed review of relevant articles in the field of SDI is presented in this chapter. Also, the importance of FEMU in SDI with respect to various techniques is explored. The developments in RSM including HDMR is also reviewed and presented. The literature study has mainly focused on three major groups (i.e., FEMU, SDI and HMDR) by highlighting the research gaps. Figure 2.1 summarizes a brief list of relevant articles reviewed in these areas.

#### **2.1 FINITE ELEMENT MODEL UPDATING**

In the modern applications of engineering and science, most of the effort and time has been invested in developing numerical models based on finite element approach. These necessity models have greater importance in predicting the responses of the systems which will be utilized in model assessments, understanding the behaviour of structures under untested loading conditions or modified structural configurations, SHM and SDI. FEM is a numerical tool based on the numerous assumptions and simplifications (Rombach 2004). Hence, there exists a lack of correlation between predicted and experimental observations due to inaccuracies in numerical models. The three model errors which are considered as the main cause of inaccuracies in numerical models prediction are the model structure error, the model parameter error and the model order error (Mottershead and Friswell 1993). The model structure error is due to uncertainty in model parameters and input data, where accuracy of a model structure depends on availability of field data. A framework which integrates quantitative and qualitative uncertainty to estimate the impact of model structural uncertainty model predictions was developed by Refsgaard et al. (2006).

The nonlinear behaviour associated with the engineering systems may also lead to model structure error. The possibility of occurring the model parameter error is due to incorrect parameters and boundary conditions selected and applied to the given model. The model parameter error occurs, when there is a limited amount of data available to estimate the parameters. This error can be estimated using confidence intervals, bootstrap technique and Bayesian estimation. In most of the finite element modeling procedures, assumptions are made in order to simplify the model, and the model parameter errors are expected to occur in case of inaccurate assumptions.

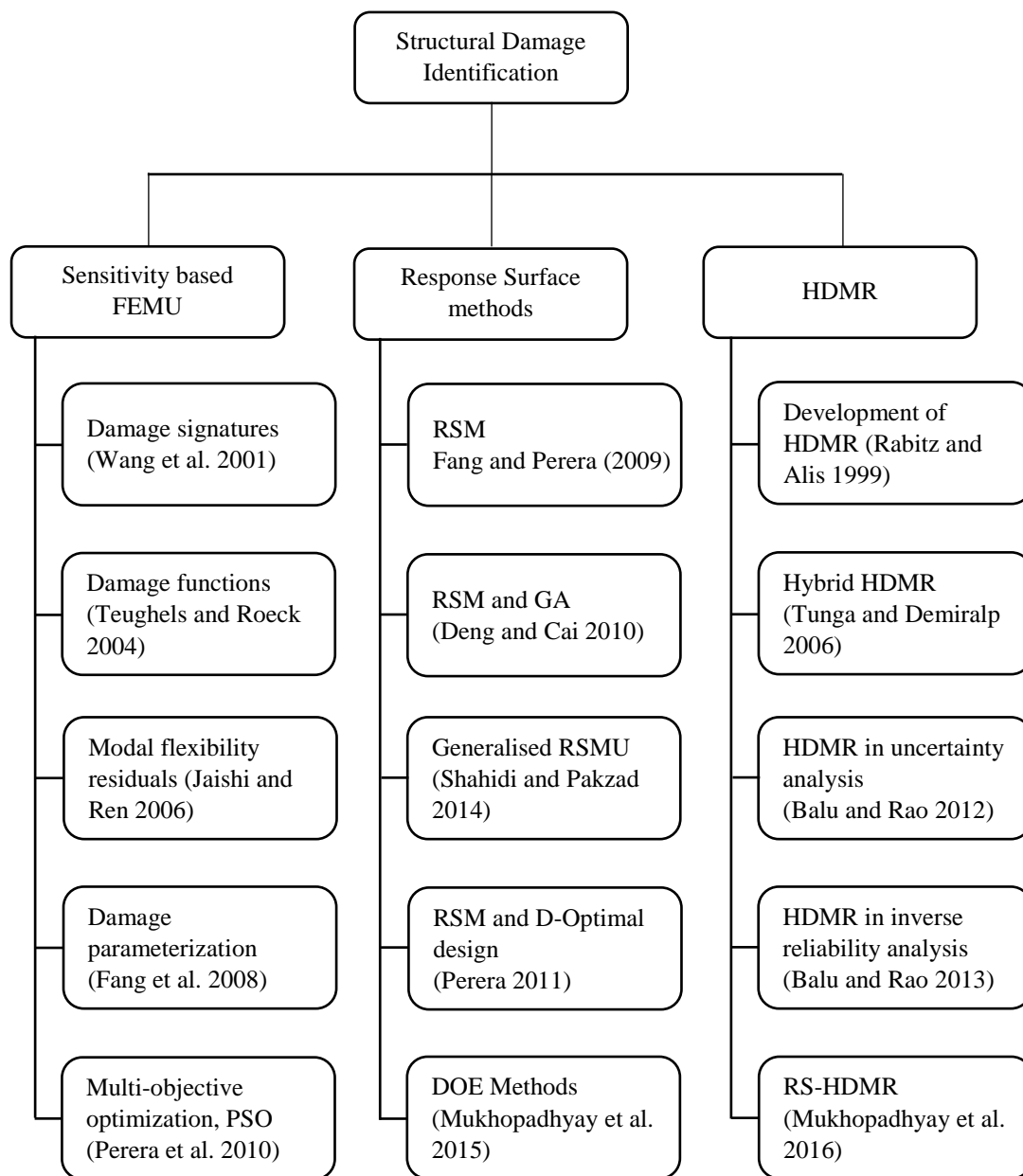


Fig. 2.1 Summary of articles

The model order errors which arise in the discretization of complex systems can result in a model of insufficient order. The model order may be considered as a part of the model structure. The main objective of model updating is to improve the correlation of results between the predicted and the observed by correcting the inaccurate modelling assumptions, and not by making other alteration to the model. Usually the parameters like mass, stiffness and damping of the numerical model are modified so that they will be in tune with the experimental test results. With the good correlation between the predicted and experimental observations, the application of FE model can be utilized in future response prediction confidently.

The FEMU emerged and became prominent in 1990s. Application concepts of FEMU techniques have gained a greater importance in the field of design and maintenance of mechanical and civil engineering structures in order to improve the performance of the products of engineering design. The procedure used to update the model is called the FEMU (Friswell and Mottershead 1995). The FEMU techniques can be broadly classified into direct and iterative techniques (Sehgal and Kumar 2015). Several FEMU techniques have been developed by different researchers on direct techniques (Baruch and Bar-Itzhack 1978; Berman and Nagy 1983; Bucher and Braun 1993; Friswell et al. 1998; Modak et al. 2002; Fang et al. 2011; Li et al. 2016) and iterative techniques (Collins et al. 1974; Levin and Lieven 1998; Modak et al. 2000; Marwala 2005; Jaishi and Ren 2007).

Imregun et al. (1995b) developed a formulation for FEMU using frequency response function (FRF), and applied for simple beam structure. The study was carried out to find the effectiveness of updating technique by considering noise and incomplete experimental data. Stability and convergence were also studied in numerical simulations, where free-free beam model was considered with known modeling errors using measured and simulated FRF data. Model updating based on FRF data was further extended by Imregun et al. (1995a), and the method was applied for a plate-beam structure consisting of 500 degrees of freedom, and after several iterations, initial FRF is updated. Hence, a better correlation with measured FRF has been obtained which was within engineering accuracy. From FRF based model updating method, it was concluded that, updating of FE model can be done by

measured data if the size of FE model is relatively small and ratio of measurement coordinates to the total number of degrees of freedom has to be high about 10%. Inverse Eigen sensitivity method (IESM) was applied by Lin et al. (1995) to update the analytical models of engineering structures. The IESM was improved by addressing the drawbacks of classical IESM methods, which are having slower convergence, and the calculated coefficients are based on modal data only. The improved IESM utilized both experimental and analytical modal data to obtain the Eigen sensitivity coefficients, which are found to be in tune with the true values. Also the method was further investigated for the case where measured coordinates are incomplete, and applied to FEMU of planar truss structure.

Structural model updating based on experimental data was carried out by Sanayei et al. (1997). The results based on the experiments performed on small scale steel frame model were presented to support the displacement equation error function, displacement output error function, and strain output error function methods of structural parameter estimation using static non-destructive test data. Parameters of the structural elements were updated using experimental static measurements and the stiffness of structural components was considered as unknown parameter. To evaluate the unknown stiffness, the measurements obtained from static displacements and static strains are used, and errors are reduced by weight factors obtained from analysis of variance of measured data. The parameters were identified with good accuracy having low deviation with respect to true values. Atalla and Inman (1998) presented NN based model updating using frequency domain data. A similar study was conducted by Chang et al. (2000) where concept of adaptive NN for model updating was applied to suspension bridge and verified both numerically and experimentally. A correlation-based model updating algorithm was proposed to update large structural dynamics models using measured response functions by Grafe (1998). The formulations developed are independent of number of measurements used, and are resistant to measurement noise. Kenigsbuch and Halevi (1998) presented a generalised reference basis approach of updating an analytical model from experimental data. The optimization was carried out using general weighting matrices. Accurate parameters like mode shapes or natural frequencies are taken while updating

the other parameters and constrained optimization problem has been solved in order to obtain the updated parameters.

Levin and Lieven (1998) utilized GA and simulated annealing (SA) as optimization algorithms for dynamic FEMU, and proposed a new variant for SA called blended-SA algorithm, which performs better than GA. The algorithms developed are based on probabilistic search approach, which are efficient in capturing the global minimum from the set of local minima, and comparison has been made between GA and SA algorithms. The choice of updating parameters has a greater impact on the accuracy of the results obtained during the optimisation process. Brownjohn and Xia (2000) investigated the application of sensitivity-based model updating technique to the dynamic assessment of the Safti Link Bridge, a curved cable-stayed bridge in Singapore. From the investigation, it was concluded that the dynamic properties obtained by the finite element analysis (FEA) for the complex structures such as the Safti Link Bridge, are not always consistent with the measured results due to the modelling errors and the uncertainties in the structure. Therefore, it is necessary to improve the FE model for successful dynamic assessment of the structure. Hence, the model updating is a feasible and effective technology for improvement of the FE model by modification of the parameters with uncertainties existing in the structure based on the prototype testing data.

Modak et al. (2002) used IESM and the response function method (RFM) of analytical model updating in their study. A detailed comparison of these two approaches of model updating was made on the basis of computer simulated experimental data. The main objective was to study the convergence of the two methods and the accuracy in the prediction of required corrections in a FE model. The updated models were compared on the basis of some error indices constructed to quantify error in the predicted natural frequencies, mode shapes and response functions. From the study it was concluded that RFM seems to have worked better than the IESM for the case of incomplete experimental data. In order to understand the structural behaviour and identify the parameters, the FEMU technique was implemented to upgrade the existing highway bridge by conducting field dynamic testing.

Using FEMU techniques, a practical method was performed to assess the load carrying capacity by utilizing the experimental data in order to upgrade and strengthen the bridge. Also, the influence of girder stiffness on post-performance of guard rail in the bridge was identified (Brownjohn et al. 2003). Particle swarm optimization (PSO) technique was utilized in FEMU by Marwala (2005). Bayesian probabilistic approach to structural model updating associated with uncertainties was proposed by utilizing the measured dynamic responses (Katafygiotis et al. 1998). A model updating approach for linear structural models called Bayesian model updating based on Gibbs sampler was proposed by Ching et al. (2006). This method not only updates the optimal estimate of the structural parameters, but also updates the associated uncertainties. Further the Gibbs sampler approach was applied to the health monitoring of existing structures with high-dimensional uncertain parameters which was effective in detecting location of the damage in an instrumented structure.

Eigen frequency residual and modal strain energy residual were used as two objective functions of the multi-objective optimization in FEMU (Jaishi and Ren 2007). Selection of updating parameters was done based on predetermined concepts of dynamic behaviour and sensitivity study. This FEMU technique based on Eigen frequency and modal strain energy detected the damage effectively when applied to a simulated simply supported beam with an assumed damage. Further the method was applied to update on-field precast continuous box girder-bridge under working conditions. In FE model applications, finding complex FRF and complex mode shapes will be difficult when damping matrices are not accounted in FEMU techniques. A method of FEMU by considering damping as a parameter was carried out by Arora et al. (2009), wherein the damping matrix was identified by the updated mass and stiffness matrices. The method was applied for a numerical beam with viscous damping. The method was more useful when dealing with complex updating parameter based FEMU, and a better matching of complex FRF with experimental data was found.

Response surface (RS) models or meta-models are considered as most efficient models in approximating the multivariate input-output relationships of a physical system, which are utilized to update the FE models by replacing the time consuming

physical based computer models. Developing RS models for model updating mainly involves implementing various sampling techniques with the aid of design of experiments (DOE) parameter screening, where important parameters to be updated are selected by screening out the non-significant ones and constructing the quadratic polynomial RS. In FEMU, setting-up of an objective function, selecting updating parameters and using robust optimization algorithm are the three crucial steps. The FEMU in structural dynamics based on RSM was carried out by Ren and Chen (2010), and applicability of the RSM was illustrated by considering a full scale precast box-girder bridge, which was tested under operational vibration conditions. Results showed faster convergence with RSM based FEMU than conventional sensitivity based FEMU methods. Bridge model updating using RSM and GA was proposed by Deng and Cai (2010), where parameters were updated using the GA by minimizing the objective function. Numerical simulations were done using the experimental design combinations of parameters and corresponding responses from the structure of interest. Second-order RS equations were developed, and in order to get accurate parameter values, third order RS equations were utilized to develop objective function. The residuals between measured and predicted responses constituted an objective function, and updated parameters were obtained by optimizing the function.

Generalized response surface model updating (GRSMU) method was developed by Shahidi and Pakzad (2014), where methodology was explained to formulate an iterative based model updating in time domain state. Also the method was implemented to update nonlinear FE model. A numerical case-study was carried out considering a steel frame with global nonlinearity. Well prediction of unknown parameters was observed using GRSMU in conjunction with optimization in simulation case studies. The case studies with large estimation error were also evaluated using GRSMU, where noise level was low. Xiao et al. (2014) presented a new model-updating method for updating the multi-scale FE model of a long-span bridge. The objective functions for model updating included both modal frequencies and multi-scale influence lines (ILs). The results showed that the differences between the measured and the computed modal frequencies, and between the measured and computed multi-scale ILs were all reduced after using the model-updating method.



The comparison of the additional measured modal frequencies and ILs with the corresponding computed results further confirmed the quality of the model-updating method.

An automated FEMU technique was developed using data obtained from a set of non-destructive tests conducted on a laboratory bridge model, where both stiffness and mass parameters were updated at the element level, simultaneously. This approach was utilized in software packages for automated and systematic FEMU (Sanayei et al. 2015). Updating a structural model is as an optimization problem, where parameters minimize the errors between the model and the actual structure. In optimization, chances of obtaining the multiple solutions are more, and hence finding the global minimum has its own importance. A combination of GA with sequential niche technique was proposed to increase the chance of finding the global minimum that best describes the system (Shabbir and Omenzetter 2016). Testing, modeling and updating of laboratory and bridge structure was carried out, where laboratory structure consists of four columns supporting the stainless plate, and bridge considered was a full scale cable stayed bridge. To obtain FRF, the spectral analysis was carried out. Further the sequential niche technique was applied for updating the numerical space frame structure. Model updating using sequential niche technique in combination with GA yielded with satisfactory results.

Pacini et al. (2017) utilized a computationally efficient modal nonlinear identification technique in FEMU, and experimentally demonstrated the ability to capture typical structural nonlinearity. Gautier et al. (2017) proposed a FE based subspace fitting approach to identify the structural parameters based on the variance analysis for model updating, where the data-related covariance was propagated to the updated model parameters through first-order sensitivity analysis, and vibration signals were used to demonstrate the accuracy and practicability of the method. In recent past, Bayesian techniques have been widely used in FEMU (Boulkaibet et al. 2017). In order to update an FE model, the Bayesian formulation requires the evaluation of the posterior distribution function. For large systems, this function is difficult to solve analytically. In such cases, the use of sampling techniques often provides a good approximation of this posterior distribution function. The hybrid

Monte Carlo method is a classic sampling method used to approximate high-dimensional complex problems.

## **2.2 STRUCTURAL DAMAGE IDENTIFICATION**

The FEMU applications have been extensively utilized in identifying the damage in civil engineering structures and health monitoring of existing bridges. In the past decade, model updating techniques have been extended not only to detect, but also to localize and quantify the structural damage. In the FE model, the damage is represented by a reduction of the stiffness properties of the elements, and by tuning the FE model to the measured modal parameters, the damages can be identified. The most common type of detecting the damages is by visual inspections. However, this method requires skilled labours, and in order to access various key structural load bearing components, dismantling of the ancillary components is must which leads to the consumption of additional time, cost and effort. Further, in case of damages detected in later stages, additional repairs and maintenance operations will become important concerns to rectify the damages.

Wang et al. (2001) developed an algorithm based on static test data and changes in natural frequencies. The method was improved by proper definition of measured and predicted damage signatures. Teughels et al. (2002) proposed a sensitivity-based FEMU method using experimental modal data to assess the damage including localization and quantification, where damage pattern was represented by a reduction factor of the element bending stiffness. Damage functions were used in order to reduce the number of unknown variables. Teughels and Roeck (2004) extended the use of damage functions in order to approximate the stiffness distribution, and optimization was done using the trust region strategy in the implementation of the Gauss–Newton method. The damage in the highway bridge was identified by updating the Young’s modulus and the shear modulus whose distribution over the FE model were approximated by piecewise linear functions. Damage detection based on modal flexibility residuals (i.e., one of the sensitivity based FEMU techniques) was carried out by Jaishi and Ren (2006). For minimization of developed objective function and damage identification, the optimization algorithm was utilized which

also considered the effect of noise. The method was found susceptible to change in the physical properties of the structure. Hence, the method identified the damage location and severity with acceptable accuracy, and the crack pattern in the damaged structure were similar to experimental observations. The complexity of finding the damage in the structure increased when all the elements of FE model became updating parameters in the SDI process. Ding et al. (2017) carried out the SDI based on the modified artificial bee colony (ABC) algorithm using modal data, and compared the method with other evolutionary algorithms.

Fang et al. (2008) investigated a RC frame, which was tested in the laboratory for damage identification using damage parameterization. Further, RSM was adopted by Fang and Perera (2009) to identify the damage. The quantification of structural damage mainly depends on the quality of the damaged model and its ability to describe the structural property changes due to damage in a physical meaningful way (Link and Weiland 2009). Two different model updating techniques were summarized in conjunction with damage identification using multi-model updating: first was based on classical modal residuals by updating undamaged and damaged models simultaneously, and second by updating the models using residuals composed of measured and analytical time histories. The PSO method was utilized in damage identification problems based on multi-objective FE updating procedures by considering modelling errors and its performance was compared with GA (Perera et al. 2010).

Damage identification by RS based model updating using D-optimal design was carried out by Fang and Perera (2011). The advantage of D-optimal design is that, updating of FE model can be done effectively with minimum number of numerical sample when the availability of samples is limited. Before updating, the non-significant parameters are screened out using D-optimal design, and FE models are replaced with first order RS models. These RS models are used to predict the dynamic behaviour of undamaged and damaged structures. The method was applied to a numerical beam, tested RC frame and full scale bridge by considering Young's modulus, section inertia as input parameter and modal frequency was the only output response. An improved PSO algorithm was developed for FEMU using experimentally

obtained natural frequencies by Mohamed et al. (2013), where the inverse diagnostic optimization procedure was adopted to detect and localise the crack in beams using frequency measurements. Additionally, the damages were detected by reducing the number of elements in FE model, where adaptive meshing was used to detect smaller damage cracks in beams. A comparative assessment of the damage identification capability of different DOE methods like  $2^k$  factorial design, central composite design (CCD), Box-Behnken design, D-optimal design and Taguchi's orthogonal array design was carried out by Mukhopadhyay et al. (2015).

A framework for SHM and SDI of civil structures was presented by Ebrahimian et al. (2016), which involves integration of advanced mechanics-based non-linear FE model updating using batch Bayesian estimation approach technique to estimate time-invariant model parameters used in the FE model. Non-linear FEMU was carried out in order to minimize the discrepancies between predicted and measured response time histories by considering excitations as input and dynamic responses as output. The updated FE model was further utilized to identify, localize and quantify the damage and to predict the remaining useful life of the structure. The application of non-linear FEMU method was validated by considering realistic structural FE models of a bridge pier and a moment resisting steel frame.

Single and multiple damage assessment was done for spring mass damper system, a beam and a composite bridge deck. From the comparative study, it was concluded that D-optimal design and CCD are efficient DOE methods for SDI. Sensitivity based parameter screening was done using RSM by  $2^k$  factorial and D-optimal design. The concepts of random sampling high dimensional model representation (RS-HDMR) were utilized to develop damage identification algorithm under the influence of noise, and also for the purpose of parameter screening, a global sensitivity analysis based on RS-HDMR was adopted by Mukhopadhyay et al. (2016). A damage identification methodology based on multivariate adaptive regression splines in conjunction with a multi-objective goal-attainment optimization algorithm was developed for the web core fibre reinforced polymer (FRP) composite bridges, and was validated for several single and multiple damage cases (Mukhopadhyay 2016). Real-time vibration-based structural damage detection using one-dimensional

convolutional neural networks was studied by Abdeljaber et al. (2017). The method adopted performs vibration-based damage detection and localization of the damage in real-time. The advantage of this approach is the ability to extract optimal damage-sensitive features automatically from the raw acceleration signals. A new sensitivity-based damage detection method was proposed to identify and estimate the location and severity of structural damage using incomplete noisy modal data. The accuracy and performance of the sensitivity method were numerically examined by a planar truss by incorporating incomplete noisy modal parameters and FE modeling errors (Entezami et al. 2017). Damage detection using power spectral density of structural response using FEMU approach was investigated both numerically and experimentally which adopts sensitivity based damage detection methodology. The method can be used to detect damages in lower frequency ranges with acceptable accuracy (Pedram et al. 2017). Roy (2017) adopted the vibration-based damage localization technique using mode shape slope and curvature, and formulated the expressions for the derivatives of mode shapes. Damage functions were used in order to reduce the number of unknown variables.

### **2.3 HIGH DIMENSIONAL MODEL REPRESENTATION**

In engineering design, spending excessive amount of time on physical experiments or expensive simulations makes the design costly and lengthy. The severity increases when the design problem has a large number of inputs, or of high dimension. The HDMR is a powerful method in approximating high dimensional, expensive, and black-box problems (Rabitz and Alis 1999). It is a set of quantitative model assessment and analysis tools for improving the efficiency of deducing high dimensional input–output system behaviour stimulated by applications in chemistry. The HDMR is an approximation tool, which expresses the input and output relationships of complex and computationally burdensome models to form a function having hierarchical correlation expansions. A family of nonparametric multivariate approximation functions were developed in order to understand the hierarchy of correlations amongst the input variables (Rabitz et al. 1999). A well-ordered mapping strategy was developed among the inputs and outputs. Alis and Rabitz (2001) assumed that the data was randomly scattered over the entire domain and formulated

HDMR expressions. Their prediction was that the dimensionality of the function was not dependent on the number of samples needed for representation to a given tolerance, which was the efficient means to perform high dimensional interpolation. It was recognised and concluded from the various studies that, only lower order interaction effect between the input variables will have an effective impact upon the output responses of a precise and explicit physical system.

The HDMR can be applied for various well-defined physical systems by making use of this property to develop a specific, ordered mapping between inputs and outputs. The HDMR approximation techniques are very useful in many domains if they can represent the output to good accuracy at sufficiently low orders. Two specific HDMR expansions are developed, i.e., analysis of variance HDMR (ANOVA-HDMR) for statistical applications and second the cut-HDMR expansion. ANOVA-HDMR has its application in statistics which utilize the computation of multidimensional integrals, where cut-HDMR does not necessitate the computation of any integrals to represent the output of a physical system. A rapid convergence in cut-HDMR approximations is found comparable to ANOVA-HDMR where approximation function can be obtained in more efficient manner. In a monomial based preconditioned HDMR method (Li et al. 2001), higher order terms of cut-HDMR expansions are expressed as lower order terms with monomial multipliers. Here additional input-output samples are used, where there is an inadequacy in the approximations given by the first and second order cut-HDMR correlated functions, which avoid the utilisation of higher order terms. The concept of HDMR is used to build simplified and efficient meta-model by replacing the original model which is complex and nonlinear in nature. The inputs may be in the form variables such as initial boundary conditions, control variables as per field data, functions and its parameters and response of the system or solutions would be the output variables (Li et al. 2002). This mathematical assumption can dramatically reduce the sampling effort in representing the multivariate function.

Sobol (2003) investigated mathematical models described by multivariable functions, theorems and examples on model functions with separated variables, and global sensitivity indices for approximations. In the study, the testing of the two

important assumptions in HDMR was done, i.e., a model can be approximated by using arbitrary reference points and fault in approximations caused due incorrect choice of reference points. Theorems and examples related to ANOVA HDMR, finite difference HDMR, model functions with separated variables, and highest order approximations for functions with separated variables were discussed by considering many numerical examples.

Kaya et al. (2004) developed a computer program that computes individual components of HDMR resolution of a given multivariate function, and also calculated the global sensitivity indices. Numerical experiments were considered, where HDMR functions and sensitivity indices were computed, and examined the effect of variables of different sets on the function outputs. In further experiments, the closeness of HDMR approximation with the real functions was estimated. The kernel function was taken as the main part of the developed algorithm where it receives a set of inputs and returns corresponding output value as integrals. The advantage of the algorithm developed was that, it can generate HDMR functions of zeroth order to  $n^{\text{th}}$  order. However, the program can be used for only model where explicit forms are known and models with simple symbolic integration.

For partitioning the given multivariate data into low-variate data, HDMR and generalized high dimensional model representation (GHDMR) methods are utilized. The above two methods worked well when multivariate data was additive in nature, and if multivariate data has multiplicative in nature then factorized high dimensional model representation (FHDMR) can be used. But when the nature of multivariate data and the sought multivariate function will have hybrid nature i.e., neither additive nor multiplicative, hybrid high dimensional model representation (HHDMR) was obtained to get the best value for the hybridity parameter (Tunga and Demiralp 2006). Chowdhury et al. (2008) utilized the technique of HDMR approximation to obtain an equivalent continuous function by replacing univariate or a multivariate piece-wise continuous function. They concluded that the HDMR is a powerful approximation tool to obtain equivalent continuous function from univariate and multivariate piece-wise continuous function even when the original function is characterized with sudden peak and fall in the domain. A dramatic reduction in approximation error can

be found in first order HDMR approximation with increase in number of samples or with utilization of higher order (second) HDMR. And also from this study, it was suggested to use Moving least square (MLS) interpolation scheme rather than Lagrange interpolation, where approximation error can be drastically reduced from MLS. A data partitioning method (Tunga 2011), which chooses the arbitrarily distributed points from the given grid, constructs an approximate analytical structure by interpolation at those chosen points of the grids by utilizing HDMR expansions to partition the given multivariate data. The above method was used to increase the approximation quality particularly for hybrid and purely multiplicative nature structures.

In recent years, the application of HDMR has been extended to uncertainty analysis. When the uncertainties are represented in terms of fuzzy membership functions, analysis of response of the structures is done using HDMR based RS models (Balu and Rao 2012). Implicit and explicit fuzzy analysis procedures are developed using integrated FE modelling and HDMR based RS generation. It was concluded that HDMR approach is mathematically elegant and computationally less expensive for the approximation of fuzzy FE response quantity. In inverse reliability analysis (Balu and Rao 2013), the HDMR is used to get the explicit expressions without requiring the derivatives of the response functions with respect to uncertain variables, and fast fourier transform (FFT) techniques are used to obtain the unknown design parameters. It was concluded that optimum number of sample points in approximating the HDMR component functions was the most important criterion. Moreover, to capture the nonlinearity outside the domain of sample points, very small number of sample points should be avoided during approximation and thereby affecting the estimated solution. Efficient uncertainty analysis was performed for estimating the possibility distribution of structural reliability in presence of mixed uncertain variables (Balu and Rao 2014).

Stochastic free vibration analysis of angle-ply composite plates using RS-HDMR approach has been carried out (Dey et al. 2015) by developing a meta-model to express stochastic natural frequencies of the system, and performance of RS-HDMR has been compared with full-scale Monte Carlo simulation results. An



efficient hybrid method based on RS-HDMR and GA coupled with a local unconstrained multivariable minimization function was investigated by Mukhopadhyay et al. (2015) for optimization of FRP composite web core bridge deck panels. The application of HDMR in stochastic multiscale modelling conjunction with multi-element least square approach was carried out by Jiang and Li (2015). A local least square HDMR was constructed in subdomains which are constructed by adoptive decomposition of randomly chosen main domains. These local HDMRs are represented by a finite number of orthogonal basis functions defined in low-dimensional random spaces, where the coefficients are determined using least square methods. Hence a global approximation HDMR was obtained by summation of all the local HDMR approximations.

An efficient uncertainty quantification scheme for frequency responses of laminated composite plates was investigated by bottom up surrogate based approach using general-high dimensional model representation (GHDMR) for achieving computational efficiency in quantifying uncertainty (Dey et al. 2016). The uncertainty based quantification using GHDMR is applied on laminated composite structure having complex configuration. Effect of noise on quantification of uncertainty of natural frequency was estimated using GHDMR. Convergence study on frequency amplitude was done for combined variation of ply orientation and the method was validated using FEA. A critical comparative assessment has been done by Dey et al. (2017) for different meta-models including polynomial regression, Kriging, D-optimal design, for stochastic natural frequency analysis of composite laminates. It was found that regression based analysis using D-optimal design was proved to be a better technique when there is individual as well as combined variation of parameters. However, the artificial neural network (ANN) was found to be computationally more expensive compared to other meta models. Further in order to construct an efficient HDMR expansion, concept of support vector regression has been adopted by Li et al. (2017) which enables efficient construction of high dimensional models with satisfactory prediction accuracy from a modest number of samples.

## 2.4 SUMMARY OF LITERATURE REVIEW

The SHM is an important process in SDI of civil engineering structures. Various techniques like vibration based and impedance based techniques have their applications in real-time monitoring of engineering structures. Many researchers in the literature have focused on the improvements with respect to the computational efficiency in the damage identification apart from the studies on the utilization of conventional NDE techniques. In the modern analysis of systems in engineering and science, much effort has been invested in developing the complex FE models. The main purpose of such models is to predict the responses of the system to disturbances and the design advantage gained by the modifications in the configurations. But there will be a lack of correlation between predictions and observations due to the inaccuracies in numerical models.

Model updating is concerned with the correction of FE models and it is rapidly developing technology. A number of techniques, as discussed in the literature review, has been developed for model updating including sensitivity based techniques. Further in the past decade, RSM based FEMU technique has become an important tool in place of conventional methods, where response equations are developed with the aid of CCD, and the optimization has been carried out using various optimization techniques (i.e., GA, NN, and PSO). Further, in order to reduce the computational effort of RSM, D-optimal design became popular. In order to increase the computational efficiency, and to reduce the complexity of modeling the real life structures, the FEMU techniques are adopted. Also the FEMU techniques are further utilised to identify the structural damages for various structures including bridges.

The choice of the input and output features of the system to be updated is the key aspect of FEMU process. Initially, before proceeding to the FEMU process, the parameters which affect the output response of the systems are found by parameter screening procedure. From the literature, it was found that, in majority of the case studies the variation of parameters (like the Young's modulus, the second moment of area, and the density) affects the dynamic behaviour of systems, and dynamic response measured is the fundamental natural frequency of the system. Most of the methods are validated by considering the experimental responses as the target results

and thereby updating the FE model by incorporating the predicted values of the parameters obtained using the FEMU techniques. The updated parameters are obtained by optimizing the objective function developed, which is nothing but the difference between the response equations developed by the approximation technique and the experimental results of interest. The FEMU has also been carried out by considering the non-linearity associated with the FE model.

In order to address the severity in the design problems having large inputs or high dimension, an approximation technique called HDMR has been developed to study the input-output relationships of a system under consideration. The concepts of HDMR have been implemented in uncertainty analysis, inverse reliability analysis, and stochastic free vibration analysis and applied to frame and bridge structures.

Hence, the concepts of HDMR have been applied in model updating in the proposed methodology. The FEMU is carried out by considering the simulation studies, and the study is further extended to the SDI. The methodology is validated using case studies from the literature.

## **2.5 OBJECTIVES OF RESEARCH WORK**

Based on the literature review, the objectives of the present research work are as follows.

1. To utilize the concepts of HDMR for the best experimental design of the parameters to be updated, so as to obtain explicit function interrelating the responses and the parameters.
2. To optimize the objective function using genetic algorithm for obtaining the updated parameters.
3. To apply the HDMR based model updating technique in structural damage identification.

## **CHAPTER 3**

### **MODEL UPDATING USING HDMR**

In any physical system, the output/response depends on the input variables. Therefore, it is necessary to learn the input-output mapping for understanding the behaviour of any physical system. The outputs of most physical systems are mathematically well behaved and the scarcity of the data is usually compensated by additional assumptions on the function. The HDMR is a particular family of representations where each term in the representation reflects the individual or cooperative contributions of the inputs upon the output. The main assumption for most well defined physical systems is that the output can be approximated by the sum of these hierarchical functions whose dimensionality is much smaller than the dimensionality of the output. The present investigation is focused on applying concepts of HDMR in FEMU by considering the simulation study.

#### **3.1 HDMR**

The HDMR is an assumed form of mathematical expression in which the higher order correlated effects of the inputs are expected to have negligible effect on the output (Rabitz et al. 1999). This mathematical assumption can dramatically reduce the sampling effort in representing the multivariate function. HDMR has a variety of applications where an efficient representation of multivariate functions arises with scarce data (Alis and Rabitz 2001).

Hence, HDMR is regarded as a general set of quantitative model assessment and analysis tools for capturing the high-dimensional relationships between sets of input and output model variables. It is a very efficient formulation of the system response, if higher order variable correlations are weak, allowing the physical model

to be captured by the first few lower order terms. In HDMR background there stands the simple observation: only low-order correlations amongst the input variables have a significant impact upon the outputs. Such a presumption permits expressing single multi-dimensional mapping as a sum of many low dimensional mappings. Its main advantages are finite order of expansion and rapid convergence for “well-defined” systems. The concepts behind HDMR aim to capitalize on the latter observations that realistic physical systems generally do not call for an exponentially growing number of samples to prescribe their input-output relationships. The HDMR technique can be applied to complex models of nonlinear nature, where an efficient and accurate simplified model to reflect the original model can be developed.

Depending on the method adopted to determine the component of functions of HDMR there are two particular HDMR expansions: ANOVA-HDMR and cut-HDMR. ANOVA-HDMR is useful for measuring the contributions of the variance of individual component functions to the overall variance of the output. On the other hand, cut-HDMR expansion is an exact representation of the output in the hyperplane passing through a reference point in the variable space. Applications of the HDMR tools can dramatically reduce the computational effort needed in representing the input-output relationships of a physical system. HDMR applications include:

- Construction of a computational model directly from laboratory/field data
- Creating an efficient fully equivalent operational model to replace an existing time consuming mathematical model
- Identification of key model variables and their interrelationships
- Assessment of global uncertainties, quantitative risks etc.
- Solving inverse problems
- In the fields of chemical kinetics, radiative transport, materials discovery, molecular physics, statistical analysis, and financial and econometrics

### **3.2 HDMR EXPANSIONS**

The HDMR expansions introduced here are especially useful for the purpose of representing the outputs of a physical system when the number of input variables are

large. The notion of “high” dimensionality is system-dependent, with some situations being considered high for practical reasons at  $N \sim 3-5$ , while others will only reach that level of complexity for  $N \sim 10$  or more. For a high dimensional system, an output  $f(\mathbf{x})$  is commonly a function of many input variables  $\mathbf{x} = \{x_1, x_2, \dots, x_N\}$  with  $n \sim 10^2$  or larger. The HDMR approximations should not be viewed as first- or second-order Taylor series expansions nor do they limit the nonlinearity of  $f(\mathbf{x})$ . Furthermore, the approximations contain contributions from all input variables. Thus, the infinite number of terms in the Taylor series is partitioned into finite different groups, and each group corresponds to one HDMR component function. The HDMR expresses the output as a hierarchical correlated function expansion in terms of the input variables as:

$$f(\mathbf{x}) = f_0 + \sum_{i=1}^N f_i(x_i) + \sum_{1 \leq i \leq j \leq N} f_{ij}(x_i, x_j) + \sum_{1 \leq i \leq j \leq k \leq N} f_{ijk}(x_i, x_j, x_k) + \dots + f_{1,2,\dots,N}(x_1, x_2, \dots, x_N) \quad (3.1)$$

where,  $f_0$  denotes the mean response to  $f(\mathbf{x})$  which is a constant. The function  $f_i(x_i)$  is a first-order term expressing the effect of variable  $x_i$  acting alone, although generally nonlinearly, upon the output  $f(\mathbf{x})$ . The function  $f_{ij}(x_i, x_j)$  is a second-order term that describes the cooperative effects of the variables  $x_i$  and  $x_j$  upon the output  $f(\mathbf{x})$ . The higher order terms give the cooperative effects of increasing numbers of input variables acting together to influence the output. The last term  $f_{1,2,\dots,N}(x_1, x_2, \dots, x_N)$  contains any residual dependence of all the input variables locked together in a cooperative way to influence the output. To determine the component functions in Eq. (3.1), cut-HDMR procedure is used in approximating a univariate or a multivariate piece-wise continuous function with an equivalent continuous function.

Using the cut-HDMR method, first a reference point  $\mathbf{c} = \{c_1, c_2, \dots, c_N\}$  is defined in the variable space. The expansion functions are determined by evaluating the input-output responses of the system relative to the defined reference point  $\mathbf{c}$  along associated lines, planes, sub-volumes, etc. (i.e. cuts) in the input variable space. This process reduces to the following relationship for the component functions in Eq. (3.1):

$$f_0 = f(\mathbf{c}) \quad (3.2)$$

$$f_i(x_i) = f(x_i^j, \mathbf{c}^i) - f_0 \quad (3.3)$$

$$f_{ij}(x_i, x_j) = f(x_i^{j_1}, x_i^{j_2}, \mathbf{c}^{i_1, i_2}) - f_i(x_i) - f_j(x_j) - f_0 \quad (3.4)$$

By evaluating the response quantities at all sample points of each variable including the reference point the following expressions are obtained.

$$f(x_i^j, \mathbf{c}^i) = f(c_1, \dots, c_{i-1}, x_i^j, c_{i+1}, \dots, c_N) \quad (3.5)$$

$$f(x_i^{j_1}, x_i^{j_2}, \mathbf{c}^{i_1, i_2}) = f(c_1, \dots, c_{i_1-1}, x_i^{j_1}, c_{i_1+1}, \dots, c_{i_2-1}, x_i^{j_2}, c_{i_2+1}, \dots, c_N) \quad (3.6)$$

Using the Lagrange interpolation or the moving least squares interpolation yields Eq. (3.7) and Eq. (3.8) for first-order and second-order expressions respectively as follows.

$$f(x_i^j, \mathbf{c}^i) = \sum_{j=1}^N \phi_j(x_i) f(c_1, \dots, c_{i-1}, x_i^j, c_{i+1}, \dots, c_N) \quad (3.7)$$

$$f(x_i^{j_1}, x_i^{j_2}, \mathbf{c}^{i_1, i_2}) = \sum_{j_1=1}^n \sum_{j_2=1}^n \phi_{j_1, j_2}(x_i, x_i) f(c_1, \dots, c_{i_1-1}, x_i^{j_1}, c_{i_1+1}, \dots, c_{i_2-1}, x_i^{j_2}, c_{i_2+1}, \dots, c_N) \quad (3.8)$$

By summing up the interpolated values of HDMR expansion terms from zeroth order to the highest order retained in keeping with the desired accuracy, the first- and second order approximations of the functions are as follows.

$$\tilde{f}(\mathbf{x}) = \sum_{i=1}^N \sum_{j=1}^n \phi_j(x_i) f(c_1, \dots, c_{i-1}, x_i^j, c_{i+1}, \dots, c_N) - (N-1)f_0 \quad (3.9)$$

$$\begin{aligned} \tilde{f}(\mathbf{x}) = & \sum_{\substack{i_1=1, i_2=1, \\ i_1 < i_2}}^N \sum_{j_1=1}^n \sum_{j_2=1}^n \phi_{j_1, j_2}(x_{i_1}, x_{i_2}) f(c_1, \dots, c_{i_1-1}, x_{i_1}^{j_1}, c_{i_1+1}, \dots, c_{i_2-1}, x_{i_2}^{j_2}, c_{i_2+1}, \dots, c_N) \\ & - (N-2) \sum_{i=1}^N \sum_{j=1}^n \phi_j(x_i) f(c_1, \dots, c_{i-1}, x_i^j, c_{i+1}, \dots, c_N) + \frac{(N-1)(N-2)}{2} f_0 \end{aligned} \quad (3.10)$$

The shape/interpolation function  $\phi_j(x_i)$  and  $\phi_{j_1, j_2}(x_{i_1}, x_{i_2})$  using the Lagrange interpolation is defined as:

$$\phi_j(x_i) = \frac{(x_i - x_i^1) \dots (x_i - x_i^{j-1})(x_i - x_i^{j+1}) \dots (x_i - x_i^n)}{(x_i^j - x_i^1) \dots (x_i^j - x_i^{j-1})(x_i^j - x_i^{j+1}) \dots (x_i^j - x_i^n)} \quad (3.11)$$

$$\begin{aligned} \phi_{j_1, j_2}(x_{i_1}, x_{i_2}) &= \frac{(x_{i_1} - x_{i_1}^1) \dots (x_{i_1} - x_{i_1}^{j_1-1})(x_{i_1} - x_{i_1}^{j_1+1}) \dots (x_{i_1} - x_{i_1}^n)}{(x_{i_1}^{j_1} - x_{i_1}^1) \dots (x_{i_1}^{j_1} - x_{i_1}^{j_1-1})(x_{i_1}^{j_1} - x_{i_1}^{j_1+1}) \dots (x_{i_1}^{j_1} - x_{i_1}^n)} \\ &\quad \times \frac{(x_{i_2} - x_{i_2}^1) \dots (x_{i_2} - x_{i_2}^{j_2-1})(x_{i_2} - x_{i_2}^{j_2+1}) \dots (x_{i_2} - x_{i_2}^n)}{(x_{i_2}^{j_2} - x_{i_2}^1) \dots (x_{i_2}^{j_2} - x_{i_2}^{j_2-1})(x_{i_2}^{j_2} - x_{i_2}^{j_2+1}) \dots (x_{i_2}^{j_2} - x_{i_2}^n)} \end{aligned} \quad (3.12)$$

HDMR expressions are obtained by evaluating the component functions in Eq. (3.1), which can be utilized to replace the original, complex, and expensive methods efficiently without compromising with the accuracy of the model. Expression for first-order approximation with uniformly distributed sample points ( $n$ ) given by  $\mu_i - (n-1)\sigma_i/2, \mu_i - (n-3)\sigma_i/2, \dots, \mu_i, \dots, \mu_i + (n-3)\sigma_i/2, \mu_i + (n-1)\sigma_i/2$ , where  $n = 3, 5, 7$  are deployed along the variable axis  $x_i$  with mean ( $\mu_i$ ) and standard deviation ( $\sigma_i$ ) through the reference point. The sampling scheme for first-order HDMR for a function having one variable ( $x$ ) and two variables ( $x_1$  and  $x_2$ ) is shown in Fig. 3.1 (a) and (b), respectively. Similarly, Fig. 3.2 represents sampling scheme for second-order HDMR for a function with two variables.

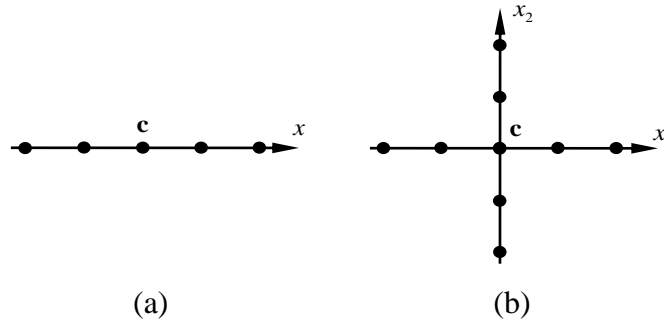


Fig. 3.1. Sampling scheme: First-order HDMR: (a) function with one variable ( $x$ ) and (b) function with two variables ( $x_1$  and  $x_2$ )



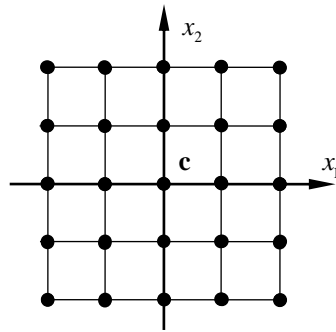


Fig. 3.2. Sampling scheme: Second-order HDMR

### 3.3 MODEL UPDAITNG USING HDMR

This section explains the proposed approach of utilizing the concepts of HDMR in model updating adopted for damage identification. FEMU has been carried out using first order HDMR approximation functions. The HDMR based SDI procedure consists of six steps as presented in Fig. 3.3.

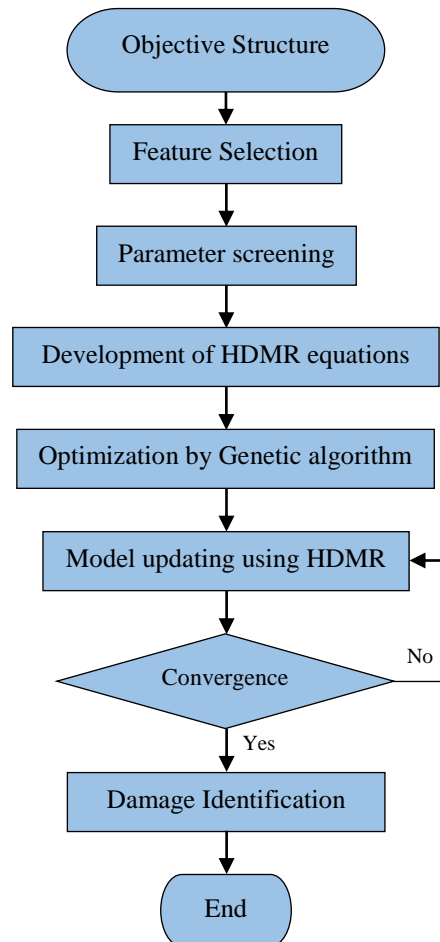


Fig. 3.3 Flow chart of HDMR based model updating and damage identification

In feature selection, the material properties, such as the Young's modulus, the density, and the geometric properties, are usually adopted as the input parameters in model updating. And, for the output features, time and frequency domain features are two feasible options. In parameter screening, non-significant inputs that have least influence on output responses are screened out using regression analysis. Further, HDMR response equations are developed to map the input-output relationships. Objective functions are built using HDMR response equations, which are optimized using GA to obtain the updated parameters. Further the updated FE model is utilized for structural damage identification.

### 3.4 NUMERICAL EXAMPLES

Two numerical examples are considered in order to study the efficiency of HDMR in predicting the updating parameters of interest. Without any physical tests, the damages are assumed at specific locations and response quantities are evaluated for further investigations.

#### 3.4.1 Example 1: Simply Supported Beam

To illustrate the applicability of HDMR technique in FEMU, a simply supported beam (Deng and Cai 2010) is considered for the present simulation study. This example demonstrates how RS generation can be done using proposed HDMR, in conjunction with the GA in order to obtain accurate parameters. The cross section and material property of the beam is assumed to be uniform throughout its length. Three parameters, the Young's modulus ( $E$ ), the density ( $\rho$ ) and the Poisson's ratio ( $\mu$ ) of the material, are chosen as the input parameters. Figure 3.4 shows the beam considered for the present study, which is divided in to 15 elements.

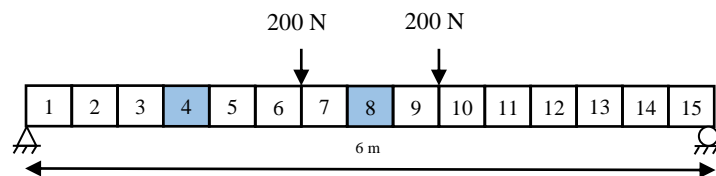


Fig. 3.4 Simply supported concrete beam

The span and cross section of the beam are taken as 6 m and 200 mm × 200 mm respectively. For the simulation study Young's modulus ( $E$ ), density ( $\rho$ ) and Poisson's ratio ( $\mu$ ) are taken as 20 GPa, 2,400 kg/m<sup>3</sup> and 0.2 respectively

For the present case, it is assumed that, elements at location 4 and 8 are damaged. The initial values of  $E$  at two locations (4 and 8) are taken as 20 GPa and  $\rho$  as 2,400 kg/m<sup>3</sup> respectively. Assuming a unit change for each of the three parameters to be 50%, 50%, and 20% of the baseline values respectively, the first three natural frequencies from the modal analysis and the deflection at the bottom of the section near the mid span of the beam from the static test are obtained as responses.

### 3.4.1.1 Response surface generation

For development of approximation equation, number of variable ( $N$ ) for the static test is taken as 3 and number of sample points ( $n$ ) as 3. The function evaluations required for developing first order HDMR approximation equation is  $(n-1)N + 1$ . Hence seven function evaluations are performed using FEA package. Considering first-order HDMR approximation technique:

$$\tilde{f}(\mathbf{x}) = f(x_1, x_2, x_3) = f_0 + \sum_{i=1}^N f_i(x_i) - (N-1)f_0 \quad (3.13)$$

$$\tilde{f}(\mathbf{x}) = f_0 + f_1(x_1) + f_2(x_2) + f_3(x_3) - (N-1)f_0 \quad (3.14)$$

$$f_0 = f(c_1, c_2, c_3) \quad (3.15)$$

$$\tilde{f}(\mathbf{x}) = f(x_1, x_2, x_3) = f(c_1, c_2, c_3) + f_1(x_1) + f_2(x_2) + f_3(x_3) - (N-1)f_0 \quad (3.16)$$

where

$$f(x_i) = f(x_i^j, \mathbf{c}^i) - f_0 \quad (3.17)$$

$$f(x_i^j, \mathbf{c}^i) = \sum_{j=1}^n \phi_j(x_i) f(c_1, \dots, c_{i-1}, x_i^j, c_{i+1}, \dots, c_N) \quad (3.18)$$

Therefore, from Eq. (3.17)

$$\begin{aligned}
f(x_1) &= f(x_1, c^1) \\
&= \phi_1(x_1) \cdot f(x_1^1, c_2, c_3) + \phi_2(x_1) \cdot f(x_1^2, c_2, c_3) \\
&\quad + \phi_3(x_1) \cdot f(x_1^3, c_2, c_3) - f_0
\end{aligned} \tag{3.19}$$

$$\begin{aligned}
f(x_2) &= f(x_2, c^2) \\
&= \phi_1(x_2) \cdot f(c_1, x_2^1, c_3) + \phi_2(x_2) \cdot f(c_1, x_2^2, c_3) \\
&\quad + \phi_3(x_2) \cdot f(c_1, x_2^3, c_3) - f_0
\end{aligned} \tag{3.20}$$

$$\begin{aligned}
f(x_3) &= f(x_3, c^3) \\
&= \phi_1(x_3) \cdot f(c_1, c_2, x_3^1) + \phi_2(x_3) \cdot f(c_1, c_2, x_3^2) \\
&\quad + \phi_3(x_3) \cdot f(c_1, c_2, x_3^3) - f_0
\end{aligned} \tag{3.21}$$

Let  $c_1, c_2, c_3$  be the reference points where output response of the system is evaluated. The values of  $c_1, c_2, c_3$  are taken as 20 GPa, 20 GPa and 2200 kg/m<sup>3</sup> respectively.  $x_1, x_2, x_3$  are the three parameters considered i.e.,  $E$  at two locations (4 and 8), and  $\rho$  of beam respectively, where  $x_1^1, x_1^2, x_1^3$  are three sample points taken as 10 GPa, 20 GPa, 30 GPa respectively. Similarly  $x_2^1, x_2^2, x_2^3 = (10, 20, 30)$  GPa and  $x_3^1, x_3^2, x_3^3 = (1920, 2200, 2880)$  kg/m<sup>3</sup>. Using the above values, the required responses are found out using FEA for the component functions in Eq. (3.18) which constitute the approximation function.

Hence,

$$f(x_1^1, c_2, c_3) = f(10, 20, 2200) = 7.11 \text{ Hz}$$

$$f(x_1^2, c_2, c_3) = f(20, 20, 2200) = 7.32 \text{ Hz}$$

$$f(x_1^3, c_2, c_3) = f(30, 20, 2200) = 7.39 \text{ Hz}$$

$$f(c_1, c_2, c_3) = f(20, 20, 2200) = 7.32 \text{ Hz}$$

Using Lagrange Interpolation function,

$$\phi_1(x_1) = (x_1 - 20)(x_1 - 30) \times 0.005 = 30 - 2.5x_1 + 0.05x_1^2$$

$$\phi_2(x_1) = (x_1 - 10)(x_1 - 30) \times -0.01 = -3 + 0.4x_1 - 0.01x_1^2$$

$$\phi_3(x_1) = (x_1 - 10)(x_1 - 20) \times 0.005 = 0.15 - 0.15x_1 + 0.005x_1^2$$

From Eq. (3.16) and Eq. (3.19),

$$\begin{aligned}\tilde{f}(\mathbf{x}) &= f(x_1, x_2, x_3) \\ &= f(c_1, c_2, c_3) + f_1(x_1) + f_2(x_2) + f_3(x_3) - (N-1)f_0 \\ f(x_1) &= f(x_1, c^1) \\ &= \phi_1(x_1) \cdot f(x_1^1, c_2, c_3) + \phi_2(x_1) \cdot f(x_1^2, c_2, c_3) + \phi_3(x_1) \cdot f(x_1^3, c_2, c_3) - f_0 \\ f(x_1, c_1) &= 192.448 - 15.955x_1 + 0.31875x_1^2\end{aligned}$$

Similarly, all the component functions are obtained using Eq. (3.20) and (3.21) as:

$$\begin{aligned}f(x_2, c_2) &= 185.562 - 15.394x_2 + 0.3082x_2^2 \\ f(x_3, c_3) &= -3.119 - 0.23x_3 - 0.009x_3^2\end{aligned}$$

Substituting the component functions in Eq. (3.19), the expression for first response i.e., first natural frequency ( $Y_1$ ) is obtained as follows.

$$\begin{aligned}Y_1 &= 360.252 - 15.955x_1 - 15.394x_2 - 0.223x_3 + 0.3192x_1^2 \\ &\quad + 0.308x_2^2 - 0.0088x_3^2\end{aligned}\tag{3.22}$$

Similarly using the above procedure, approximation functions for second natural frequency ( $Y_2$ ) third natural frequency ( $Y_3$ ) and the deflection at mid span ( $Y_4$ ) are obtained as follows.

$$\begin{aligned}Y_2 &= 1457.93 - 61.451x_1 - 65.3054x_2 - 1.03054x_3 + 1.2303x_1^2 \\ &\quad + 1.30613x_2^2 + 0.05452x_3^2\end{aligned}\tag{3.23}$$

$$\begin{aligned}Y_3 &= 3215.443 - 141.238x_1 - 138.429x_2 - 3.6532x_3 + 2.8267x_1^2 \\ &\quad + 2.77145x_2^2 + 0.20964x_3^2\end{aligned}\tag{3.24}$$

$$\begin{aligned}Y_4 &= 380.4051 - 15.386x_1 - 17.003x_2 - 4.209346x_3 + 0.3075x_1^2 \\ &\quad + 0.3394x_2^2 + 0.8162x_3^2\end{aligned}\tag{3.25}$$

### 3.4.1.2 Optimization using GA

Since no physical tests are conducted, an assumption has been made that the damage in numerical beam at locations 4 and 8 is due to reduction in  $E$  from 20 GPa to 15 and

12 GPa respectively with an assumed value of  $\rho$  as 2,200 kg/m<sup>3</sup>. The reduction of  $E$  and  $\rho$  at location 4 and 8 are taken as true values. An objective function is then built up which is nothing but the difference between the responses predicted from HDMR approximation function and the true values.

The responses considered for the present simulation case are natural frequencies from the first three modes from modal analysis and deflection at the mid-span of the beam due to application of the static loads, which are found to be 6.954, 28.459, 69.916Hz, and 7.249 mm, respectively. Further, the effect number of HDMR response quantities required to build an objective function for accurately predicting the values of the updating parameters is studied. Four objective functions are built with each function having one to four response quantities, and are shown below.

$$F_{obj}^1 = \sqrt{(Y_1 - 6.954)^2} \quad (3.26)$$

$$F_{obj}^2 = \sqrt{(Y_1 - 6.954)^2 + (Y_4 - 7.249)^2} \quad (3.27)$$

$$F_{obj}^3 = \sqrt{(Y_1 - 6.954)^2 + (Y_2 - 28.459)^2 + (Y_4 - 7.249)^2} \quad (3.28)$$

$$F_{obj}^4 = \sqrt{(Y_1 - 6.954)^2 + (Y_2 - 28.459)^2 + (Y_3 - 69.916)^2 + (Y_4 - 7.249)^2} \quad (3.29)$$

The updated parameters obtained by minimising the all the four objective function with different number of response equations are presented in Table 3.1. Results from Table 3.1 indicate that the number of responses needed in objective function should be at least no less than the number of parameters to be identified. Hence, for  $F_{obj}^4$  case, updated parameters are close to true values. Further the study is extended to utilize HDMR response equations in FEMU.

In order to know the effect of number of sample points on the accuracy of the updated parameters, same simulated beam as shown in Fig. (3.4) is considered and in this case, the responses considered are first four natural frequencies of the beam. Also the efficiency of HDMR is compared with the RSM in terms of difference values with respect to true parameters, and number of function evaluations.

Table 3.1 Identified values of parameters using GA

Objective Function	Identified values		
	Parameters	True Value	HDMR 1st Order
$F_{obj}^1$	$x_1$ (GPa)	15	18.98
	$x_2$ (GPa)	12	15.46
	$x_3$ ( $10^3$ kg/m <sup>3</sup> )	2.2	2.57
$F_{obj}^2$	$x_1$ (GPa)	15	15.52
	$x_2$ (GPa)	12	19.29
	$x_3$ ( $10^3$ kg/m <sup>3</sup> )	2.2	2.3
$F_{obj}^3$	$x_1$ (GPa)	15	14.31
	$x_2$ (GPa)	12	21.5
	$x_3$ ( $10^3$ kg/m <sup>3</sup> )	2.2	2.48
$F_{obj}^4$	$x_1$ (GPa)	15	15.94
	$x_2$ (GPa)	12	11.55
	$x_3$ ( $10^3$ kg/m <sup>3</sup> )	2.2	2.65

Before proceeding to RS generation, a three factor CCD with 18 trials (i.e., eight corner points, six star points and four replicates at centre points) are utilized to perform the simulation study (Deng and Cai 2010). Parameter screening has been carried out using regression analysis to find the percentage contribution of each parameter to the total variance of the output. From the initial values, the parameter bounds ( $\pm 1$ ) are fixed to  $\pm 30\%$ . Frequencies from the first four modes is evaluated using numerical simulations, and screening results are presented in Fig. 3.5. From the screening results, the values of  $E$  and  $\rho$  are considered for further investigation, and  $\mu$  is screened out as it has zero contribution towards the total variance.

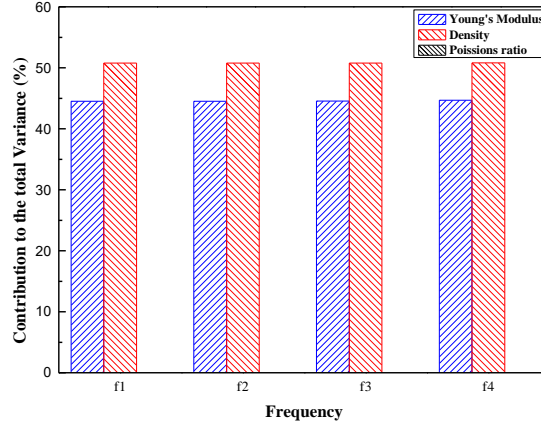


Fig. 3.5 Parameter screening results

Based on the assumption that the beam is damaged at element locations 4 and 8, the true values are as follows.  $E_4 = 15$  GPa,  $E_8 = 12$  GPa and  $\rho_{4,8} = 2200$  kg/m<sup>3</sup>. Further in order to obtain the true values of the parameters ( $E_4$ ,  $E_8$  and  $\rho_{4,8}$ ), the concept of model updating using HDMR is applied to the numerical beam. Let  $c_1, c_2, c_3$  be the reference points where output response of the system is evaluated. The values of  $c_1, c_2, c_3$  are taken as 20 GPa, 20 GPa and 2200 kg/m<sup>3</sup> respectively. The beam is updated by considering different number of sample points (ie,  $n = 3, 5 \& 7$ ). The HDMR approximation equations for first four natural frequencies are developed. Then an objective function which is the difference between the responses obtained (natural frequencies: 6.951 Hz, 10.771 Hz, 28.415 Hz and 35.667 Hz) based on the true parameter values ( $E_4 = 15$  GPa,  $E_8 = 12$  GPa and  $\rho_{4,8} = 2200$  kg/m<sup>3</sup>) and the HDMR response equations. Table 3.2 shows the responses obtained from function evaluations.

$$F_{obj} = \sqrt{(Y_1 - 6.951)^2 + (Y_2 - 10.771)^2 + (Y_3 - 28.415)^2 + (Y_4 - 35.667)^2} \quad (3.30)$$

where  $Y_1, Y_2, Y_3$  and  $Y_4$  denote the HDMR response equations, for first four natural frequencies.

The objective function developed in Eq. (3.30) is optimized using GA by defining the lower and upper bounds of three parameters ( $E_4$ ,  $E_8$  and  $\rho_{4,8}$ ) as [10 GPa, 10 GPa, 1920 kg/m<sup>3</sup>] and [30 GPa, 30 GPa, 2880 kg/m<sup>3</sup>] respectively. Numerical beam is



investigated by updating the model for  $n = 3, 5 \& 7$  in order to minimize the errors of all the parameters. The sample points for  $n = 3, 5 \& 7$  considered are within the parameter bounds. Results obtained for all the sample points are compared with RSM (Deng and Cai 2010).

Table 3.2 Responses for development of HDMR expression (Beam example)

$f(c_1, \dots, c_{i-1}, x_i^j, c_{i+1}, \dots, c_N)$	$f_1$ (Hz)	$f_2$ (Hz)	$f_3$ (Hz)	$f_4$ (Hz)
$f(10, 20, 2400)$	7.04	10.84	27.24	34.49
$f(13.33, 20, 2400)$	7.15	11.07	28.00	35.40
$f(16.66, 20, 2400)$	7.21	11.22	28.51	36.02
$f(20, 20, 2400)$	7.25	11.32	28.87	36.47
$f(23.33, 20, 2400)$	7.28	11.40	29.14	36.81
$f(26.66, 20, 2400)$	7.31	11.47	29.35	37.08
$f(30, 20, 2400)$	7.33	11.50	29.52	37.29
$f(20, 10, 2400)$	6.82	10.61	28.82	36.06
$f(20, 13.33, 2400)$	7.02	10.95	28.85	36.26
$f(20, 16.66, 2400)$	7.16	11.17	28.86	36.38
$f(20, 23.33, 2400)$	7.32	11.44	28.88	36.54
$f(20, 26.66, 2400)$	7.38	11.52	28.89	36.59
$f(20, 30, 2400)$	7.42	11.59	28.90	36.63
$f(20, 20, 1920)$	7.40	11.52	29.26	37.03
$f(20, 20, 2080)$	7.35	11.45	29.13	36.84
$f(20, 20, 2240)$	7.30	11.33	29.00	36.65
$f(20, 20, 2560)$	7.21	11.26	28.75	36.29
$f(20, 20, 2720)$	7.16	11.20	28.62	36.11
$f(20, 20, 2880)$	7.12	11.14	28.50	35.93

Table 3.3 presents the variation of values obtained using HDMR, and the second- and third-order RSM (Deng and Cai 2010). The model updating using HDMR with  $n = 5$  results in less absolute error of 0.5%, 1.71% and 0.07% for  $E_4$ ,

$E_8$  and  $\rho_{4,8}$  respectively, which is more accurate than the results reported using conventional RSM (Deng and Cai 2010). Also, the computational effort is calculated in terms of number function evaluations required for construction of the functions.

Table 3.3 Variation of values (Error percentage) for Beam

Variables	True Values	% Error				
		RSM (Deng and Cai 2010)		HDMR		
		Second order	Third order	$n=3$	$n=5$	$n=7$
$E_4$ (GPa)	15	5.99	2.22	3.59	0.50	0.45
$E_8$ (GPa)	12	13.31	0.55	4.7	1.71	1.70
$\rho_{4,8}$ (kg/m <sup>3</sup> )	2200	0.55	0.91	0.19	0.07	0.06

Table 3.4 presents the number of function evaluations required for RSM and HDMR methods. The conventional RSM requires 18 function evaluations whereas the HDMR requires only 7 function evaluations, and provides more accurate prediction than the RSM. In the proposed work, number of sample points in an axis considered for evaluation is increased to investigate the parametric study.

Table 3.4 Computational effort (Beam Example)

	RSM (Deng and Cai 2010)		HDMR		
	Second Order	Third Order	$n = 3$	$n = 5$	$n = 7$
# Fn. Evaluations	18	18	7	13	19

It is observed that the increase in number of sample points results in more accurate prediction of results. However, a little more computational effort is required which is still less than the RSM. Therefore, the proposed approach is able to obtain the accurate parameters with less computational effort.

### 3.4.2 Example 2: Reinforced Concrete Box Culvert

The concept of HDMR based model updating has been applied for an existing RC box culvert located at Surathkal, India. Over the RC box culvert a four lane highway traffic flow is present which is along the length of the culvert. The RC box culvert has an expansion joint, hence two box culvert structures are present, each providing a path

for traffic traveling in one direction. Hence only one box culvert is considered for the present investigation. The RC box culvert structure under study has a total width of 54 m, where expansion joint is located a 27 m and length of each span measures 6 m, and both the thickness of deck slab and RC wall are 0.8 m. Based on the configuration of the box culvert, a numerical model was created using a commercial FE software. A fixed boundary condition has been assigned between RC slab and vertical wall system. Similar to the simply supported beam study, the box culvert is assumed to have damages or stiffness changes due to moving load of the vehicle at two locations, (location A and location B) one at the middle of first span and second at the corner of the second span as shown in Fig. 3.6. Three parameters are considered as variables i.e., Young's modulus of concrete at location A ( $E_A$ ), Young's modulus of concrete at location B ( $E_B$ ) and the density of concrete at two locations ( $\rho_{A,B}$ ).

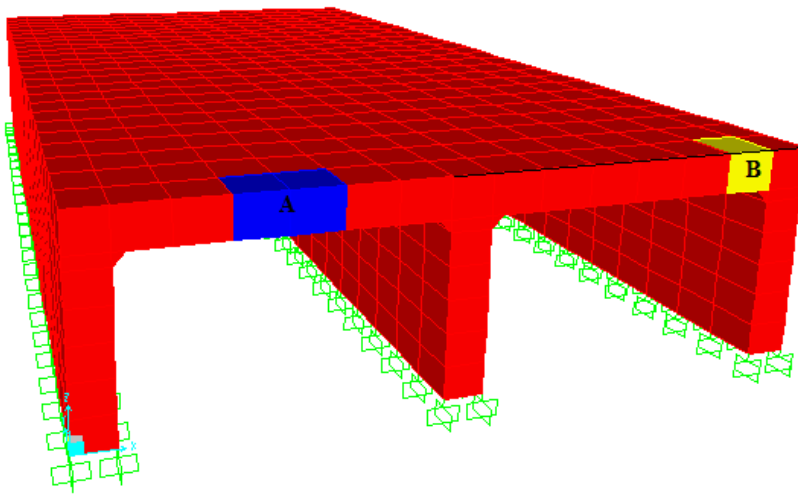


Fig. 3.6 Finite element model of RC box culvert

For the simulation study, the values of  $E$ ,  $\mu$ , and  $\rho$  are taken as 30 GPa, 0.2, and 2,500 kg/m<sup>3</sup> respectively. Truck loadings are considered as per IRC: 3-1983 and type of vehicle considered is Type 3-S2. Let  $c_1, c_2, c_3$  be the reference point (30 GPa, 30 GPa, 2500 kg/m<sup>3</sup>) where output responses of the system is evaluated. It is assumed that damages have occurred at location A and location B, and the true values for the  $E$  at two locations are taken as 25 GPa and 22 GPa. The true value for  $\rho$  is taken as 2,300 kg/m<sup>3</sup>.

The expressions for first, second and third natural frequencies are developed using first-order HDMR as follows.

$$\begin{aligned}
Y_1 = & 3.97 \times 10^{-5} x_1^6 - 6.22 \times 10^{-10} x_2^6 + 2.35 \times 10^{-30} x_3^6 - 0.069 x_1^5 + 1.133 \times 10^{-7} x_2^5 \\
& + 5.832 \times 10^{-20} x_3^5 + 0.468 x_1^4 - 8.388 \times 10^{-6} x_2^4 - 7.29 \times 10^{-16} x_3^4 - 17.8 x_1^3 \\
& + 3.22 \times 10^{-4} x_2^3 + 3.62 \times 10^{-12} x_3^3 + 356.63 x_1^2 - 0.0068 x_2^2 - 8.97 \times 10^{-9} x_3^2 \\
& - 3701.3 x_1 + 0.0749 x_2 - 1.896 \times 10^{-5} x_3 + 15563
\end{aligned} \quad (3.31)$$

$$\begin{aligned}
Y_2 = & 6.76 \times 10^{-5} x_1^6 - 1.51 \times 10^{-9} x_2^6 + 1.03 \times 10^{-18} x_3^6 - 0.011 x_1^5 - 2.76 \times 10^{-7} x_2^5 \\
& - 1.55 \times 10^{-14} x_3^5 + 0.827 x_1^4 + 2.04 \times 10^{-5} x_2^4 + 9.68 \times 10^{-11} x_3^4 - 30.27 x_1^3 \\
& - 7.88 \times 10^{-4} x_2^3 - 3.20 \times 10^{-7} x_3^3 + 606.19 x_1^2 + 0.0165 x_2^2 + 5.94 \times 10^{-4} x_3^2 \\
& - 6291.4 x_1 - 0.178 x_2 - 0.585 x_3 + 26694
\end{aligned} \quad (3.32)$$

$$\begin{aligned}
Y_3 = & 8.47 \times 10^{-5} x_1^6 + 3.88 \times 10^{-19} x_2^6 - 0.0147 x_1^5 - 8.00 \times 10^{-9} x_2^5 \\
& - 5.899 \times 10^{-15} x_3^5 + 1.036 x_1^4 + 1.266 \times 10^{-6} x_2^4 + 3.711 \times 10^{-11} x_3^4 \\
& - 37.91 x_1^3 - 7.83 \times 10^{-5} x_2^3 - 1.23 \times 10^{-7} x_3^3 + 759.163 x_1^2 + 0.0023 x_2^2 \\
& + 2.31 \times 10^{-4} x_3^2 - 7878.9 x_1 - 0.0331 x_2 - 0.2302 x_3 + 33224
\end{aligned} \quad (3.33)$$

The HDMR functions are developed for deflection at the center of each span ( $Y_4$  and  $Y_5$ ). Deflections are taken on the upper portion of the concrete slab where moving loads are considered. The response functions for deflection at center of the first span are developed using first-order HDMR as follows.

$$\begin{aligned}
Y_4 = & 8.390 \times 10^{-8} x_1^6 + 5.333 \times 10^{-33} x_2^6 - 1.456 \times 10^{-5} x_1^5 - 8.094 \times 10^{-29} x_2^5 \\
& + 0.001 x_1^4 + 5.101 \times 10^{-25} x_2^4 - 0.0375 x_1^3 - 1.708 \times 10^{-21} x_2^3 + 0.7518 x_1^2 \\
& + 3.207 \times 10^{-18} x_2^2 - 7.803 x_1 - 3.199 \times 10^{-15} x_2 + 32.834
\end{aligned} \quad (3.34)$$

$$\begin{aligned}
Y_5 = & 9.165 \times 10^{-8} x_1^6 - 1.777 \times 10^{-11} x_2^6 + 5.421 \times 10^{-33} x_3^6 - 1.590 \times 10^{-5} x_1^5 \\
& + 3.466 \times 10^{-9} x_2^5 - 8.228 \times 10^{-29} x_3^5 + 0.001 x_1^4 - 2.711 \times 10^{-7} x_2^4 \\
& + 5.186 \times 10^{-25} x_3^4 - 0.041 x_1^3 - 1.083 \times 10^{-5} x_2^3 - 1.737 \times 10^{-21} x_3^3 \\
& + 0.821 x_1^2 - 2.312 \times 10^{-4} x_2^2 + 3.260 \times 10^{-18} x_3^2 - 8.524 x_1 + 0.002 x_2 \\
& - 3.252 \times 10^{-15} x_3 + 35.834
\end{aligned} \quad (3.35)$$

The HDMR approximation equations for five responses are developed i.e., first three natural frequencies and deflection at the center of two spans of box culvert. Then an objective function is developed which is the difference between the responses obtained (21.319 Hz, 36.251 Hz, 45.328 Hz, 0.159 mm, 0.157 mm) based on the true

parameter values ( $E_A, E_B$  and  $\rho_{A,B}$ ), and the HDMR response equations. The objective function is as shown in Eq. (3.36):

$$F_{obj} = \sqrt{(Y_1 - 23.319)^2 + (Y_2 - 36.251)^2 + (Y_3 - 45.328)^2 + (Y_4 - 0.159)^2 + (Y_5 - 0.157)^2} \quad (3.36)$$

where  $Y_1, Y_2$  and  $Y_3$  denote the first three natural frequencies of the bridge,  $Y_4$  denotes deflection at center of first span, and  $Y_5$  denotes the deflection at center of second span obtained using HDMR.

The objective function developed in Eq. (3.36) is optimized using the GA by defining the lower and upper bounds as [30 GPa, 30 GPa, 2500 kg/m<sup>3</sup>] and [45 GPa, 45 GPa, 3000 kg/m<sup>3</sup>] respectively. The predicted values and the percentage variation of true values of  $E_A, E_B$  and  $\rho_{A,B}$  for  $n = 3, 5 \& 7$  are presented in Table 3.5.

The values of absolute errors diminish when sample points ( $n$ ) are increased from  $n = 3$  to  $n = 5$  and converges at sample point  $n = 7$ . It is observed that for  $n = 7$ , the error with respect to  $\rho_{A,B}$  is only 0.26% while for  $E_A$  and  $E_B$ , it is around 2.63% and 2.21% respectively. Since there is no significant improvement in reduction of percentage error between  $n = 5$  and  $n = 7$ , the optimum number of sample points is considered as 5. The function evaluations required for the HDMR functions are 7, 13 and 19 for  $n = 3, 5 \& 7$  respectively. It is observed that the increase in the number of sample points results in more accurate prediction of results, but with a little more computational effort.

Table 3.5 Variation of values (Error percentage) for Box-culvert

Variables	True Values	% Error		
		$n = 3$	$n = 5$	$n = 7$
$E_A$ (GPa)	25	35.88	2.64	2.63
$E_B$ (GPa)	22	6.16	2.32	2.21
$\rho_{A,B}$ (kg/m <sup>3</sup> )	2300	13.04	0.28	0.26

In order to make the parameters in Eq. (3.36) dimensionless, the normalization procedure is tested. Since the identified parameters are insensitive to the normalization procedure, the results are not presented. Therefore, the methodology proposed is suitable for accurate prediction of parameters for model update, and the method is computationally efficient. Hence the HDMR based FEMU is further employed in SDI.

### **3.5 SUMMARY**

The concept of HDMR is applied to update the FE model in order to obtain the accurate parameters. Two numerical simulations (a simulated simply supported beam and an existing RC box culvert) have been carried out. In the numerical simulations, damages are assumed at particular locations due to reduction of stiffness. From the simulation study, the applicability of HDMR in FEMU has been studied by conducting a parametric study with respect to number of sample points. And the results of the proposed method are compared with conventional RSM.



## CHAPTER 4

# STRUCTURAL DAMAGE IDENTIFICATION USING HDMR

In order to validate the proposed methodology, HDMR based FEMU is applied to find out the damage pattern, location and severity. Unlike numerical beam examples, the damages are not known in advance, while updating FE model of the real structures. Hence, it is interesting to solve the case-study example with respect to identification of the damage location, which defines the objective of the problem as shown in Fig. 3.2. Three case studies have been considered in this work to validate the proposed methodology. The damage pattern, location and severity are correlated with the experimental investigations from the literature.

### 4.1 SIMULATION STUDY: SIMPLY SUPPORTED BEAM

In this simulation study, selected elements of the simply supported beam are assumed to have damage at three locations, and rest of the beam was considered with no damage elements (Jaishi and Ren 2006). The density ( $\rho$ ) and Young's modulus ( $E$ ) of the concrete are  $2500 \text{ kg/m}^3$  and  $3.2\text{e}+10 \text{ N/m}^2$ , respectively. Size of the beam considered is  $250 \text{ mm} \times 200 \text{ mm}$  as shown in Fig. 4.1. Modal analysis is performed by using FEA package for both damaged and undamaged beam. Damages are assumed by reducing the  $E$  of the three elements (3, 8 & 10) by 20%, 50% and 30% respectively.

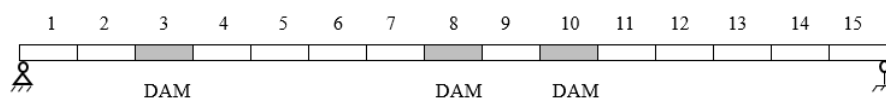


Fig. 4.1 A simulated simply supported beam



To develop the response equations using HDMR, the elastic modulus is considered as variable, and elastic moduli of the 15 elements of the beam are considered as updating parameters ( $x_1$  to  $x_{15}$ ). The first ten fundamental natural frequencies are considered as output responses. The objective of the proposed methodology is to find out the damage location and severity by updating the undamaged beam by considering the first order approximation equation with number of variables,  $N=15$  and sample points  $n=3,5 \& 7$ . Using the above values, responses are found out for functions using FEA for all the three parameters to constitute the component functions of HDMR.

Let  $c_1$  to  $c_{15}$  be the reference point, where output response of the system is evaluated and taken as 32 GPa. The lower and upper bounds considered for  $E$  are 16 GPa and 48 GPa respectively and sample point for  $n=3,5, \& 7$  are taken within the parameter bounds. The HDMR expressions are developed for first ten natural frequencies and objective function can be written as follows:

$$F_{obj} = \sqrt{\begin{aligned} &(Y_1 - 8.25)^2 + (Y_2 - 34.85)^2 + (Y_3 - 74.68)^2 + (Y_4 - 135.43)^2 \\ &+ (Y_5 - 141.06)^2 + (Y_6 - 204.69)^2 + (Y_7 - 298.58)^2 \\ &+ (Y_8 - 386.98)^2 + (Y_9 - 417.32)^2 + (Y_{10} - 494.62)^2 \end{aligned}} \quad (4.1)$$

where,  $Y_1$  to  $Y_{10}$  denote the first ten natural frequencies of the beam obtained using HDMR. Objective function developed in Eq. (4.1) is optimized using the GA. Table 4.1 shows the initial frequencies of undamaged and damaged beam where frequencies of damaged beam are taken as true values.

The beam is updated first by considering three sample points ( $n=3$ ). It is found that, after FEMU, the frequency values are close to damage state model with the maximum difference of 5.92% in mode 1 (Fig. 4.2).

Table 4.1 Initial frequencies of FE model: Simulated beam

Mode	Undamaged beam (Hz)	Damaged beam (Hz)	Difference in frequencies (%)
1	9.00	8.26	8.22
2	35.86	34.84	2.84
3	80.13	74.69	6.78
4	141.03	135.43	3.97
5	149.00	141.06	5.32
6	217.39	204.69	5.84
7	307.52	298.58	2.90
8	409.13	386.98	5.41
9	445.38	417.32	6.30
10	519.16	494.62	4.72

Figure 4.2 indicates the variation of percentage frequencies with respect to damaged beam frequencies in ten modes after model updating for  $n = 3$  and the results show the reduction in percentage difference after updating. However, the values are slightly high, and it requires further refinement of parameter values. Also from Fig. 4.3, the prediction of damage location and severity is found to be less accurate, since percentage damage at location 3, 8 and 10 are found to be 5.3%, 26.9% and 4.1% respectively, which less than the assumed damage percentage. Hence the HDMR based model updating is carried out for  $n = 5$ .

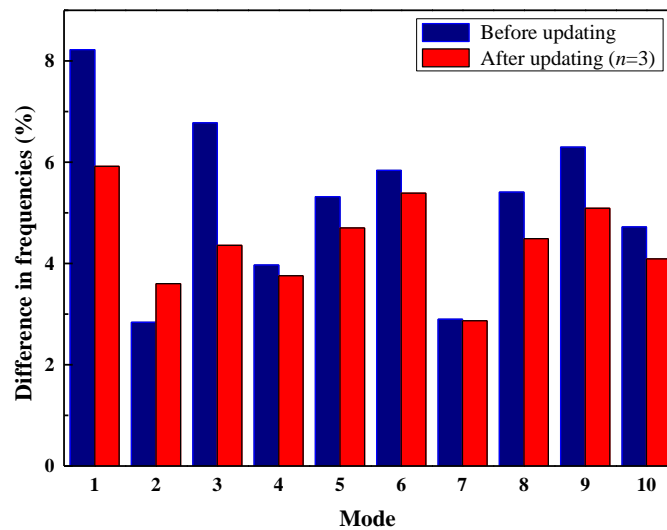


Fig. 4.2 Difference in frequencies after model updating ( $n = 3$ )

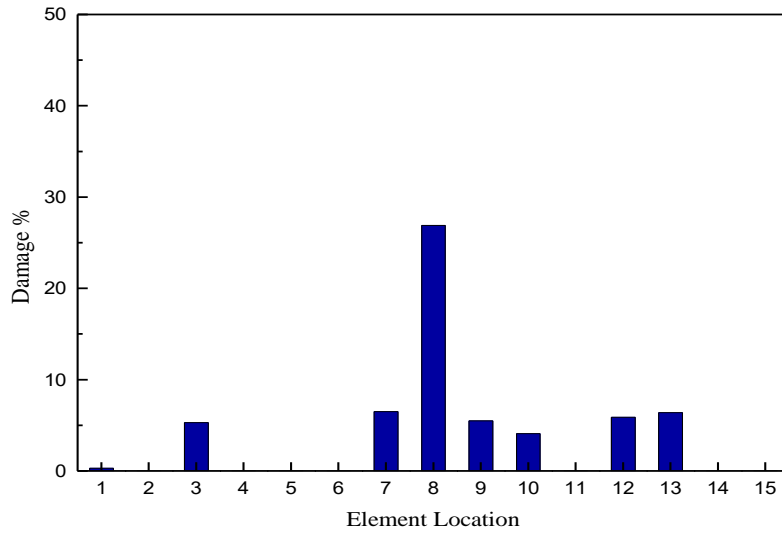


Fig. 4.3 Identified damage locations and stiffness distribution ( $n = 3$ )

When number of sample points is increased from 3 to 5, significant improvement in the predicted frequencies are found, since reduction of difference in frequencies is witnessed from 5.92% for  $n = 3$  (Fig. 4.2) to 0.48% for  $n = 5$  (Fig. 4.4) in mode 1, and also in other modes. Also improvement in prediction of damage location is observed. The variation of difference in frequencies after updating, using  $n = 5$  is presented in Fig. 4.4, which shows a good agreement with the true responses in the damaged beam.

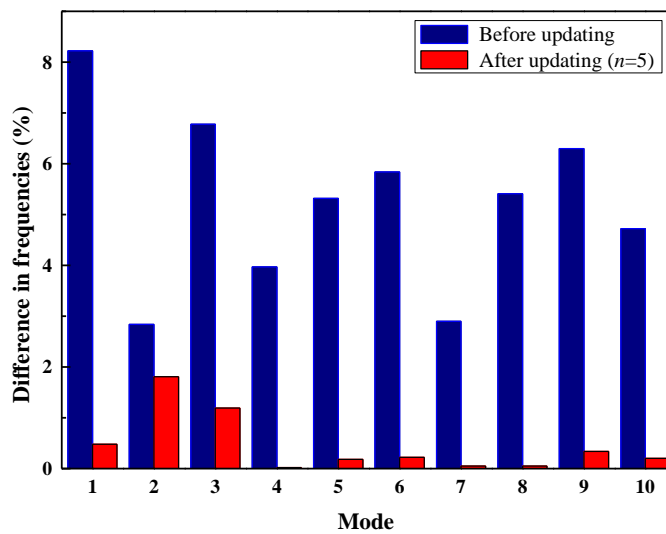


Fig. 4.4 Difference in frequencies after model updating ( $n = 5$ )

Results obtained by updating the value of  $E$  of the 15 beam elements using five sample points are presented in Table 4.2.

Table 4.2 Updated frequencies of simulated beam ( $n = 5$ )

Mode	Before updating (Hz)	Damaged beam (Hz)	After updating (Hz)	Difference in frequencies (%)
1	9.00	8.26	8.22	0.48
2	35.86	34.84	34.21	1.81
3	80.13	74.69	75.58	1.19
4	141.03	135.43	135.47	0.02
5	149.00	141.06	141.32	0.18
6	217.39	204.69	204.22	0.22
7	307.52	298.58	298.41	0.05
8	409.13	386.98	387.19	0.05
9	445.38	417.32	418.76	0.34
10	519.16	494.62	495.62	0.20

Figure 4.5 indicates that the damage has been located at element 3, 8 and 10 with the damage percentage of 31% 45% and 34% respectively. Values of damages have appeared on the undamaged elements i.e., 5, 11 and 12, damage is found to be 13% and for element location 6 and 15 it is found to be 6% and 9% respectively.

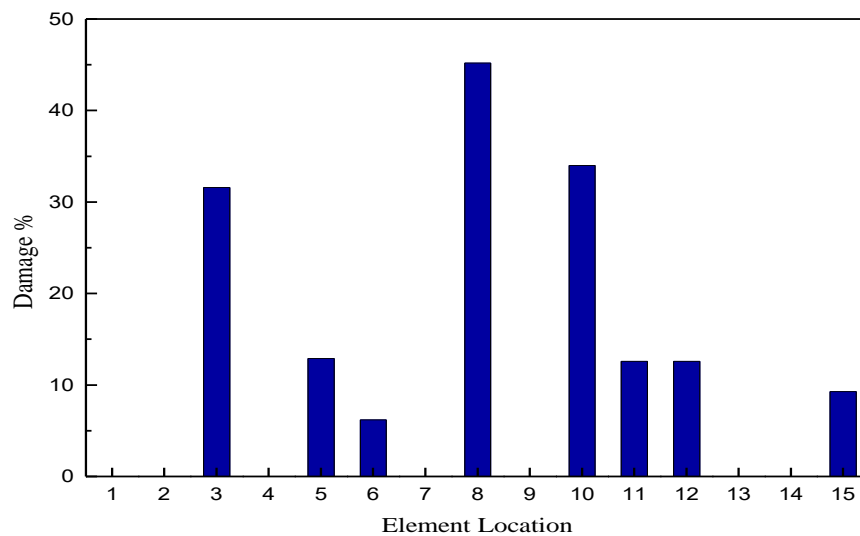


Fig. 4.5 Identified damage locations and stiffness distribution ( $n = 5$ )

Even though the damage percentage in three elements are higher than the assumed ones, the results are acceptable due to a significant reduction in the differences observed in frequencies. Hence the updated FE model is able to predict the responses with good accuracy with the difference in frequencies less than 0.5%, except for mode 2 and 3 which is found to be 1.81% and 1.19% respectively as shown in Table 4.2. From the parametric study, it is found that, increase in number of sample points yields better responses with lesser percentage difference in frequencies in comparison with damaged beam frequencies. Hence after updating, the average difference between the experimental and numerical frequencies decreases from 4.42% (Fig. 4.2) to 0.45% (Table 4.2) with the increase in sample points from  $n=3$  to 5 respectively. Similar study is extended to update the model for finding the damage locations and severity using  $n=7$ . As the obtained results for  $n=7$  do not exhibit any remarkable changes in the percentage of difference in frequencies compared with  $n=5$ , considering the efficiency with respect to computational effort as crucial, the higher number of sample points is not reported in this work. Hence optimum number of sample points for better prediction of true response is taken as  $n=5$ .

## 4.2 CASE STUDY 1: EXPERIMENTAL BEAM

The cross section of the RC beam tested in laboratory (Jaishi and Ren 2006) is shown in Fig. 4.6. The RC beam consists of three 16 mm diameter bars provided on tension and compression sides with 1.4% of reinforcement ratio. Two legged stirrups of 8 mm diameter with 200 mm centre to centre is provided as shear reinforcement along the length of the beam. The beam is with a mass of 750 kg and  $\rho$  value of 2500 kg/m<sup>3</sup>. Two point symmetric loading has been applied which are at distance of 2 m.

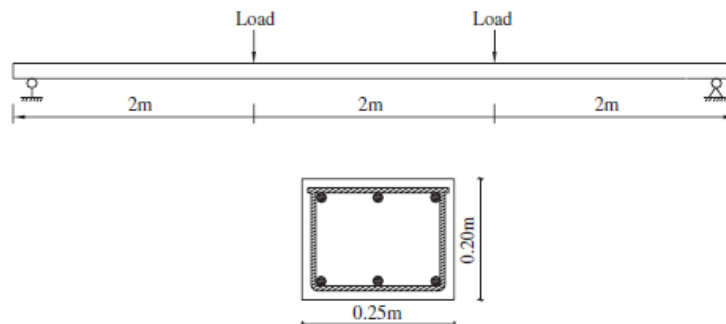


Fig. 4.6 Beam cross section and with two point loading (Jaishi and Ren 2006)

Damages at regular intervals are introduced into the beam by a six-step static load arrangement (Fig. 4.7). Dynamic measurements are recorded after each loading intervals to get the dynamic responses of the beam at different damage conditions. The magnitude of the loads applied during each load step is given in Table 4.3.

Table 4.3 Six step static load magnitude

Load Step No.	1	2	3	4	5	6
Load (kN)	4.0	6.0	12.0	18.0	24.0	26.0

In the test setup, first for simply supported beam a static load is applied at two locations and after successive damage the static load is removed. Then beam was rested on flexible springs in order to eliminate the effect of inadequate support conditions on dynamic characteristics (modal frequencies). A non measured dynamic input in the form of impulses was created and supplied to the beam resting on flexible springs. With the said test procedure, initially the modal frequencies are recorded for simply supported beam without having damage, which was called as initial state of the beam. Before FE model updating, the responses from the initial state of the beam is considered to build the reference state FE model. Similar tests are carried out for all the static load steps and dynamic measurements are done. The dynamic responses from 5<sup>th</sup> load step are considered for updating the reference state model in order to obtain the final damage state FE model. For updating process, the test beam is analytically modelled with 30 beam elements using commercial FEA software.

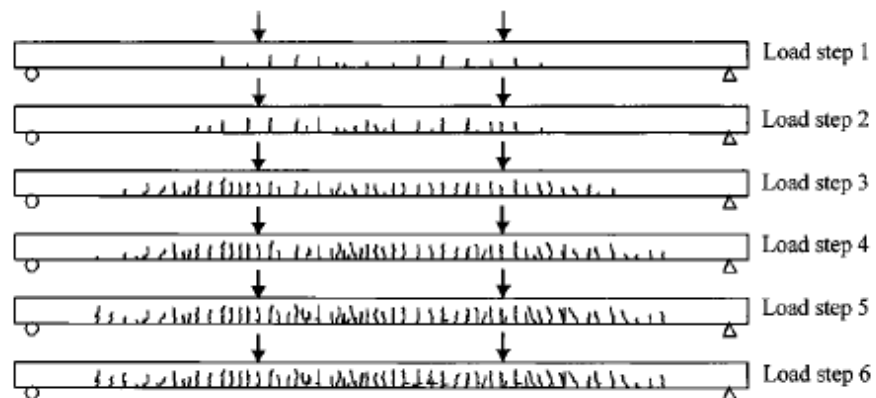


Fig. 4.7 Crack pattern at each load steps (Jaishi and Ren 2006)

The modulus of elasticity ( $E$ ) of 38 GPa and second moment of area ( $I$ ) of  $66 \times 10^{-4} \text{m}^4$  as material and inertial properties are considered in the original FE model respectively. The  $E$  of all the 30 elements of numerical model is used as updating parameters ( $N=30$ ). Acceptable bounds are considered for all the parameters and HDMR response equations are used to develop the objective function. The function is minimized using GA to obtain the updated values of  $E$ . In this case study  $x_1 - x_{30}$  are the 30 parameters considered which are the elastic modulus of individual elements of FE model. The values of the reference points ( $c_1 - c_{30}$ ) is taken as 38 GPa for evaluating the output response of the system. Sample points for  $n=3$  are 22, 38, 54 GPa, and similarly the sample points for  $n=5$  are 22, 30, 38, 46, 54 GPa. The spacing between the two sample points in an axis is maintained as constant.

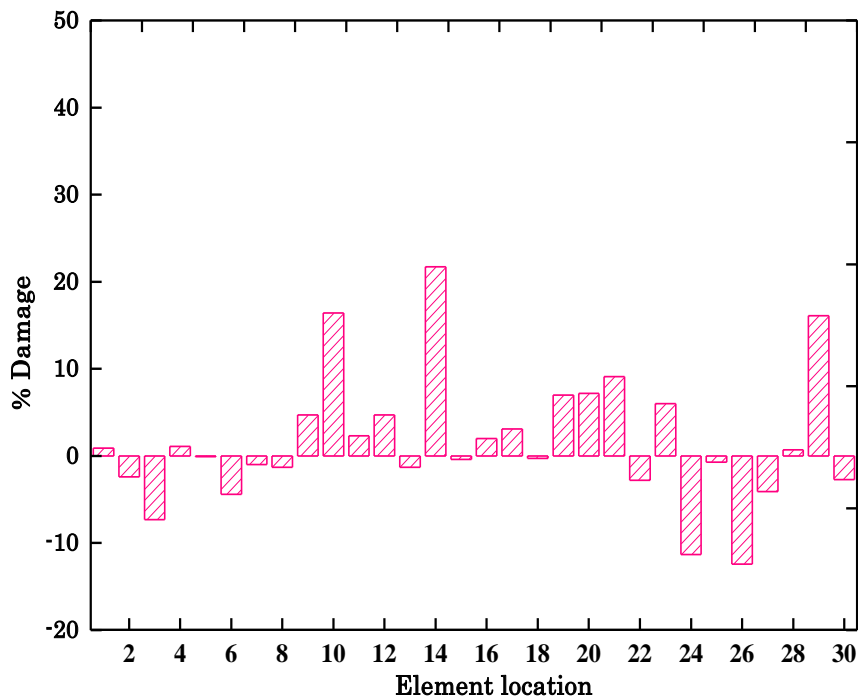


Fig. 4.8 Stiffness distribution: Reference state model (After updating:  $n = 3$ )

The model updating procedure is first implemented for  $n=3$ . The HDMR response equations are developed for first four modal frequencies. Once HDMR response equations are developed, the objective function is built up and the same is optimized using GA. From Fig. 4.8, it is observed that the reference state model has several damages at different location at the mid span of the beam between element 10,

14 and 21 and damage percentage is found to be high with the values of 16.4%, 21.7% and 9% respectively.

Moreover, the damage at support is detected about 16% in element 29 and which needs further refinement. Hence study is extended to  $n=5$ . The SDI based on HDMR is carried out for  $n=5$  in order to obtain a better reference state model so that, damage pattern is found out which can be correlate with the experimental observations. Considering first-order HDMR expression from Eq. (3.9), for  $N=30$  and  $n=5$ :

$$\tilde{f}(\mathbf{x}) = \sum_{i=1}^{30} \sum_{j=1}^5 \phi_j(x_i) f(c_1, \dots, c_{i-1}, x_i^j, \dots, c_{i+1}, \dots, c_N) + (N-1) f_0 \quad (4.3)$$

$$\begin{aligned} \tilde{f}(\mathbf{x}) = & \sum_{j=1}^5 \phi_j(x_1) f(x_1^j, c_2, c_3, \dots, c_{38}) + \sum_{j=1}^5 \phi_j(x_2) f(c_1, x_2^j, c_3, \dots, c_{38}) \\ & + \dots + \sum_{j=1}^5 \phi_j(x_{30}) f(c_1, c_2, \dots, x_{30}^j) + (30-1) f(c_2, c_3, \dots, c_{38}) \end{aligned} \quad (4.4)$$

In the above expression the functions  $f(c_1, \dots, c_{i-1}, x_i^j, \dots, c_{i+1}, \dots, c_N)$  are evaluated from FEA tool and responses of first four bending modes in vertical direction are considered to develop HDMR expansion. The evaluations of first five component functions are presented as below.

$$\begin{aligned} f(x_1^1, c_2, c_3, \dots, c_{38}) &= f(22, 38, 38, \dots, 38) \\ &= 21.947 \text{ Hz}, 60.071 \text{ Hz}, 116.670 \text{ Hz}, 190.578 \text{ Hz} \end{aligned}$$

$$\begin{aligned} f(x_1^2, c_2, c_3, \dots, c_{38}) &= f(30, 38, 38, \dots, 38) \\ &= 21.946 \text{ Hz}, 60.072 \text{ Hz}, 116.679 \text{ Hz}, 190.615 \text{ Hz} \end{aligned}$$

$$\begin{aligned} f(x_1^3, c_2, c_3, \dots, c_{38}) &= f(38, 38, 38, \dots, 38) \\ &= 21.947 \text{ Hz}, 60.073 \text{ Hz}, 116.673 \text{ Hz}, 190.636 \text{ Hz} \end{aligned}$$

$$\begin{aligned} f(x_1^4, c_2, c_3, \dots, c_{38}) &= f(46, 38, 38, \dots, 38) \\ &= 21.947 \text{ Hz}, 60.073 \text{ Hz}, 116.673 \text{ Hz}, 190.650 \text{ Hz} \end{aligned}$$

$$\begin{aligned} f(x_1^5, c_2, c_3, \dots, c_{38}) &= f(54, 38, 38, \dots, 38) \\ &= 21.947 \text{ Hz}, 60.073 \text{ Hz}, 116.673 \text{ Hz}, 190.689 \text{ Hz} \end{aligned}$$



In first order-approximations,  $(n-1)N+1$  function evaluations are required, hence 131 function evaluations are done to obtain the HDMR expression for four bending modes. Based on the experimental results, the objective function for the first four bending frequencies is written as follows:

$$F_{obj} = \sqrt{(Y_1 - 18.005)^2 + (Y_2 - 50.204)^2 + (Y_3 - 98.219)^2 + (Y_4 - 161.876)^2} \quad (4.5)$$

Initial model is updated to obtain reference state FE model. The stiffness distribution of reference state FE model is shown in Fig. 4.9. A decrease in stiffness of 9.7% is observed at element location 24. Also, increase in stiffness has been observed in some elements of the FE model. For example, the stiffness at element 13 is found to be 14.9%, which is higher compared to all other elements.

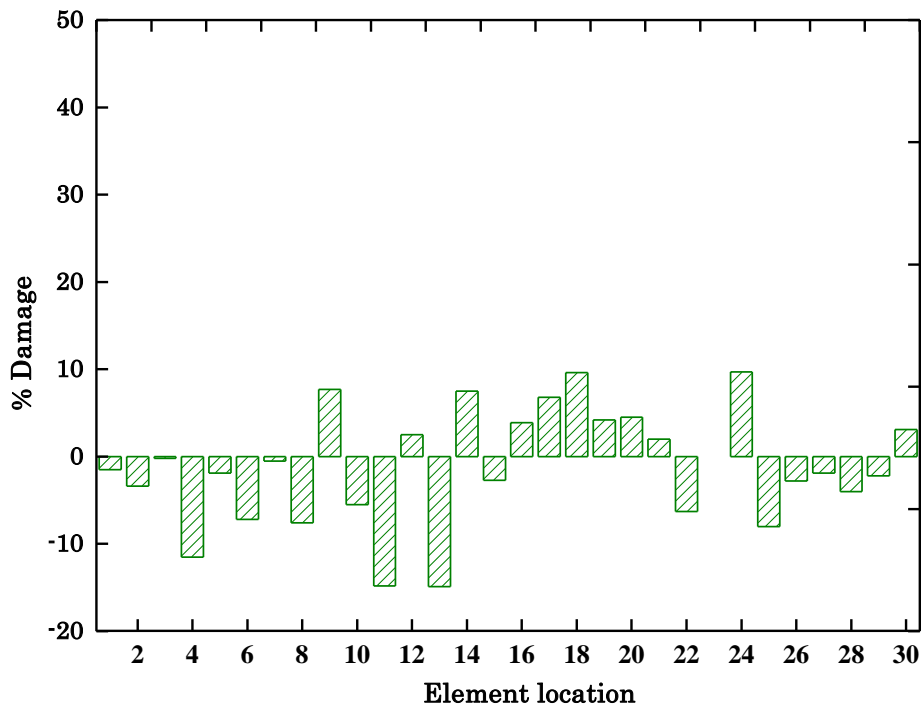


Fig. 4.9 Stiffness distribution: Reference state model (After updating:  $n = 5$ )

Table 4.4 shows the recognized modal parameters for the experimental beam, the frequencies of the initial FE model and its percentage differences. From the results it is observed that, initial FE model is in tune with the reference state of the test beam having variation of percentage frequencies from 0.191 to  $-0.723$ . The FE model has to be updated since the difference in damage state frequencies are found to be high

(21.18%). Frequencies from first four bending modes are utilized to construct objective functions and further optimization using GA.

Further by considering the  $E$  values obtained in reference state model, new lower bound, upper bound and mean [23 GPa, 43 GPa and 33 GPa] for all the 30 updating parameters are fixed to carry out the updating process for second iteration. Table 4.5 presents the frequencies of the damage state FE model obtained by updating the reface state FE model using HDMR, and this model is called reference damage state (Ref.-damage). The stiffness distribution of Ref.-damage state model is shown in Fig.4.10. From Table 4.5 the percentage difference between experimental values and updated model in Ref.-damage state is found to be more than 5%, which is slightly high.

Table 4.4 Frequencies and their differences: Experimental beam ( $n = 5$ )

Mode	Experimental Value (Hz)	Initial FE Value (Hz)	Difference in frequencies (%)
<i>Reference State</i>			
1	21.904	21.946	0.191
2	60.329	60.072	-0.425
3	117.022	116.680	-0.292
4	192.026	190.636	-0.723
<i>Damaged State</i>			
1	18.005	21.819	21.183
2	50.204	60.285	20.080
3	98.219	116.949	19.069
4	161.876	191.944	18.574

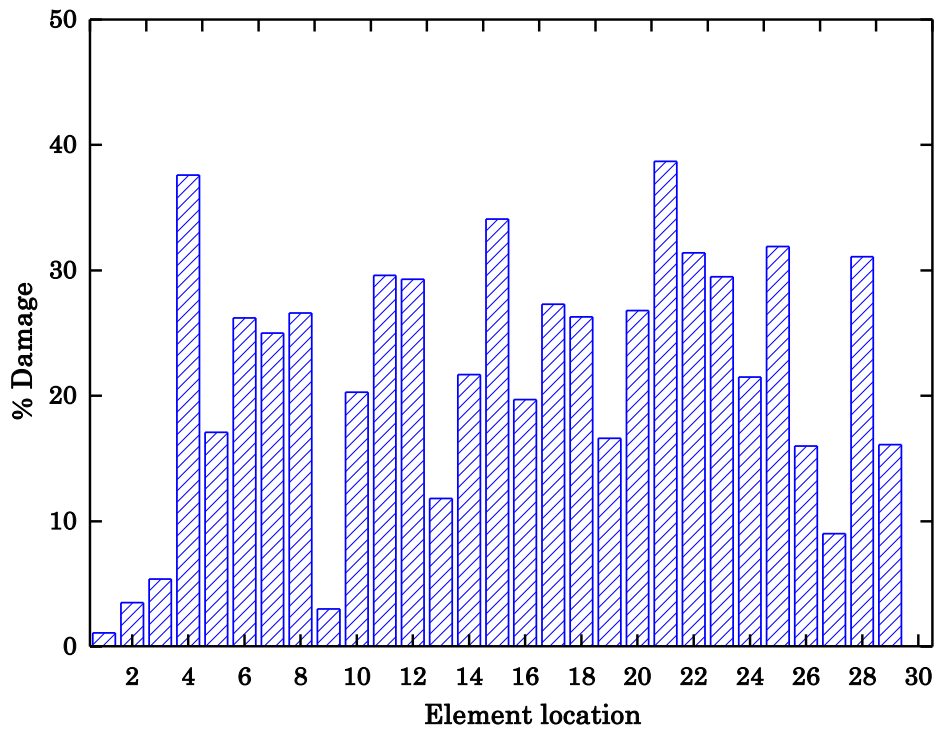


Fig. 4.10 Stiffness distribution: Ref.-damage state model (After updating:  $n = 5$ )

Hence in order to reduce the percentage difference and to obtain the better correlation between experimental and FE model, the values of  $E$  from Ref.-damage state model is further updated to obtain the modal parameters.

Table 4.5 Frequencies and its differences of Ref.-damage model: Experimental beam ( $n = 5$ )

Mode	Experimental Value (Hz)	After updating (Hz)	Differences in frequencies (%)
<i>Reference State</i>			
1	21.904	21.819	-0.388
2	60.329	60.285	-0.072
3	117.022	116.949	-0.062
4	192.026	191.944	-0.042
<i>Damaged State</i>			
1	18.005	18.980	5.415
2	50.204	51.928	3.433
3	98.219	101.314	3.151
4	161.876	166.357	2.768

The comparison of Table 4.4 and 4.5 shows that a significant improvement in tuning the natural frequencies is observed except for mode 1 in reference state. And for other modes, the difference in frequencies are reduced further, where experimental and FE values are almost found equal with a minimum difference of  $-0.042\%$  and maximum difference of  $-0.388\%$ . From the model updating procedure using HDMR, accurate modal frequencies are obtained which are having values closer to experimental damage beam. By updating, percentage differences are found to reduce from 21.81% to 5.41% in the first mode and also in the higher modes. The detected damage distribution is shown in Fig. 4.10 without the assumed damage pattern.

New lower bounds, upper bounds and mean [22.8 GPa, 41.8 GPa and 32.3 GPa] are considered for third iteration for further refinement of responses. After updating for third iteration, good convergence of frequencies between experimental and FE model is obtained. Table 4.6 presents the updated modal parameters obtained and variation in comparison with experimental values. It can be observed that the percentage difference reduces from 5% to  $-1.89\%$  in first mode, and in other three modes also a reduction in difference is observed as shown in Table 4.6.

Table 4.6 Frequencies and its differences in damage state model: Experimental beam ( $n = 5$ )

Mode	Experimental Value (Hz)	After updating (Hz)	Differences in frequencies (%)
<i>Reference State</i>			
1	21.904	21.819	$-0.388$
2	60.329	60.285	$-0.072$
3	117.022	116.949	$-0.062$
4	192.026	191.944	$-0.042$
<i>Damaged State</i>			
1	18.005	18.347	1.899
2	50.204	50.735	1.057
3	98.219	99.090	0.886
4	161.876	163.32	0.892

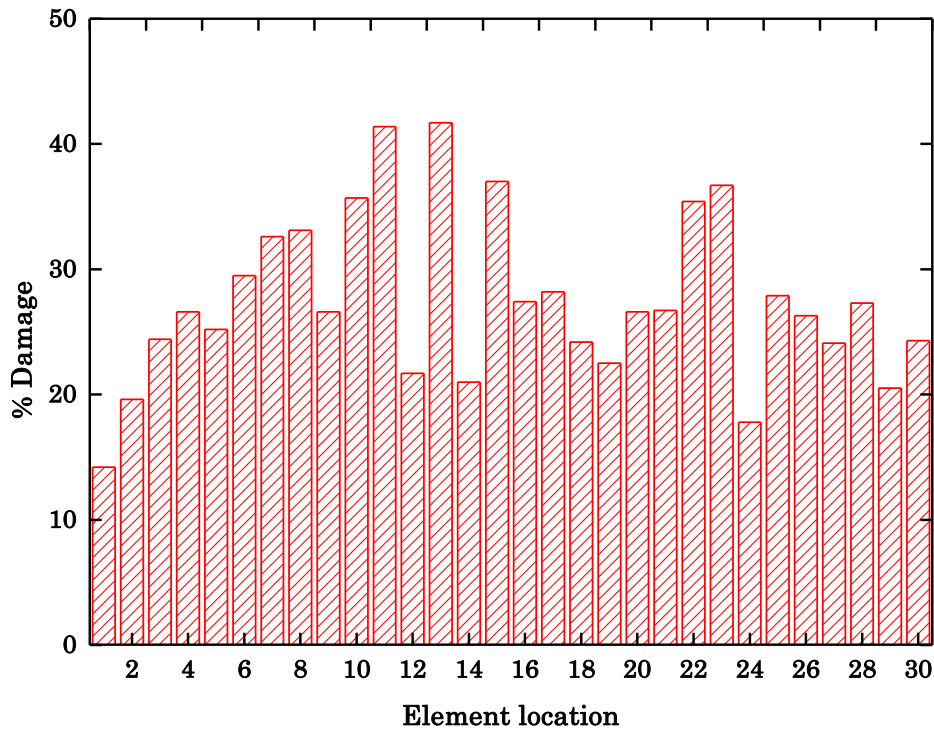


Fig. 4.11 Stiffness distribution: Damage state model (After updating:  $n = 5$ )

Figure 4.11 shows the damage distribution in terms of percentage reduction in  $E$  for all the 30 elements of the FE model. Reduction in  $E$  is found to be more than 30% between the elements 7 and 23.

Further in order to know the effect of increase in number of sample points on accuracy of the updated FE model, study is extended to  $n = 7$ . From the obtained results no significant reduction of difference in frequencies for damage state model is found when sample points are increased from  $n = 5$  to  $n = 7$ . Hence similar damage pattern is observed as in case of  $n = 5$  (Fig. 4.12). Hence five sample points are considered as optimum for this study.

Tables 4.7 and 4.8 present the comparison between FEMU based on modal flexibility residual method (Jaishi and Ren 2006) and HDMR. From the results, it is observed that the HDMR based SDI predicts results with less percentage variation than modal flexibility in both reference state and damage state. In final damage state model, the mean error of frequency is found to be 1.18% using HDMR based SDI in comparison with modal flexibility residual method wherein the error is 4.86%.

Table 4.7 Differences in frequencies of Modal flexibility residual (Jaishi and Ren 2006) and HDMR before updating: Experimental beam (Reference state)

Mode	Experimental Value (Hz)	Differences in frequencies (%) (Jaishi and Ren 2006)	Differences in frequencies (%) HDMR
<i>Reference State</i>			
1	21.904	1.410	0.191
2	60.329	1.219	-0.425
3	117.022	1.898	-0.292
4	192.026	2.187	-0.723
<i>Damaged State</i>			
1	18.005	21.466	21.183
2	50.204	21.416	20.080
3	98.219	20.361	19.069
4	161.876	19.953	18.574

Table 4.8 Differences in frequencies of Modal flexibility residual (Jaishi and Ren 2006) and HDMR after updating: Experimental beam (Damaged state)

Mode	Experimental Value (Hz)	Differences in frequencies (%) (Jaishi and Ren 2006)	Differences in frequencies (%) HDMR
<i>Reference State</i>			
1	21.904	-0.155	-0.388
2	60.329	1.039	-0.072
3	117.022	1.022	-0.062
4	192.026	1.119	-0.042
<i>Damaged State</i>			
1	18.005	-1.144	1.899
2	50.204	4.923	1.057
3	98.219	6.845	0.886
4	161.876	6.519	0.892

Figure 4.12 shows the variation of  $E$  at different updating states, where straight line (i.e., horizontal line) indicates the  $E$  values are taken as 35.5 GPa throughout the length of the beam for 30 elements. However in real time situations, it is not the case, and there is a variation of  $E$  in reference state model. Further in

iteration 2 after updating the reference state model, values of  $E$  will converge, so that, modal frequencies are in tune with the experimental observations and the variation is found to be 5% more than the experimental values. Also the updated values of  $E$  are reduced (Ref.-Damage) compared to reference state. In order to reduce the variation further, iteration 3 is performed, where excellent convergence of modal frequencies are found. The final variation of  $E$  values of damage state model for iteration-3 is shown in Fig. 4.13. The damage distribution for  $n=5$  and  $n=7$  is found to be similar with no significant improvement. Hence, with minimum number of sample the frequency responses from updated FE model are found to be in tune with the experimental observations.

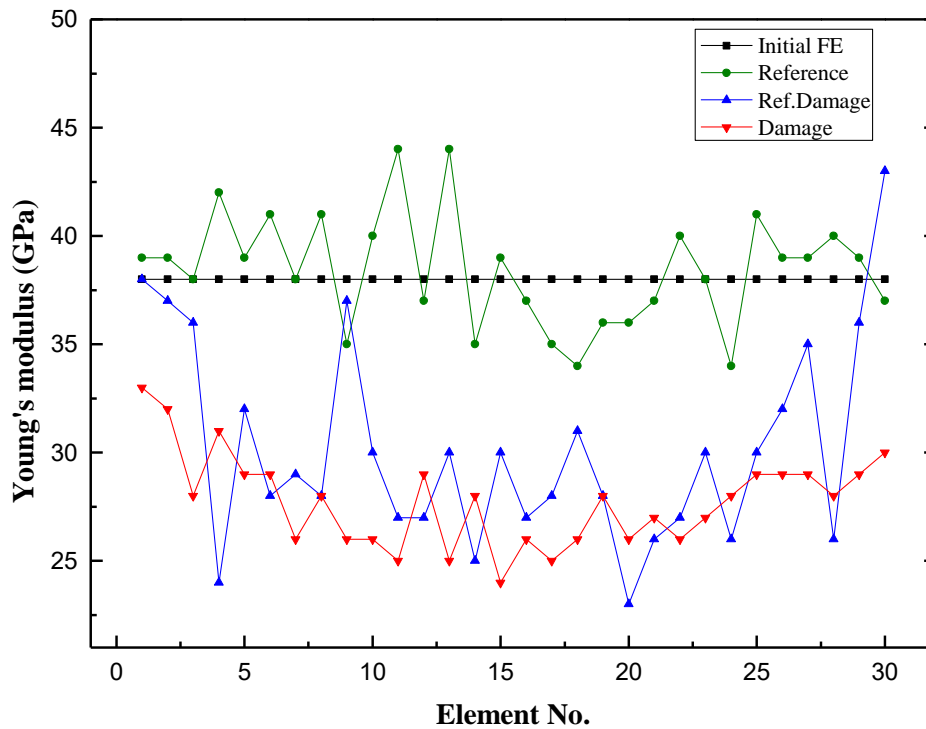


Fig. 4.12 Variation of Young's modulus at different updating states

In order to know the exact damage pattern due to variation of Young's modulus ( $E$ ), the damaged beam is modelled using FEA software ABAQUS (Hibbitt et al. 2000). Total number of nodes used are 8092, and total number of elements are 5656. To model the concrete beam, 4800 linear hexahedral elements of type C3D8R (Continuum 3D 8-node Reduced integration) are used. Reduced integration elements increase computational efficiency without losing the accuracy. Figure 4.13 shows the discretisation of FE model into 30 elements in which updated values of  $E$  are given.

Figure 4.14 shows the reinforcement provided as per the experimental beam. Reinforcements are modelled using 856 linear line elements of type T3D2 i.e., 2-noded linear 3-D stress/displacement truss element.

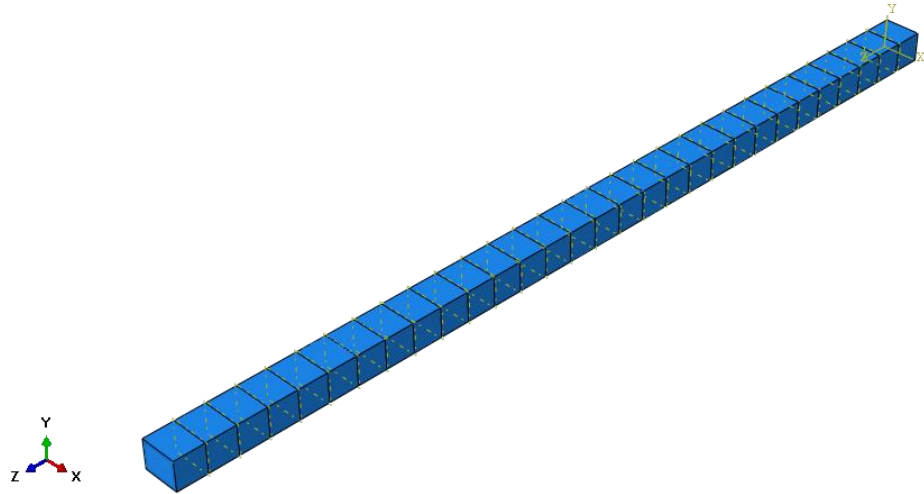


Fig. 4.13 3D Numerical model of experimental beam

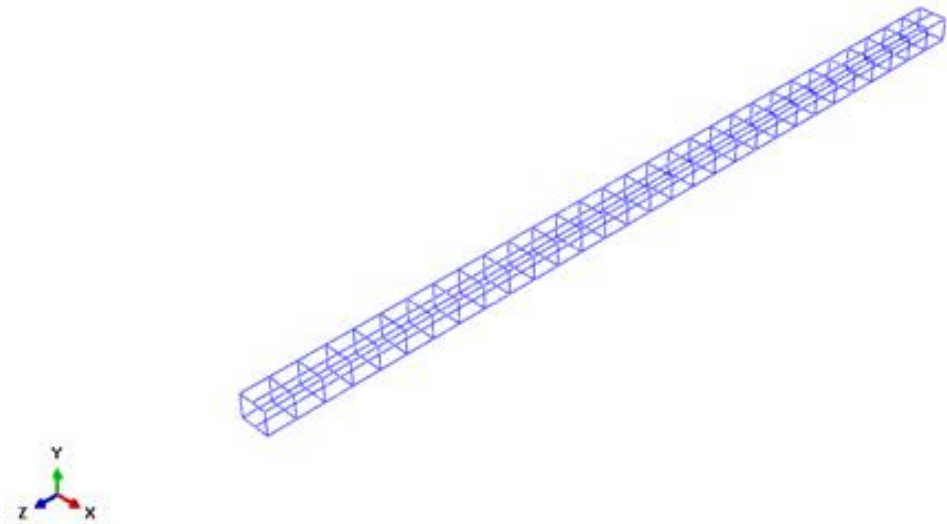


Fig. 4.14 Reinforcement bars (Linear line elements of type T3D2)

Figure 4.15 shows the tension cracks generated due to static load step 5 in experimental case study and damage state FE model. The crack pattern obtained in the final updated FE model is found to be in well agreement with the experimental observations, where most of the cracks are under the applied load and no cracks are found at the supports for both the cases. Hence, SDI based on HDMR can be effectively utilized in SDI and damage pattern recognition.



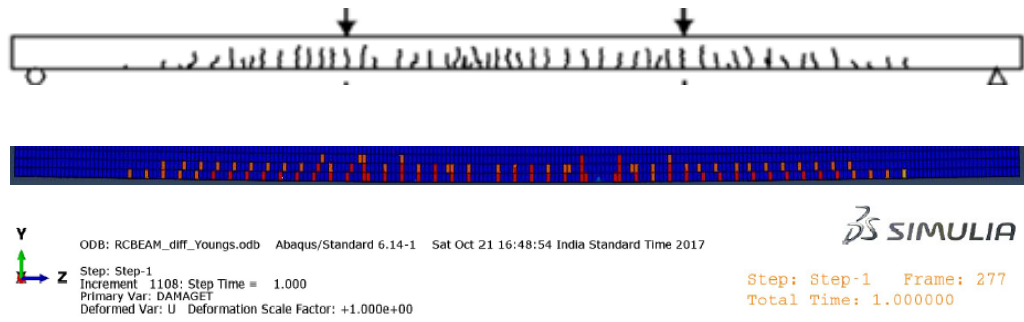


Fig. 4.15 Comparison of cracks

### 4.3 CASE STUDY 2: REINFORCED CONCRETE FRAME

A single storey and single bay laboratory-scale RC frame tested under static and dynamic conditions (Fang et al. 2008) is considered for further validation of the proposed methodology. The geometric dimensions, reinforcement layout and in-situ modal test setup are as shown in Figs.4.16 and 4.17 respectively. Modal parameters of the intact and damaged frame are obtained by performing dynamic test and are used to validate the proposed method. The RC frame is modelled using commercial FE software with two-dimensional beam element. The actual  $E$  of concrete is taken as 35.5 GPa and  $\rho$  as 2400 kg/m<sup>3</sup> with  $\mu$  of 0.2.

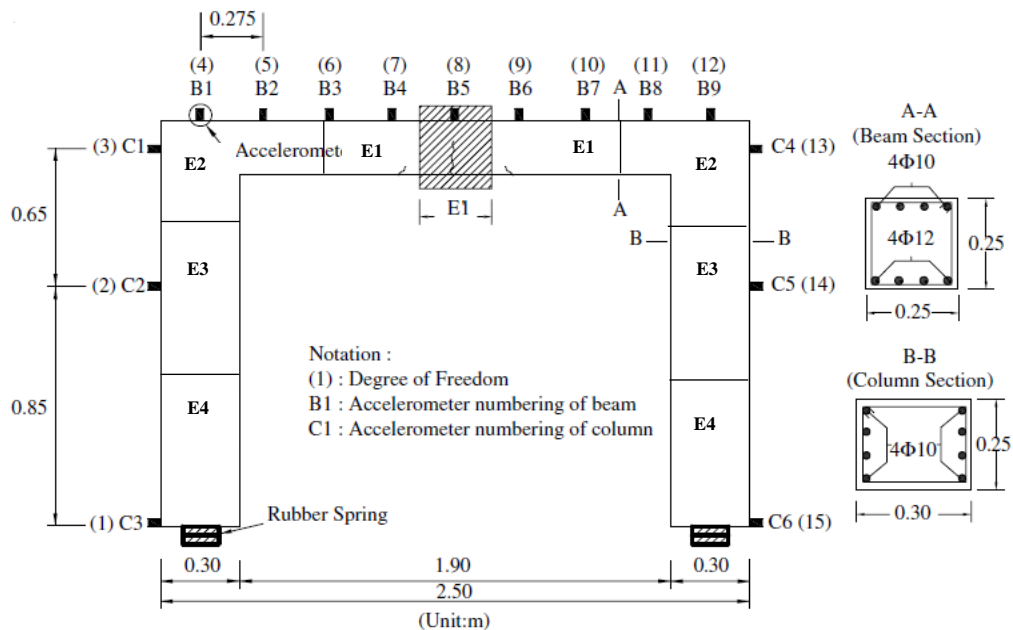


Fig. 4.16 RC frame: Geometric dimensions and accelerometer arrangement (Fang et al. 2008)



Fig. 4.17 Modal test of an RC frame: (a) In-situ modal test with spring boundary condition (top right corner). (Fang et al. 2008)

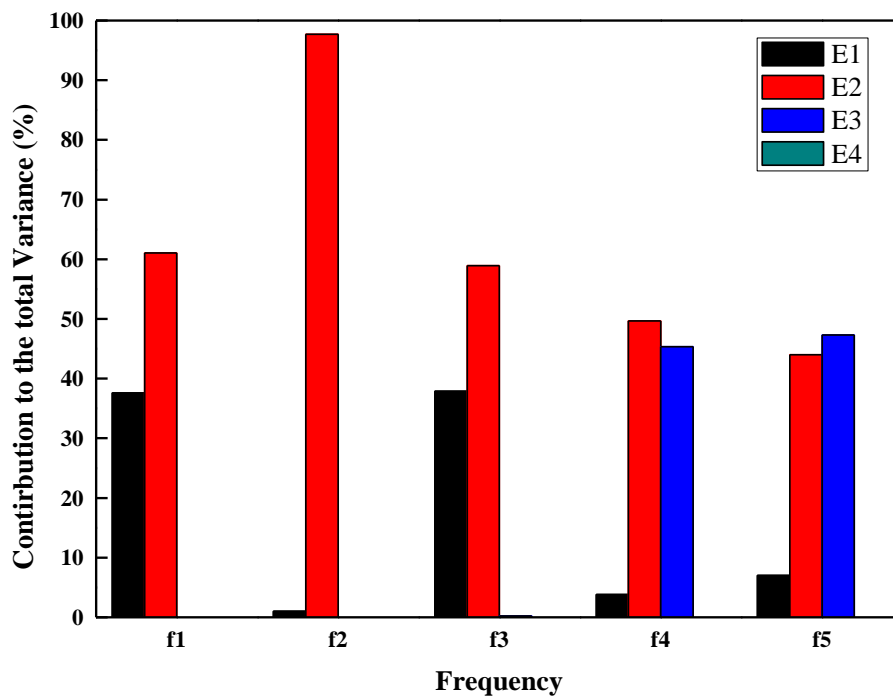


Fig. 4.18 Parameter screening results (RC frame)

Before proceeding to further development of HDMR response equations, parameter screening has been carried out to know the effect of  $E$  on response

characteristics of four substructures of RC frame. Figure 4.18 shows the contribution of four substructures on first five frequencies of the RC frame. From the results of parameter screening, E4 substructure has no contribution on variation of the frequencies. Since, the Young's modulus is the only property used as updating parameter, all the four substructures are considered as for identifying the damage location. Young's modulus of the four substructure ( $E_1, E_2, E_3$  and  $E_4$ ) is considered as input parameters and nine modal frequencies are considered as output responses. The study is carried out for  $n = 3, 5 \& 7$ . The lower bound, upper bound values of  $E$  considered are 30.2 GPa, 40.8 GPa respectively, and 35.5 GPa as mean (reference point,  $c$  in HDMR expansions). The damage identification is performed in three updating steps. In the first step, the four substructures E1, E2, E3 and E4 having 35.5 GPa each are updated. These updated values are used to build the damage state model.

Table 4.9 Updated values of  $E$  for reference state model: Experimental RC frame

Substructure	Initial State (GPa)	Reference State	Reference State
		(GPa) ( $n=3$ )	(GPa) ( $n=5$ )
E1	35.5	38.56	31.23
E2	35.5	40.55	40.80
E3	35.5	40.80	40.49
E4	35.5	36.59	39.81

Initially, SDI using HDMR technique is implemented in order to update the model and to identify the damage location and severity using  $n = 3$ . From Table 4.9, it can be observed that the updated values of  $E$  of reference state model has no significance, since the values of  $E$  are higher than 35.5 GPa in all the substructures.

The frequency errors of reference state model is found to be very high i.e., 16.81% in first mode itself (Table 4.10), which is not acceptable, and a maximum error of 5.33% in mode 7 is found (Table 4.10). Hence, the possibility of detecting the damage location is found to be less. Therefore the investigation is further carried out for  $n = 5$ , where an attempt has been made to reduce the percentage error and to

detect damage location in order to make FE model in tune with the experimental damage frame.

By considering the parameter bounds similar to the case for  $n=3$ , the study is carried out for  $n=5$ . In this case, from the updated values in the first iteration, reduction in  $E$  for substructure one (E1) is observed and the corresponding values of  $E$  for all the substructures are shown in Table 4.9. From Table 4.10 frequency differences are found to reduce significantly from 16.81% to 3.85% in reference state with the increase in sample points from  $n=3$  to  $n=5$  respectively. Also from Fig. 4.19, it is clear that, in the reference state model, the absolute errors significantly reduce except for first frequency.

Table 4.10 Modal frequencies of reference state model: Experimental RC frame

Mode	Undamaged					
	Experimental	FEA <sub>Initial</sub>	FEA <sub>Ref</sub> (Hz)	Error (%)	FEA <sub>Ref</sub> (Hz)	Error (%)
	(Hz)	(Hz)	$n=3$	$n=3$	$n=5$	$n=5$
1	30.16	30.51	35.23	16.81	31.32	3.85
2	69.34	65.51	72.64	4.76	70.17	1.19
3	178.11	163.58	173.57	2.54	167.36	6.04
4	339.06	317.01	348.00	2.63	337.44	0.48
5	348.74	322.43	351.14	0.68	339.67	2.60
6	509.78	463.40	494.58	2.98	480.40	5.76
7	709.86	682.30	747.70	5.33	686.30	3.32
8	790.07	750.52	796.76	0.84	768.00	2.79
9	948.13	890.53	965.45	1.82	952.60	0.47

As observed from Table 4.9, the updated values of  $E_1-E_4$  obtained from reference state model, it is clear that the substructure E1 is damaged due to reduction in  $E$ . Hence, the reference state model is further updated to find out the exact location of damage in substructure E1. Further the substructure E1 is subdivided into three divisions (E11, E12 and E13) and updated for the new bounds (lower bound 25.056 GPa, upper bound 31.32 and mean 28.18 GPa).

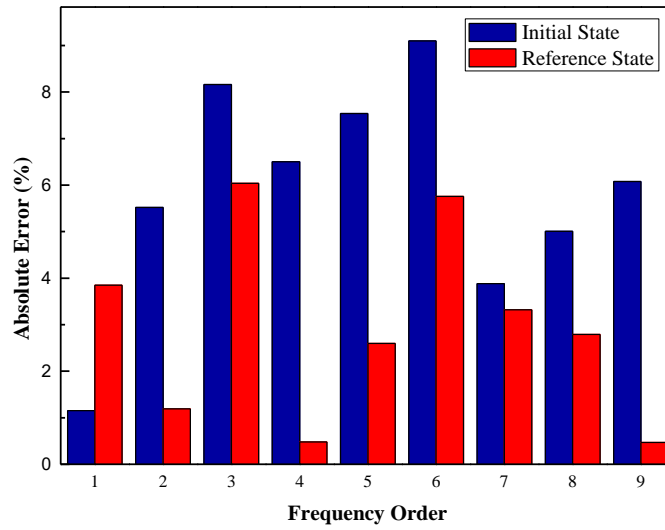


Fig. 4.19 Comparison of absolute errors (%) of initial and reference state model ( $n = 5$ )

The updated values of three substructures (E11, E12 and E13) are shown in Table 4.11. From the results it is clear that, damage at the substructure E11 is found to be more due to reduction in  $E$  from 31.23 GPa to 26.79 GPa. Hence, the damage is located at the mid span of the beam element. Finally, the  $E$  of four substructure and frequencies of damage state is shown in Table 4.12 and 4.13 respectively

Table 4.11 Updated values  $E$  of E1 substructures: Experimental RC frame ( $n = 5$ )

Initial State(GPa)	Reference State (GPa)	Damage State (GPa)
E1	E1	E1'=E11-E12-E13
35.5	31.23	26.79, 29.77, 29.77

Table 4.12 Values of  $E$  at different updating states: Experimental RC frame ( $n = 5$ )

Substructure	Initial (GPa)	Reference State (GPa)	Damage State (GPa)
E1	35.5	31.23	26.79
E2	35.5	40.80	40.80
E3	35.5	40.49	40.49
E4	35.5	39.81	39.81

Table 4.13 Modal frequencies of damage state model: Experimental RC frame ( $n = 5$ )

Mode	Damaged				
	Experimental (Hz)	FEA <sub>Ref</sub> (Hz)	Error (%)	FEA <sub>Dam</sub> (Hz)	Error (%)
1	29.10	31.32	7.64	30.81	5.88
2	68.05	70.17	3.11	70.17	3.11
3	170.24	167.36	1.69	166.82	2.01
4	335.53	337.44	0.57	336.11	0.17
5	344.65	339.67	1.44	339.43	1.52
6	499.53	480.40	3.83	480.48	3.81
7	679.41	686.30	1.01	674.92	0.66
8	768.70	768.00	0.09	763.44	0.68
9	933.98	952.60	1.99	953.50	2.09

From the results of reference state (Table 4.10) and damage state (Table 4.13) reduction in mean error is observed, i.e., the mean error is found to be 2.94% in reference state and in case of damage stage model it is 2.21%. Also frequencies of the damage state model are in tune with the experimental observations. With maximum error of 5.88% in mode one and 0.17% to 3.81% in remaining modes.

Figure 4.20 shows the absolute percentage variation of reference state and damage state beam with respect to results of test beam for nine frequencies. It is found that absolute error is found to reduce in damage state model from 7.64% to 5.88% in mode 1, and reduction in absolute error is also found in higher modes. Finally, Fig. 4.21 represents the variation of  $E$  at different updating states.

The study has been extended for  $n = 7$ , to know any further improvement in updated parameters. From the updated values of  $E_1 - E_4$  it is observed that, there is no significant improvement in the responses of the damage state model. The mean error for  $n = 5$  and  $n = 7$  is found to be the same i.e., 2.2%. Hence the optimum number of sample points is found to be  $n = 5$  for this case study.

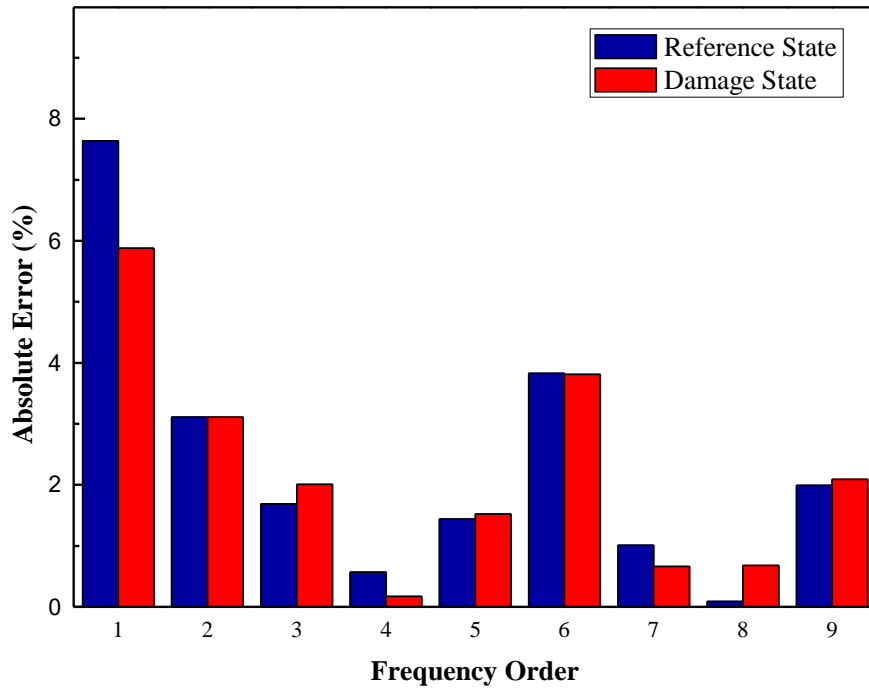


Fig. 4.20 Comparison of absolute error (%) of reference and damage state model ( $n = 5$ )

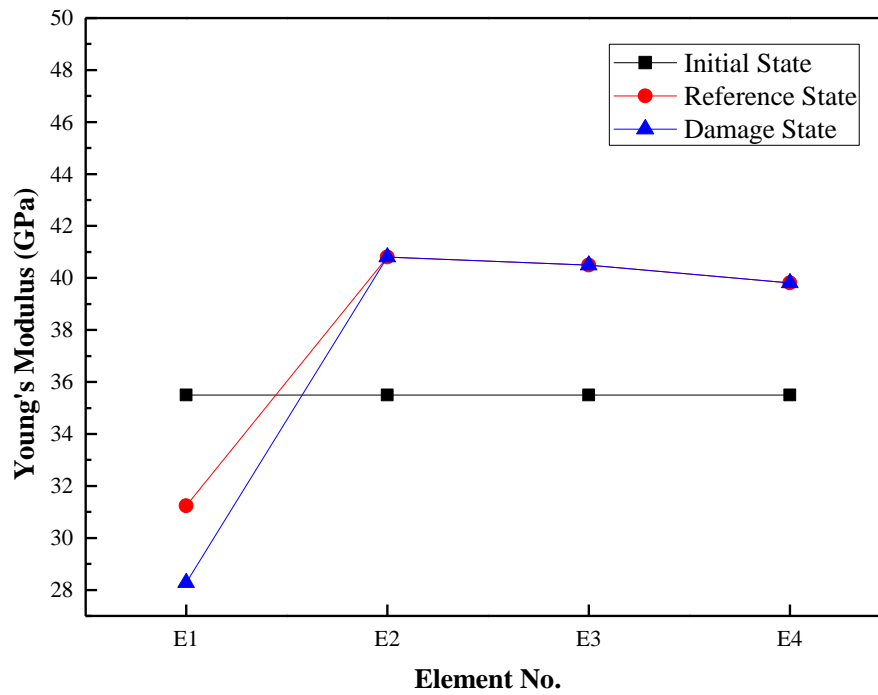


Fig. 4.21 Variation of  $E$  at different updating states

#### 4.4 CASE STUDY 3: BRIDGE STRUCTURE

In order to find out the efficiency of HDMR based SDI, a tested (Farrar et al. 1996) full scale I – 40 bridge constructed over the Rio Grande is considered (Fig. 4.22). In order to investigate the dynamic behaviour of the bridge, different damage scenarios are introduced in web and flange portion of a girder. First stage of damage in the form of two foot web cut at girder mid span, second stage of damage as six foot cut from the centre of the web to bottom flange at girder mid span, third Stage of damage as six foot cut in the web plus half bottom flange cut at girder mid-span, and fourth stage of damage as six foot cut in the web plus full bottom flange cut at girder mid-span (Figs. 4.23 and 4.24).



Fig. 4.22 General view of I – 40 Bridge

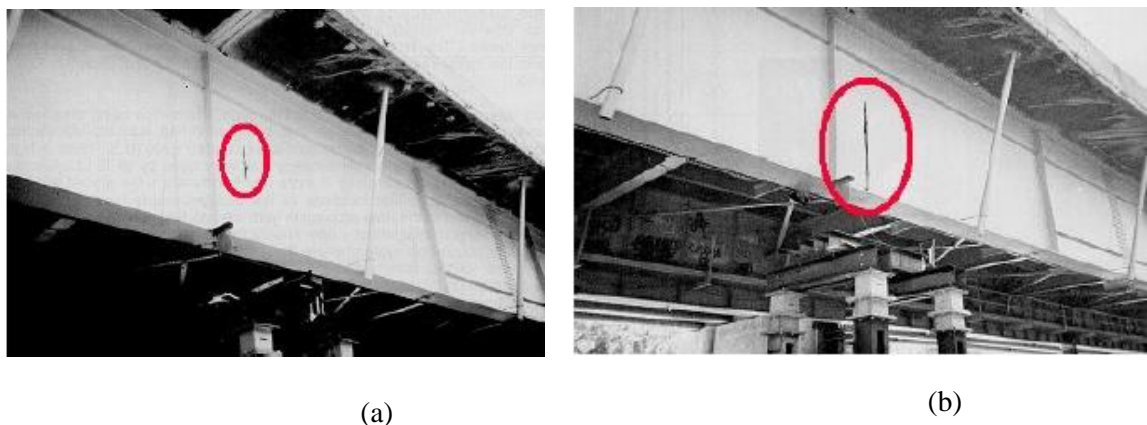


Fig. 4.23 Damage scenarios (a) First stage damage (b) Second stage damage



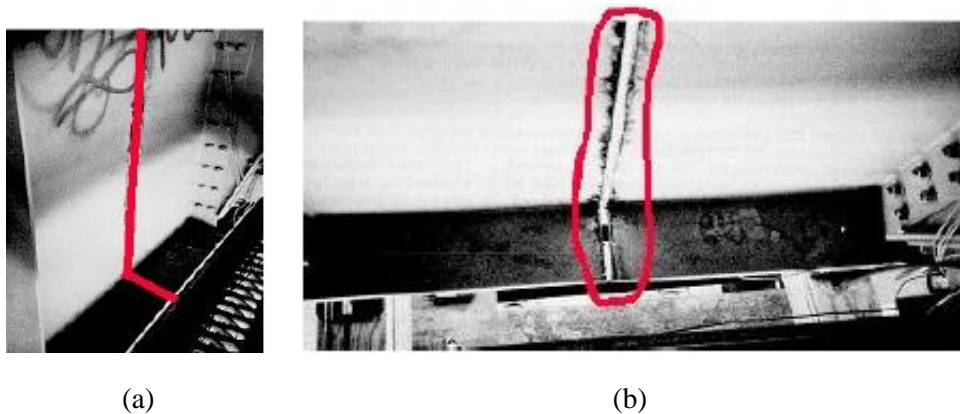


Fig. 4.24 Damage scenario (a) Third stage damage (b) Fourth stage damage

The bridge has three continuous spans each of 39.9 m, 49.7 m and 39.9 m (Fig. 4.25). To understand the dynamic behaviour of the bridge, three torsional and three bending modes are recorded from the experimental investigation. To apply the concept of HDMR based SDI, the three dimensional model is simplified to two-dimensional beam model. Hence, only bending modes are considered as the target values which are obtained from extraction of frequencies due to fourth damage scenario.

Figure 4.26 shows the simplified two dimensional beam model resting on three piers, which have a rigid connection at the bottom and rotatable connections between top of the pier and the girder. The beam model is divided into 9 substructures (thin girders 7 numbers and thick girders 2 numbers-S3 and S7). The values of  $E$  for both girders are taken as 200 GPa and flange dimensions of thick girder are higher than thin girders. The section properties considered in the present study are cross sectional area ( $A$ ) and second moment of area ( $I$ ). The initial values of cross section area of thin girder ( $A_1$ ) and thick girder ( $A_2$ ) are taken as 0.5685 and 0.6436 respectively. The values of second moment of area of thin section ( $I_1$ ) and thick section ( $I_2$ ) is considered as  $0.512 \text{ m}^4$  and  $0.812 \text{ m}^4$  respectively. A total of 61 beam elements were generated to simulate the equivalent girder, and 10 beam elements were used for each equivalent pier.

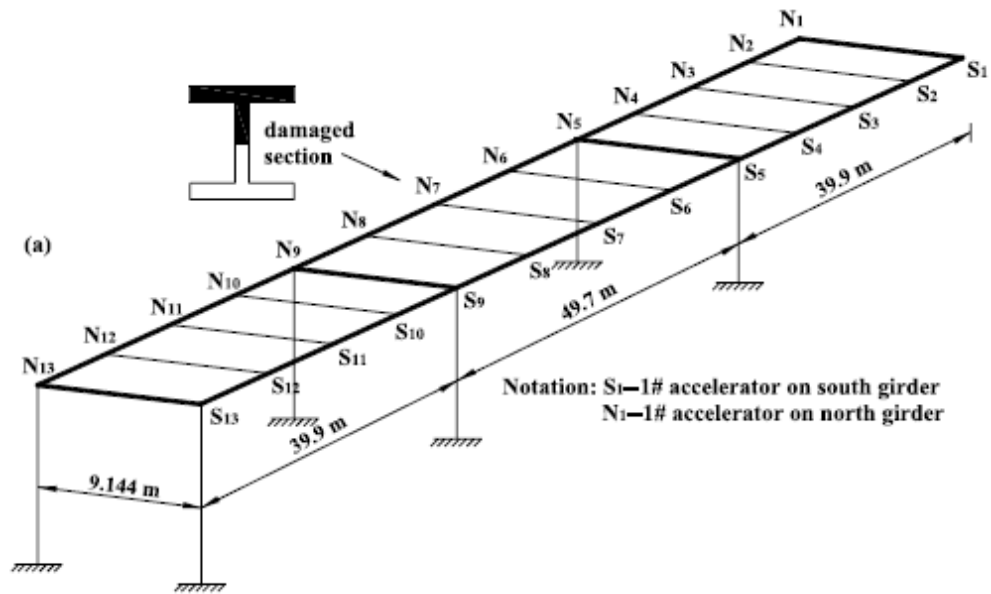


Fig. 4.25 Simplified I-40 bridge model with accelerometer layout

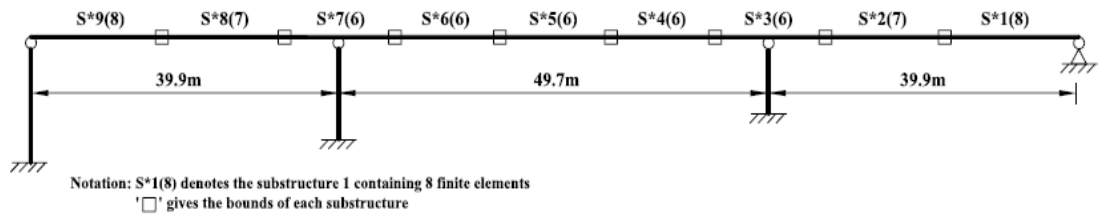


Fig. 4.26 Two dimensional beam model of bridge

Similar to the first two case studies, a parametric study has been carried out for  $n = 3, 5 \& 7$ . In this case-study, as damage locations are predetermined in the field study, first the second moment of area of thin girder is taken as updating parameter ( $I_1$ ). Lower bound and upper bound for ( $I_1$ ) is taken as  $0.340 \text{ m}^4$  and  $0.684 \text{ m}^4$  respectively with mean value of  $0.512 \text{ m}^4$  for all the sample points. Frequencies of initial state model before updating for first three bending modes are presented in Table 4.14.

Table 4.14 Frequency errors before updating: Bridge example

Mode	Experimental Un-damage Frequency (Hz)	Frequency (Hz) (Initial State)	Frequency Errors (%)
1	2.48	2.45	-1.2
2	3.50	3.69	5.1
3	4.08	3.90	-4.6

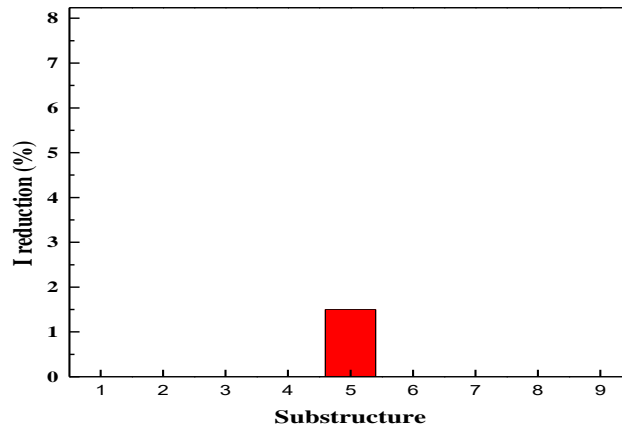


Fig. 4.27 Identified damage location at substructure S5 ( $n = 3$ )

From Fig. 4.27 it is observed that the damage is detected at substructure S5 which agrees with the experimental value. However, the damage percentage is found to be less than 2% with mean percentage error 6.01%. Hence the study is extended using  $n = 5$  to obtain the accurate reference state model, with less frequency errors.

From model updating using HDMR, for  $n = 5$ , reduction in section inertia of  $I_1$  (7.5%) is found at S5 substructure, and hence damage is found to be at S5 location as shown in Fig. 4.28. Table 4.15 presents percentage difference of frequencies between predicted and experimental observations in reference and damage state. Also the mean error is found to be reduced from 6% ( $n = 3$ ) to 5.8% in reference state model for  $n = 3$ . Model is further updated to obtain damage distribution (Fig. 4.29) and frequency errors of damage stage model is presented in Table 4.15.

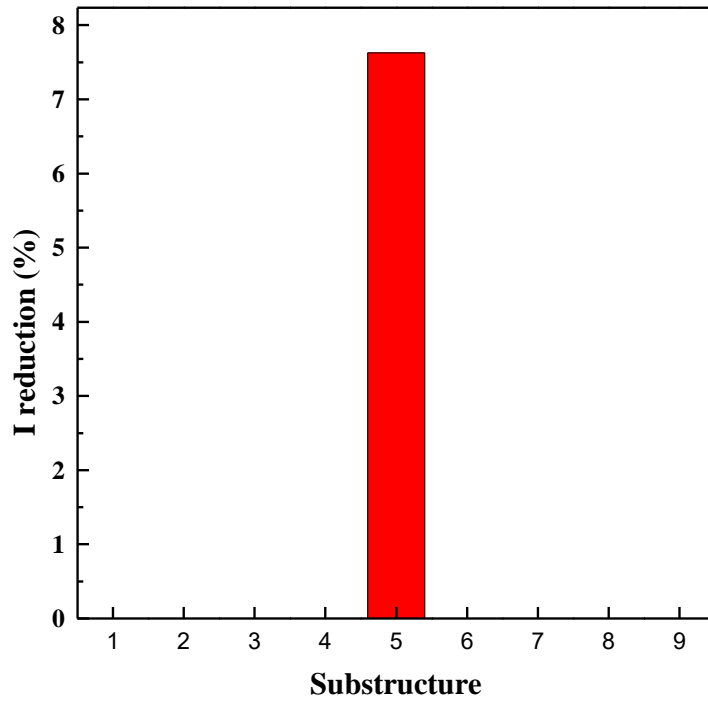


Fig. 4.28 Identified damage location at substructure S5 ( $n = 5$ )

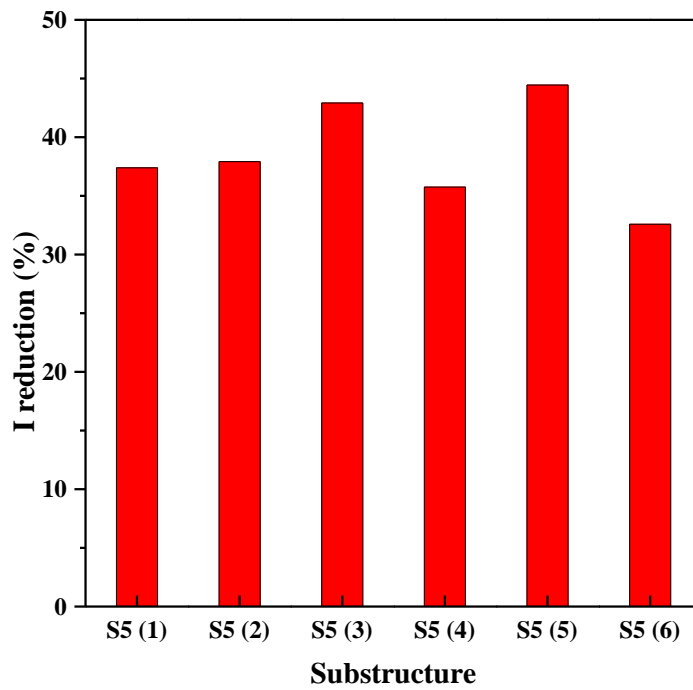


Fig. 4.29 Stiffness distribution at S5 substructure ( $n = 5$ )

Table 4.15 Frequency errors after updating: Bridge model in damage state ( $n = 5$ )

Mode	Experimental Damage Frequency (Hz)	Frequency Errors (%) (Reference state)	Frequency Errors (%) (Damage State)
1	2.30	6.90	6.88
2	3.49	7.90	3.59
3	3.99	-3.00	-2.57

Finally, by further updating the S5 substructure elements of FE model, the mean error is found to be reduced to 4.34%. The study is further carried out for  $n = 7$  and no reduction in mean error of percentage difference is found out. Values of parameter bounds and percentage frequency error of initial state is taken similar to  $n = 5$ . From the results observed it is found that, the mean error of damage state model for  $n = 5$  and  $n = 7$  is found to be 4.34% and 4.29% respectively. Hence the values of frequency are converged for  $n = 5$ .

## 4.5 SUMMARY

The concept of HDMR is applied to three case studies in this chapter. In case-study 1 an attempt has been made to update the initial FE model to final damage state model so that the dynamic responses obtained are in tune with the experimental observations. The dynamic responses i.e., frequencies at different modes are in well agreement with the experimental ones, also the crack pattern in damaged beam matches with the experimental beam.

In case-study 2, the responses from single bay single story tested under laboratory conditions (Fang et al. 2008) are considered to build objective function, where the function is minimized using GA to obtain the updated parameters. In this case-study, location of damage has been identified using HDMR accurately.

In case-study 3, HDMR based SDI is extended to identify the damage location in a real bridge structure, where damage location is found with minimum number of sample points ( $n = 3$ ). However, the precise location is identified when the number of

sample points are increased. Since the variation of experimental frequencies between the undamaged and damaged states are very less, percentage frequency errors are found to be slightly high (i.e., 6.8%) in mode 1. And subsequently, the percentage errors are reduced in other two modes in damage state. Using second-order HDMR, the errors can be further minimized, with additional computational effort.



## **CHAPTER 5**

### **CONCLUSIONS**

#### **5.1 SUMMARY AND RESEARCH FINDINGS**

The HDMR techniques are effectively applied for construction of a computational model directly from laboratory or field data, creating an efficient fully equivalent operational model to replace an existing time-consuming mathematical model, and for identification of key model variables, global uncertainty assessments, and efficient quantitative risk assessments, etc.

In this work, a computationally efficient FEMU method using the HDMR is applied in conjunction with GA. Initially, HDMR response equations are generated by considering a simulated beam using three sample points and development of an objective function for minimum number of sample points is developed. Based on the accuracy of the results it is concluded that, in order to obtain acceptable true parameters, response equations in objective functions required should be greater than the number of parameters utilized. The method has been applied to model updating of a simply supported beam as well as a RC box culvert. Suitable parameters are first selected for model updating and numerical simulations are performed using the combinations of parameters. First order HDMR expressions are used to develop the response equations. An objective function is built up using the residuals between measured and predicted responses from the developed HMDR equations, and updated parameters are obtained using the GA. From the numerical examples presented, the computational efficiency is studied.

In the proposed work, HDMR based FEMU is carried out for SDI. To locate the damage, and to observe its pattern, all elements in FE model are considered as parameters to be updated. First the proposed damage detection procedure was



illustrated with an example of simulated simply supported concrete beam, and damage patterns are identified using HDMR based model updating. The SDI procedure is then verified with the experimental results available in the literature.

The identified damage distribution obtained from HDMR (without assuming the damaged pattern of the tested beam) is compared with the test results reported in literature. The comparison of the damage patterns obtained using the proposed method with the experimental observations shows well agreement. The minimum and maximum percentage differences between the experimental values and HDMR in updating the reference state model are  $-0.72\%$  and  $0.19\%$ , which is much better than the values obtained using modal flexibility residual that ranges between  $1.41\%$  and  $2.19\%$ . Similarly, in case of damaged state model after updating, the minimum and maximum differences in frequencies between the experimental values and HDMR are found to be  $-1.899$  and  $-0.892\%$  respectively, and  $-1.14\%$  and  $6.52\%$  for the modal flexibility residual. Hence, it is concluded that the proposed method using HDMR predicts the frequencies of damaged beam more efficiently than other methods such as modal flexibility residual method.

The methodology is further applied to RC frame, where damage is located using substructure based approach, where the frame is divided in to four substructures considering Young's modulus as variable. It is found that the damage is occurred with reduction in Young's modulus at beam mid-span. The frequencies are found to be in tune with the experimental observations with percentage error of  $5.48\%$  in mode 1 and  $0.15\%$  to  $3.98\%$  in all other modes.

Finally, the concept of HDMR based SDI is applied to real bridge structures, in which the frequencies are efficiently computed with less computational effort, with a mean error of  $4.29\%$ . Mean error is converged with the sample points  $n=7$ . Also in the present work, a parametric study is conducted with respect to the number of sample points used in approximation of HDMR component functions in model updating, and its effect on absolute error of updating parameters with respect to true values. It is observed that an improvement in accuracy is witnessed with increase in number of sample points from three to five. With the increase in sample point from five to seven, no significant tuning of parameters and responses are identified.

Therefore, the optimum number of sample points is taken as five for all the cases. Hence the proposed FEMU using the HDMR is promising in SDI.

## **5.2 SUGGESTIONS FOR FUTURE WORK**

- i. In the present work, first order HDMR expansions are utilized to develop the response equations. Further, the accuracy can be significantly improved by employing the second order HDMR, but with slightly increased computational effort. Finally, the updated FE model can be utilized in structural damage identification.
- ii. In the present study, Lagrange interpolation functions are utilized. Further, other interpolation techniques like moving least squares can be used and the accuracy of the parameters and responses of updated FE model can be investigated.
- iii. The present study has been conducted with limited information. However, this could be extended by incorporating changes in damping, and also the RS designs could be coupled with neural networks.
- iv. The stochastic variation of material parameters can also be considered by proper uncertainty analysis tools.
- v. Different kinds of uncertainties can be characterised and included in the model based on the real time data.



## APPENDIX

### DEVELOPMENT OF HDMR APPROXIMATION EQUATIONS USING THREE SAMPLE POINTS ( $n=3$ ) IN CONJUNCTION WITH GENETIC ALGORITHM

#### Case study – 1: SDI of experimental beam

The general form of HDMR expression is given as:

$$f(\mathbf{x}) = f_0 + \sum_{i=1}^N f_i(x_i) + \sum_{1 \leq i < j \leq N} f_{ij}(x_i, x_j) + \sum_{1 \leq i < j < k \leq N} f_{ijk}(x_i, x_j, x_k) + \dots + f_{12\dots N}(x_1, x_2, \dots, x_N)$$

Considering first order HDMR expression to develop response equations:

$$\tilde{f}(\mathbf{x}) = \sum_{i=1}^N \sum_{j=1}^n \phi_j(x_i) f(c_1, \dots, c_{i-1}, \dots, x_i^j, \dots, c_{i+1}, \dots, c_N) + (N-1)f_0$$

For  $N = 30$  and  $n = 3$ :

$$\tilde{f}(\mathbf{x}) = \sum_{i=1}^{30} \sum_{j=1}^3 \phi_j(x_i) f(c_1, \dots, c_{i-1}, \dots, x_i^j, \dots, c_{i+1}, \dots, c_N) + (N-1)f_0$$

The expanded form the above expression is given as:

$$\tilde{f}(\mathbf{x}) = \sum_{j=1}^3 \phi_j(x_1) f(x_1^j, c_2, c_3, \dots, c_{38}) + \sum_{j=1}^3 \phi_j(x_2) f(c_1, x_2^j, c_3, \dots, c_{38}) + \dots + \sum_{j=1}^3 \phi_j(x_{30}) f(c_1, c_2, \dots, x_{30}^j) + (30-1)f(c_2, c_3, \dots, c_{38})$$

For  $i = 1$  and  $j = 1 - 3$

*Expansion – 1*

$$\phi_1(x_1) \times f(x_1^1, c_2, c_3, \dots, c_{30}) + \phi_2(x_1) \times f(x_1^2, c_2, c_3, \dots, c_{30}) + \phi_3(x_1) \times f(x_1^3, c_2, c_3, \dots, c_{30})$$

For  $i = 2$  and  $j = 1 - 3$

*Expansion – 2*

$$\phi_1(x_2) \times f(c_1, x_2^1, c_3, \dots, c_{30}) + \phi_2(x_2) \times f(c_1, x_2^2, c_3, \dots, c_{30}) + \phi_3(x_2) \times f(c_1, x_2^3, c_3, \dots, c_{30})$$

Similarly from  $i = 3$  to 30 and  $j = 1 - 3$  expression are given by

*Expansion – 3*

$$\phi_1(x_3) \times f(c_1, c_2, x_3^1, c_4, \dots, c_{30}) + \phi_2(x_3) \times f(c_1, c_2, x_3^2, c_4, \dots, c_{30}) + \phi_3(x_3) \times f(c_1, c_2, x_3^3, c_4, \dots, c_{30})$$

*Expansion – 4*

$$\phi_1(x_4) \times f(c_1, c_2, c_3, x_4^1, \dots, c_{30}) + \phi_2(x_4) \times f(c_1, c_2, c_3, x_4^2, \dots, c_{30}) + \phi_3(x_4) \times f(c_1, c_2, c_3, x_4^3, \dots, c_{30})$$

*Expansion – 5*

$$\phi_1(x_5) \times f(c_1, c_2, \dots, x_5^1, \dots, c_{30}) + \phi_2(x_5) \times f(c_1, c_2, \dots, x_5^2, \dots, c_{30}) + \phi_3(x_5) \times f(c_1, c_2, \dots, x_5^3, \dots, c_{30})$$

*Expansion – 6*

$$\phi_1(x_6) \times f(c_1, c_2, \dots, x_6^1, \dots, c_{30}) + \phi_2(x_6) \times f(c_1, c_2, \dots, x_6^2, \dots, c_{30}) + \phi_3(x_6) \times f(c_1, c_2, \dots, x_6^3, \dots, c_{30})$$

*Expansion – 7*

$$\phi_1(x_7) \times f(c_1, c_2, \dots, x_7^1, \dots, c_{30}) + \phi_2(x_7) \times f(c_1, c_2, \dots, x_7^2, \dots, c_{30}) + \phi_3(x_7) \times f(c_1, c_2, \dots, x_7^3, \dots, c_{30})$$

*Expansion – 8*

$$\phi_1(x_8) \times f(c_1, c_2, \dots, x_8^1, \dots, c_{30}) + \phi_2(x_8) \times f(c_1, c_2, \dots, x_8^2, \dots, c_{30}) + \phi_3(x_8) \times f(c_1, c_2, \dots, x_8^3, \dots, c_{30})$$

*Expansion – 9*

$$\phi_1(x_9) \times f(c_1, c_2, \dots, x_9^1, \dots, c_{30}) + \phi_2(x_9) \times f(c_1, c_2, \dots, x_9^2, \dots, c_{30}) + \phi_3(x_9) \times f(c_1, c_2, \dots, x_9^3, \dots, c_{30})$$

*Expansion – 10*

$$\phi_1(x_{10}) \times f(c_1, c_2, \dots, x_{10}^1, \dots, c_{30}) + \phi_2(x_{10}) \times f(c_1, c_2, \dots, x_{10}^2, \dots, c_{30}) + \phi_3(x_{10}) \times f(c_1, c_2, \dots, x_{10}^3, \dots, c_{30})$$

.

.

$i = 30: j = 1 - 3$

$$\phi_1(x_{30}) \times f(c_1, c_2, c_3, \dots, x_{30}^1) + \phi_2(x_{30}) \times f(c_1, c_2, c_3, \dots, x_{30}^2) + \phi_3(x_{30}) \times f(c_1, c_2, c_3, \dots, x_{30}^3)$$

In order to obtain the HDMR expression for the desired response, the functions

$f(c_1, \dots, c_{i-1}, \dots, x_i^j, \dots, c_{i+1}, \dots, c_N)$  are evaluated using FEA package. The responses in Hz for the function evaluations in the above expansion are as below:

*Function Evaluations in Expansion – 1*

$$f(x_1^1, c_2, c_3, \dots, c_{30}) = f(22, 38, 38, \dots, 38) = 21.947, 60.071, 116.670, 190.578$$

$$f(x_1^2, c_2, c_3, \dots, c_{30}) = f(38, 38, 38, \dots, 38) = 21.947, 60.073, 116.684, 190.636$$

$$f(x_1^3, c_2, c_3, \dots, c_{30}) = f(5438, 38, \dots, 38) = 21.947, 60.073, 116.689, 190.659$$

*Function Evaluations in Expansion – 2*

$$f(c_1, x_2^1, c_3, \dots, c_{30}) = f(38, 22, 38, \dots, 38) = 21.945, 60.050, 116.537, 190.083$$

$$f(c_1, x_2^1, c_3, \dots, c_{30}) = f(38, 38, 38, \dots, 38) = 21.947, 60.073, 116.684, 190.636$$

$$f(c_1, x_2^1, c_3, \dots, c_{30}) = f(38, 54, 38, \dots, 38) = 21.949, 60.082, 116.743, 190.856$$

*Function Evaluations in Expansion – 3*

$$f(c_1, c_2, x_3^1, c_4, \dots, c_{30}) = f(38, 38, 22, 38, \dots, 38) = 21.940, 59.972, 116.105, 188.737$$

$$f(c_1, c_2, x_3^1, c_4, \dots, c_{30}) = f(38, 38, 38, 38, \dots, 38) = 21.947, 60.073, 116.684, 190.636$$

$$f(c_1, c_2, x_3^1, c_4, \dots, c_{30}) = f(38, 38, 54, 38, \dots, 38) = 21.949, 60.113, 116.914, 190.389$$

*Function Evaluations in Expansion – 4*

$$f(c_1, c_2, c_3, x_4^1, \dots, c_{30}) = f(38, 38, 38, 22, \dots, 38) = 21.928, 59.799, 115.331, 187.009$$

$$f(c_1, c_2, c_3, x_4^2, \dots, c_{30}) = f(38, 38, 38, 38, \dots, 38) = 21.947, 60.073, 116.684, 190.636$$

$$f(c_1, c_2, c_3, x_4^3, \dots, c_{30}) = f(38, 38, 38, 54, \dots, 38) = 21.954, 60.182, 117.228, 192.144$$

*Function Evaluations in Expansion – 5*

$$f(c_1, c_2, \dots, x_5^1, \dots, c_{30}) = f(38, 38, \dots, 22, \dots, 38) = 21.904, 59.528, 114.460, 186.097$$

$$f(c_1, c_2, \dots, x_5^2, \dots, c_{30}) = f(38, 38, \dots, 38, \dots, 38) = 21.947, 60.073, 116.684, 190.636$$

$$f(c_1, c_2, \dots, x_5^3, \dots, c_{30}) = f(38, 38, \dots, 54, \dots, 38) = 21.964, 60.293, 117.609, 192.686$$

*Function Evaluations in Expansion – 6*

$$f(c_1, c_2, \dots, x_6^1, \dots, c_{30}) = f(38, 38, \dots, 22, \dots, 38) = 21.866, 59.195, 113.880, 186.612$$

$$f(c_1, c_2, \dots, x_6^2, \dots, c_{30}) = f(38, 38, \dots, 38, \dots, 38) = 21.947, 60.073, 116.684, 190.636$$

$$f(c_1, c_2, \dots, x_6^3, \dots, c_{30}) = f(38, 38, \dots, 54, \dots, 38) = 21.976, 60.433, 117.910, 192.586$$

*Function Evaluations in Expansion – 7*

$$f(c_1, c_2, \dots, x_7^1, \dots, c_{30}) = f(38, 38, \dots, 22, \dots, 38) = 21.813, 58.872, 113.849, 188.166$$

$$f(c_1, c_2, \dots, x_7^2, \dots, c_{30}) = f(38, 38, \dots, 38, \dots, 38) = 21.947, 60.073, 116.684, 190.636$$

$$f(c_1, c_2, \dots, x_7^3, \dots, c_{30}) = f(38, 38, \dots, 54, \dots, 38) = 22.001, 60.577, 117.983, 191.851$$

*Function Evaluations in Expansion – 8*

$$f(c_1, c_2, \dots, x_8^1, \dots, c_{30}) = f(38, 38, \dots, 22, \dots, 38) = 21.747, 58.635, 114.372, 189.761$$

$$f(c_1, c_2, \dots, x_8^2, \dots, c_{30}) = f(38, 38, \dots, 38, \dots, 38) = 21.947, 60.073, 116.684, 190.636$$

$$f(c_1, c_2, \dots, x_8^3, \dots, c_{30}) = f(38, 38, \dots, 54, \dots, 38) = 21.028, 60.692, 117.772, 191.040$$

Similarly, all the function evaluations are carried out up to  $i = 30$  and  $j = 1 - 3$

*Function Evaluations in Expansion – 30*

$$f(c_1, c_2, c_3, \dots, x_{30}^1) = f(38, 38, 38, \dots, 22) = 21.947, 60.071, 116.670, 190.578$$

$$f(c_1, c_2, c_3, \dots, x_{30}^2) = f(38, 38, 38, \dots, 38) = 21.947, 60.073, 116.684, 190.615$$

$$f(c_1, c_2, c_3, \dots, x_{30}^3) = f(38, 38, 38, \dots, 54) = 21.947, 60.073, 116.689, 190.636$$

The shape/interpolation function  $\phi_j(x_i)$  is evaluated using the Lagrange interpolation:

$$\phi_j(x_i) = \frac{(x_i - x_i^1) \dots (x_i - x_i^{j-1})(x_i - x_i^{j+1}) \dots (x_i - x_i^n)}{(x_i^j - x_i^1) \dots (x_i^j - x_i^{j-1})(x_i^j - x_i^{j+1}) \dots (x_i^j - x_i^n)}$$

Considering the first component function

For  $i = 1$  and  $j = 1 - 3$ , the expression of Expansion 1 is given by

$$\begin{aligned} \text{Expansion} - 1 &= \phi_1(x_1) \times f(x_1^1, c_2, c_3, \dots, c_{30}) + \phi_2(x_1) \times f(x_1^2, c_2, c_3, \dots, c_{30}) \\ &\quad + \phi_3(x_1) \times f(x_1^3, c_2, c_3, \dots, c_{30}) \\ &= 0.002x_1^2 - 0.179x_1 + 4.007 \times f(22, 38, 38, \dots, 38) - 0.004x_1^2 + 0.296x_1 \\ &\quad - 4.640 \times f(38, 38, 38, \dots, 38) + 0.031x_1^2 - 1.875x_1 + 26.125 \times f(54, 38, 38, \dots, 38) \\ &= 0.002x_1^2 - 0.179x_1 + 4.007 \times 21.947 - 0.004x_1^2 + 0.296x_1 \\ &\quad - 4.640 \times 21.947 + 0.031x_1^2 - 1.875x_1 + 26.125 \times 21.947 \end{aligned}$$

Hence from the *Expansion – 1* first component function in HDMR expansion is given by:

$$\text{HDMR Component function} - 1 = 0.643x_1^2 - 38.578x_1 + 559.477$$

Similarly,

$$\text{HDMR Component function} - 2 = -3.9 \times 10^{-6} x_2^2 + 3.593 \times 10^{-4} x_2 + 21.939$$

$$\text{HDMR Component function} - 3 = -9.756 \times 10^{-6} x_3^2 + 0.001x_3 + 21.922$$

$$\text{HDMR Component function} - 4 = -2.343 \times 10^{-4} x_4^2 + 0.0026x_4 + 21.882$$

$$\text{HDMR Component function} - 5 = -5.078 \times 10^{-5} x_5^2 + 0.0057x_5 + 21.802$$

Similarly all the 30 HDMR component functions are evaluated and summation of all gives the HDMR approximation equation for first response ie natural frequency in mode 1 ( $Y_1$ ) as below:

$$\begin{aligned}
Y_1 = & 0.64x_1^6 - 38.58x_1 - 3.90 \times 10^{-6}x_2^2 + 3.59 \times 10^{-4}x_2 - 9.76 \times 10^{-6}x_3^2 + 1.02 \times 10^{-3}x_3 \\
& - 1.56 \times 10^{-4}x_7^2 + 0.017x_7 - 9.76 \times 10^{-6}x_{28}^2 + 1.023 \times 10^{-3}x_{28} - 3.90 \times 10^{-6}x_{29}^2 \\
& + 3.59 \times 10^{-4}x_{29} + 2.59 \times 10^{-3}x_4 + 5.73 \times 10^{-3}x_5 + 0.01x_6 + 0.143x_8 + 0.036x_9 \\
& + 0.0468x_{10} + 0.057x_{11} + 0.066x_{12} + 0.074x_{13} + 0.079x_{14} + 0.082x_{15} + 0.082x_{16} \\
& + 0.079x_{17} + 0.074x_{18} + 0.063x_{19} + 0.057x_{20} + 0.047x_{21} + 0.036x_{22} + 0.026x_{23} \\
& + 0.134x_{24} + 0.014x_{25} + 5.73 \times 10^{-3}x_{26} + 2.59 \times 10^{-3}x_{27} - 2.34 \times 10^{-5}x_4^2 \\
& - 5.078 \times 10^{-5}x_5^2 - 1.015 \times 10^{-4}x_6^2 - 2.18 \times 10^{-3}x_8^2 - 3.18 \times 10^{-4}x_9^2 - 4.08 \times 10^{-4}x_{10}^2 \\
& - 4.98 \times 10^{-4}x_{11}^2 - 5.76 \times 10^{-4}x_{12}^2 - 6.38 \times 10^{-4}x_{13}^2 - 6.83 \times 10^{-4}x_{14}^2 - 7.07 \times 10^{-4}x_{15}^2 \\
& - 7.07 \times 10^{-4}x_{16}^2 - 6.83 \times 10^{-4}x_{17}^2 - 6.83 \times 10^{-4}x_{18}^2 - 5.76 \times 10^{-4}x_{19}^2 - 4.98 \times 10^{-4}x_{20}^2 \\
& - 4.08 \times 10^{-4}x_{21}^2 - 3.18 \times 10^{-4}x_{22}^2 - 2.32 \times 10^{-4}x_{23}^2 - 2.10 \times 10^{-4}x_{24}^2 - 1.58 \times 10^{-4}x_{25}^2 \\
& - 5.07 \times 10^{-5}x_{26}^2 - 2.34 \times 10^{-5}x_{27}^2 + 530.32
\end{aligned}$$

Similarly, the HDMR approximation equations are developed for the frequency responses of second, third and fourth mode ie.  $Y_2, Y_3$  and  $Y_4$  and utilized to develop objective functions. Then the objective function is minimized using GA to obtain the updated parameters. Using updated parameters, initial FE model is updated to obtain reference state, reference damage state and damage state models, so that, responses of FE model were in tune with the experimental observations.





## REFERENCES

- [1] Abdeljaber, O., Avci, O., Kiranyaz, S., Gabbouj, M. and Inman, D.J. (2017). “Real-time vibration-based structural damage detection using one-dimensional convolutional neural networks.” *J. Sound Vib.*, 388, 154–170.
- [2] Alis, O.F. and Rabitz, H. (2001). “Efficient implementation of high dimensional model representations.” *J. Math. Chem.*, 29(2), 127–142.
- [3] Arora, V., Singh, S.P. and Kundra, T.K. (2009). “Comparative study of damped FE model updating methods.” *Mech. Syst. Signal Process.*, 23, 2113–2129.
- [4] Atalla, M.J. and Inman, D.J. (1998). “On model updating using neural networks.” *Mech. Syst. Signal Process.*, 12(1), 135–161.
- [5] Balageas, D., Fritzen, C. and Guemes, A. (2006). “Structural health monitoring.” *ISTE Ltd.*, London.
- [6] Balu, A.S. and Rao, B.N. (2012). “High dimensional model representation based Formulations for fuzzy finite element analysis of structures.” *Finite Elem. Anal. Des.*, 50, 217–230.
- [7] Balu, A.S. and Rao, B.N. (2013). “Confidence bounds on design variables using high-dimensional model representation based inverse reliability analysis.” *J. Struct. Eng.*, 139(6), 985–996.
- [8] Balu, A.S. and Rao, B.N. (2014). “Efficient assessment of structural reliability in presence of random and fuzzy uncertainties.” *J. Mech. Des.*, 136, 051008.
- [9] Baruch, I.Y. and Bar-Itzhack (1978). “Optimal weighted orthogonalization of measured modes.” *Am. Inst. Aeronaut. Astronaut. J.*, 16(4), 346–351.
- [10] Berman, A. and Nagy, E.J. (1983). “Improvement of a large analytical model using test data.” *Am. Inst. Aeronaut. Astronaut. J.*, 21, 1168–1173.
- [11] Boulkaibet, I., Mthembu, L., Marwala, T., Friswell, M.I. and Adhikari, S. (2017). “Finite element model updating using Hamiltonian Monte Carlo techniques.” *Inv. Prob. Sci. Eng.*, 25 (7), 1042–1070.

- [12] Brownjohn, J and Xia, P. (2000). “Dynamic assessment of curve cable-stayed bridge by model updating.” *J. Struct. Eng.*, 126(2), 252–260.
- [13] Brownjohn, J.M.W., Moyo, P., Omenzetter, P. and Lu, Y. (2003). “Assessment of highway bridge upgrading by dynamic testing and finite-element model updating.” *J. Bridge Eng.*, 8(3), 162–172.
- [14] Bucher, I. and Braun, S. (1993). “The structural modification inverse problem: an exact solution.” *Mech. Syst. Signal Process.*, 7(3), 217–238.
- [15] Chang, C.C., Chang, T.Y.P. and Xu, Y.G. (2000). “Adaptive neural networks for model updating of structures.” *Smart Mater. Struct.*, 9, 59–68.
- [16] Ching, J., Muto, M. and Beck, J.L. (2006). “Structural model updating and health monitoring with incomplete modal data using Gibbs sampler.” *Comput.-Aided Civ. Infrastruct. Eng.*, 21(4), 242–257.
- [17] Chowdhury, R., Rao, B.N. and Prasad, A.M. (2008). “High dimensional model representation for piece-wise continuous function approximation.” *Commun. Numer. Methods Eng.*, 24, 1587–1609.
- [18] Collins, J.D., Hart, G.C., Haselman, T.K. and Kennedy, B. (1974). “Statistical identification of structures.” *Am. Inst. Aeronaut. Astronaut. J.*, 12(2) 185–190.
- [19] Deng, L. and Cai, C.S. (2010). “Bridge model updating using response surface method and genetic algorithm.” *J. Bridge Eng.*, 15(5), 553–564.
- [20] Dey, S., Mukhopadhyay, T. and Adhikari, S. (2015). “Stochastic free vibration analysis of angle-ply composite plates – A RS-HDMMR approach.” *Compos. Struct.*, 122, 526–536.
- [21] Dey, S., Mukhopadhyay, T. and Adhikari, S. (2017). “Metamodel based high-fidelity stochastic analysis of composite laminates: a concise review with critical comparative assessment.” *Compos. Struct.*, 171, 227–250.
- [22] Dey, S., Mukhopadhyay, T., Spickenheuer, A., Adhikari, S. and Heinrich, G. (2016). “Bottom up surrogate based approach for stochastic frequency response analysis of laminated composite plates.” *Compos. Struct.*, 140, 712–727.

- [23] Ding, Z., Yao, R., Li, J. and Lu, Z. (2017). “Structural damage identification based on modified artificial bee colony algorithm using modal data.” *Inv. Prob. in Sci. Eng.*, 1–21.
- [24] Doebling, S.W., Farrar, C.R. and Prime, M.B. (1998). “Summary review of vibration-based damage identification methods.” *Shock and Vib. Digest*, 30, 91–105.
- [25] Dutta, A. and Talukdar, S. (2004). “Damage detection in bridges using accurate modal parameters.” *Finite Elem. Anal. Des.*, 40, 287–304.
- [26] Ebrahimian, H., Astroza, R., Conte, J.P. and Callafon, R.A. (2016). “Nonlinear finite element model updating for damage identification of civil structures using batch Bayesian estimation.” *Mech. Syst. Signal Process.*, 84, 194–222.
- [27] Entezami, H., Shariatmadar and Sarmadi, H. (2017). “Structural damage detection by a new iterative regularization method and an improved sensitivity function,” *J. Sound Vib.*, 399, 285–307.
- [28] Fang, H., Wang, T.J. and Chen, X. (2011). “Model updating of lattice structures: a substructure energy approach.” *Mech. Syst. Signal Process.*, 25(5), 1469–1484.
- [29] Fang, S.E. and Perera, R. (2009). “A response surface methodology based damage identification technique.” *Smart Mater. Struct.*, 18, 1–14.
- [30] Fang, S.E. and Perera, R. (2011). “Damage identification by response surface based model updating using D-optimal design.” *Mech. Syst. Signal Process.*, 25, 717–733.
- [31] Fang, S.E., Perera, R. and Roeck, G.D. (2008). “Damage identification of a reinforced concrete frame by finite element model updating using damage parameterization.” *J. Sound Vib.*, 313, 544–559.
- [32] Farrar, C. R., Baker, W. E., Bell, T. M., Cone, K. M., Darling, T. W., Duffey, T. A., Eklund, A. and Migliori, A. (1996) “Dynamic characterization and damage detection in the I-40 bridge over the Rio Grande.” *Los Alamos National Laboratory Report*, LA-12767-MS.

- [33] Friswell, M.I. (2007). “Damage identification using inverse methods.” *Philos. Trans. R. Soc. A.*, 365, 393–410.
- [34] Friswell, M.I. and Mottershead, J.E. (1995). “Finite element model updating in structural dynamics.” *Kluwer Academic Publishers*, Dordrecht, The Netherlands.
- [35] Friswell, M.I., Inman, D.J. and Pilkey, D.F. (1998). “The direct updating of damping and stiffness matrices,” *Am. Inst. Aeronaut. Astronaut. J.*, 36(3), 491–493.
- [36] Gautier, G., Mevel, L., Mencik, J., Serra, R. and Döhler, M. (2017). “Variance analysis for model updating with a finite element based subspace fitting approach.” *Mech. Syst. Signal Process.*, 91, 142–156.
- [37] Grafe, H. (1998). “Model updating of large structural dynamics models using measured response functions.” Doctoral thesis, *Imperial College of Science, Technology and Medicine University of London*, South Kensington.
- [38] Hejll, A. (2007). “Civil structural health monitoring - strategies, methods and applications.” Doctoral Thesis, *Luleå Univ. of Tech.*, Sweden.
- [39] Hibbitt, Karlsson and Sorensen (2000). “ABAQUS/Standard user's manual, version 6.14.” *Simulia*, Providence, RI.
- [40] Imregun, M., Sanliturk K.Y. and Ewins, D. J. (1995a). “Finite element model updating using frequency response function data - II. Case study on a medium – size finite element model.” *Mech. Syst. Signal Process.*, 9(2), 203–213.
- [41] Imregun, M., Visser, W. J. and Ewins, D. J. (1995b). “Finite element model updating using frequency response function data - I. Theory and initial investigation.” *Mech. Syst. Signal Process.*, 9(2), 187–202.
- [42] Jaishi B. and Ren, W. (2006). “Damage detection by finite element model updating using modal flexibility residual.” *J. Sound Vib.*, 290, 369–387.
- [43] Jaishi, B. and Ren, W. (2007). “Finite element model updating based on eigenvalue and strain energy residuals using multi-objective optimization technique.” *Mech. Syst. Signal Process.*, 21(5), 2295–2317.

- [44] Jaishi, B. and Ren, W. (2007). “Finite element model updating based on eigenvalue and strain energy residuals using multiobjective optimization technique.” *Mech. Syst. Signal Process.*, 21(5), 2295–2317.
- [45] Jiang, L. and Li, X. (2015). “Multi-element least square HDMR methods and their applications for stochastic multiscale model reduction.” *J. Comput. Phys.* 294, 439–461.
- [46] Katafygiotis, L.S., Papadimitriou, C. and Lam, H. (1998). “A probabilistic approach to structural model updating.” *Soil Dyn. Earthquake Eng.*, 17, 495–507.
- [47] Kaya, H., Kaplan, M. and Saygin, H. (2004). “A recursive algorithm for finding HDMR terms for sensitivity analysis.” *Comput. Phys. Commun.*, 158, 106–112.
- [48] Kenigsbuch, R. and Halevi, Y. (1998). “Model updating in structural dynamics: A generalized reference basis approach.” *Mech. Syst. Signal Process.*, 12(1), 75–90.
- [49] Levin, R.I. and Lieven, N.A.J. (1998). “Dynamic finite element model updating using simulated annealing and genetic algorithm.” *Mech. Syst. Signal Process.*, 12(1), pp. 91–120.
- [50] Li, G., Wang, S., Rosenthal, C. and Rabitz, H. (2001). “High dimensional model representations generated from low dimensional data samples. I. mp-Cut-HDMR.” *J. Math. Chem.*, 30(1), 1–30
- [51] Li, G., Wang, S.W., Rabitz, H. and Wang, S. Jaffé P. (2002), “Global uncertainty assessments by high dimensional model representations (HDMR)” . *Chem. Eng. Sci.*, 57(21), 4445–4460.
- [52] Li, G., Xing, X., Welsh, W. and Rabitz, H. (2017). “High dimensional model representation constructed by support vector regression. I. Independent variables with known probability distributions.” *J. Math. Chem.*, 55(1), 278–303.
- [53] Li, J., Hao, H. and Fan, G. (2016). “Damping ratios identification by sensitivity-based model updating: Experimental investigation.” *Proceedings of*

*the 24<sup>th</sup> Australian Conference on the Mechanics of Structures and Materials: Advancements and Challenges*, 1349–1354.

- [54] Lin, R.M., Lim, M.K. and Du, H. (1995). “Improved inverse eigen sensitivity method for structural analytical model updating.” *J. Vib. Acou.*, 117, 192–198.
- [55] Link, M. and Weiland, M. (2009). “Damage identification by multi-model updating in the modal and in the time domain.” *Mech. Syst. Signal Process.*, 23, 1734–1746.
- [56] Liu, J., Sun, X., Han, X., Jiang, C. and Yu, D. (2015). “Dynamic load identification for stochastic structures based on Gegenbauer polynomial approximation and regularization method.” *Mech. Syst. Signal Process.*, 56, 35–54.
- [57] Marwala (2005). “Finite element model updating using particle swarm optimization.” *Int. J. Eng. Simul.*, 6(2), 25–30.
- [58] Modak, S.V., Kundra, T.K. and Nakra, B.C. (2000). “Model updating using constrained optimization.” *Mech. Res. Commun.*, 27(5), 543–551.
- [59] Modak, S.V., Kundra, T.K. and Nakra, B.C. (2002), “Comparative study of model updating methods using simulated experimental data.” *Compu. Struct.*, 80, 437–447.
- [60] Modak, S.V., Kundra, T.K. and Nakra, B.C. (2002). “Prediction of dynamic characteristics using updated finite element models.” *J. Sound Vib.*, 254(3), 447–467.
- [61] Mohamed, M. S., Mustafa, H. A. and Ashraf, O. N. (2013) “Finite element model updating approach to damage identification in beams using particle swarm optimization.” *Eng. Optim.*, 45(6), 677–696.
- [62] Mottershead, J.E. and Friswell M.I. (1993). “Model updating in structural dynamics: A Survey.” *J. Sound Vib.*, 167(2), 347–375.
- [63] Mukhopadhyay, T. (2016). “A multivariate adaptive regression splines based damage identification methodology for web core composite bridges including the effect of noise.” *J. Sandwich Struct. Mater.*, doi: 10.1177/1099636216682533.

- [64] Mukhopadhyay, T., Chowdhury, R. and Chakrabarti, A. (2016). “Structural damage identification: a random sampling-high dimensional model representation approach.” *Adv. Struct. Eng.*, 19(6), 908–927.
- [65] Mukhopadhyay, T., Dey, T.K., Chowdhury, R. and Chakrabarti, A. (2015). “Structural damage identification using response surface-based multi-objective optimization: a comparative study.” *Arab. J. Sci. Eng.*, 40(4), 1027–1044.
- [66] Mukhopadhyaya, T., Dey, T.K., Chowdhury, R., Chakrabarti, A. and Adhikari, S. (2015). “Optimum design of FRP bridge deck: an efficient RS-HDMR based approach.” *Struct. Multidiscip. Optim.*, 52, 459–477.
- [67] Pacini B.R., Mayes R.L., Owens B.C. and Schultz R.A. (2017). “Nonlinear finite element model updating, Part I: Experimental techniques and nonlinear modal model parameter extraction.” *Dynamics of Coupled Struct.*, 4, 263–274.
- [68] Park, G., Harley, H., Cudney and Inman, D.J. (2000). “Impedance-based health monitoring of civil structural components.” *J. Infrastruct. Syst.*, 6(4), 153–160.
- [69] Pedram, M., Esfandiari, A. and Khedmati, M.R. (2017). “Damage detection by a FE model updating method using power spectral density: Numerical and experimental investigation.” *J. Sound Vib.*, 397, 51–76.
- [70] Perera, R., Fang, S.E. and Ruiz, A. (2010). “Application of particle swarm optimization and genetic algorithms to multi-objective damage identification inverse problems with modelling errors.” *Meccanica*, 45, 723–734.
- [71] Rabitz, H. and Alis, O.F. (1999). “General foundations of high-dimensional model representations.” *J. Math. Chem.*, 25, 197–233.
- [72] Rabitz, H., Alis, O.F., Shorter, J. and Shim, K. (1999). “Efficient input-output model representations.” *Comput. Phys. Commun.*, 117, 11–20.
- [73] Refsgaard, J.C., Sluijs, J.P., Brown, J. and Keur P. (2006). “A framework for dealing with uncertainty due to model structure error.” *Adv. Water Resour.*, 29, 1586–1597.



- [74] Ren, W.X. and Chen, H. B. (2010). “Finite element model updating in structural dynamics by using the response surface method.” *Eng. Struct.*, 32, 2455–2465.
- [75] Rombach, G.A. (2004). “Finite Element Design of Concrete Structures: Practical problems and their solutions” *Thomas Telford Ltd.*, London.
- [76] Roy, K. (2017). “Structural damage identification using mode shape slope and curvature.” *J. Eng. Mech.*, 143(9), 04017110.
- [77] Salawu, O.S. (1997). “Detection of structural damage through changes in frequency: a review.” *Eng. Struct.*, 19 (9), 718–723.
- [78] Sanayei, A. Khaloo, M. Gul and Catbas, F.N. (2015). “Automated finite element model updating of a scale bridge model using measured static and modal test data,” *Eng. Struct.*, 102, 66–79.
- [79] Sanayei, M., Imbaro, G.R., McClain, J.A.S. and Brown, L.C. (1997). “Structural model updating using experimental static measurements.” *J. Struct. Eng.*, 123 792–798.
- [80] Sehgal, S. and Kumar, H. (2015). “Structural dynamic model updating techniques: a state of the art review.” *Arch. Computat. Methods Eng.*, 23(3), 515–533.
- [81] Shabbir, F. and Omenzetter, P. (2016). “Model updating using genetic algorithms with sequential niche technique.” *Eng. Struct.*, 120, 166–182.
- [82] Shahidi, G.S. and Pakzad S.N. (2014). “Generalized response surface model updating using time domain data.” *J. Struct. Eng.*, 140(8):A4014001.
- [83] Sobol, I.M. (2003). “Theorems and examples on high dimensional model representation.” *Reliab. Eng. Sys. Saf.*, 79, 187–193.
- [84] Sohn H., Farrar, C., Hunter, N.F. and Worden, K. (2001). “Structural health monitoring using statistical pattern recognition techniques.” *J. Dyn. Syst. Meas. Contr.*, 123, 706–711.
- [85] Teughels, A. and Roeck, D.G. (2004). “Structural damage identification of the highway bridge Z24 by FE model updating.” *J. Sound Vib.*, 278, 589–610.

- [86] Teughels, A., Maeck, J. and Roeck, D.G. (2002). “Damage assessment by FE model updating using damage functions.” *Comput. Stru.*, 80, 1869–1879.
- [87] Tunga, M.A. (2011). “An approximation method to model multivariate interpolation problems: Indexing HDMR.” *Math. Comput. Modell.*, 53, 1970–1982.
- [88] Tunga, M.A. and Demiralp, M. (2006). “Hybrid high dimensional model representation (HHDMR) on the partitioned data.” *J. Comput. Appl., Math.*, 185, 107–132.
- [89] Wang, X., Hu, N., Fukunaga, H. and Yao Z.H. (2001). “Structural damage identification using static test data and changes in frequencies.” *Eng. Struct.*, 23, 610–621.
- [90] Xiao, X., Xu, Y.L. and Zhu, Q. (2014). “Multiscale modelling and model updating of a cable-stayed bridge. II: Model updating using modal frequencies and influence lines.” *J. Bridge Eng.*, 20(10), 1–12.
- [91] Zhao, L., Choi, K.K. and Lee, I. (2011). “Metamodeling Method Using dynamic kriging for design optimization.” *Am. Inst. Aeronaut. Astronaut. J.*, 49(9), 2034–2046.
- [92] Zou, Y., Tong, L. and Steven, G.P. (2000). “Vibration-based model-dependent damage (delamination) identification and health monitoring for composite structures – a review.” *J. Sound Vib.*, 230(2), 357–378.

## PUBLICATIONS

### International Journals

1. Naveen, B.O. and Balu, A.S. (2018). “HDMR based model update in structural damage identification.” *International Journal of Computational Methods*, 15(2), 1–14.
2. Naveen, B.O. and Balu, A.S. (2017). “High dimensional model representation based bridge model update for structural damage identification.” *International Journal of Advances in Engineering Sciences and Applied Mathematics*. (Under review)
3. Naveen, B.O. and Balu, A.S. (2017). “Efficient finite element model update using HDMR for damage identification in bridges.” *Engineering Structures*. (Under review)
4. Naveen, B.O. and Balu, A.S. (2018). “Application of HDMR in assessment of structural damages.” *Advances in Structural Engineering*. (Under review)

### International Conferences

1. Naveen, B.O. and Balu, A.S. (2016). “HDMR based model updating in structural damage identification.” *Proceedings of Sixth International Congress on Computational Mechanics and Simulation*, June 27–July 1, 2016, IIT Bombay, India.
2. Naveen, B.O. and Balu, A.S. (2016). “Structural damage identification by model updating using HDMR.” *Structural Engineering Convention*, December 21–23, CSIR, Chennai, India.
3. Naveen, B.O. and Balu, A.S. (2017). “HDMR based finite element model update in structural damage identification.” *Seventh International Conference on Theoretical, Applied, Computational and Experimental Mechanics*, December 28–30, 2017, IIT Kharagpur, India.

## CURRICULUM VITAE

1. NAME : NAVEEN, B.O.
  2. DATE OF BIRTH : October 13, 1984
  3. EDUCATIONAL QUALIFICATIONS
    - Degree : Bachelor of Engineering (B.E.)
    - Specialization : Civil Engineering
    - Institute : B.I.E.T Davangere, Visvesvaraya Technological University, Belgavai, India
    - Year : 2006
    - Degree : Master of Engineering (M.E.)
    - Specialization : Industrial Structures
    - Institute : S.J.C.E Mysuru under Visvesvaraya Technological University, Belagavi, India.
    - Year : 2009
    - Degree : Doctor of Philosophy (Ph.D)
    - Specialization : Structural Engineering
    - Institute : National Institute of Technology Karnataka, Surathkal, India
    - Registration Date : July 17, 2014
  4. ADDRESS : S/o B.D.Onkareswara,  
#3371/3B, 3rd Cross, M.C.C. B-Block,  
Davangere - 577 004, Karnataka, India  
Mobile: +91 9611691111/8762097978  
Email: bonaveen3@gmail.com
-